

**IMPROVED BIOAVAILABILITY OF RIFAMPICIN
NANOPARTICLES FROM FIXED DOSE COMBINATION WITH
ISONIAZID, PYRAZINAMIDE AND ETHAMBUTOL**

A Dissertation submitted to

**THE TAMILNADU Dr. M.G.R. MEDICAL UNIVERSITY
Chennai-600032**

In partial fulfillment of the requirements for the award of degree of

**MASTER OF PHARMACY
IN
PHARMACEUTICS**

Submitted by

REG. NO: 261210606

Under the Guidance of

K.MOHAN KUMAR, M.pharm.



DEPARTMENT OF PHARMACEUTICS

SWAMY VIVEKANANDHA COLLEGE OF PHARMACY

ELAYAMPALAYAM

TIRUCHENGODE-637205

TAMILNADU

APRIL-2014



SWAMY VIVEKANANDHA COLLEGE OF PHARMACY

Elayampalayam, Tiruchengode, 637 205

Namakkal (DT), Tamilnadu.

Phone: 04288-234417 (8lines)

Fax: 04288-234417

Dr. N. N. RAJENDRAN, M.Pharm., Ph.D.,
Principal

CERTIFICATE

This is to certify that the dissertation entitled **“IMPROVED BIOAVAILABILITY OF RIFAMPICIN NANOPARTICLES FROM FIXED DOSE COMBINATION WITH ISONIAZID, PYRAZINAMIDE AND ETHAMBUTOL”** submitted to The Tamilnadu Dr. M.G.R Medical University, Chennai, is a bonafide project work of **Reg. No: 261210606**, carried out in the Department of Pharmaceutics, Swamy Vivekanandha College of Pharmacy, Tiruchengode in partial fulfillment for the degree of Master of Pharmacy under the guidance of **K.MOHAN KUMAR, M.Pharm.** Swamy Vivekanandha College of Pharmacy Tiruchengode.

[Dr. N. N. RAJENDRAN]



SWAMY VIVEKANANDHA COLLEGE OF PHARMACY

Elayampalayam, Tiruchengode, 637 205

Namakkal (DT), Tamilnadu.

Phone: 04288-234417 (8lines)

Fax: 04288-234417

Dr. N. N. RAJENDRAN, M.Pharm., Ph.D.,

Director of P.G. studies and Research

CERTIFICATE

This is to certify that the dissertation entitled **“IMPROVED BIOAVAILABILITY OF RIFAMPICIN NANOPARTICLES FROM FIXED DOSE COMBINATION WITH ISONIAZID, PYRAZINAMIDE AND ETHAMBUTOL”** submitted to The Tamilnadu Dr. M.G.R Medical University, Chennai, is a bonafide project work of **Reg. No: 261210606**, carried out in the Department of Pharmaceutics, Swamy Vivekanandha College of Pharmacy, Tiruchengode in partial fulfillment for the degree of Master of Pharmacy under the guidance of **K.MOHAN KUMAR, M.Pharm.** Swamy Vivekanandha College of Pharmacy Tiruchengode.

[Dr. N. N. RAJENDRAN]



SWAMY VIVEKANANDHA COLLEGE OF PHARMACY

Elayampalayam, Tiruchengode, 637 205

Namakkal (DT), Tamilnadu.

Phone: 04288-2344178lines)

Fax: 04288-234417

K.MOHAN KUMAR, M.Pharm.

Assistant professor

CERTIFICATE

This is to certify that the dissertation entitled **“IMPROVED BIOAVAILABILITY OF RIFAMPICIN NANOPARTICLES FROM FIXED DOSE COMBINATION WITH ISONIAZID, PYRAZINAMIDE AND ETHAMBUTOL”** submitted to The Tamilnadu Dr. M.G.R. Medical University, Chennai, is a bonafide project work of **Reg. No: 261210606**, carried out in the Department of Pharmaceutics, Swamy Vivekanandha College of Pharmacy, Tiruchengode in partial fulfillment for the degree of Master of Pharmacy under my direct supervision and guidance.

This work is original and has not been submitted earlier for the award of any other degree or diploma of this or any other university.

[**K.MOHAN KUMAR**]



SWAMY VIVEKANANDHA COLLEGE OF PHARMACY

Elayampalaym, Tiruchengode, 637205

Namakkal (DT), Tamilnadu.

Phone: 04288-234417(8lines)

Fax: 04288-234417

Prof. R. NATARAJAN, M .Pharm., Ph.D,

Head, Department of Pharmaceutics

CERTIFICATE

This is to certify that the Dissertation entitled **“IMPROVED BIOAVAILABILITY OF RIFAMPICIN NANOPARTICLES FROM FIXED DOSE COMBINATION WITH ISONIAZID, PYRAZINAMIDE AND ETHAMBUTOL”** submitted to The Tamilnadu Dr. M.G.R. Medical University, Chennai, is a bonafide project work of **Reg.No: 261210606**, carried out in the Department of Pharmaceutics, Swamy Vivekanandha College of Pharmacy, Tiruchengode in partial fulfillment for the degree of Master of Pharmacy under the guidance of **K.MOHAN KUMAR, M.Pharm.**, Swamy Vivekanandha College of Pharmacy, Tiruchengode.

[R. NATARAJAN]

ACKNOWLEDGEMENT

The Joyness, satisfaction and euphoria that comes along with successful completion of any work would be incomplete unless we mention the names of people who made it possible, whose constant guidance and encouragement served as a beam of light crowned out effects.

First and foremost I bow down before **Lord Almighty** for his splendid blessings and care in completing my project work and throughout my life till this very second.

I render my sincere thanks to our honorable Chairman and Secretary, **Vidhyaratna, Rashtriya Rattan, Hind Rattan, DR. M. KARUNANITHI., B.Pharm., M.S., Ph.D, D.Litt.**, for providing all facilities for my study and rendering his noble hand in the upliftment of women education in all the disciplines.

I consider it as a great honor to express my heartfelt appreciation to my guide **K.MOHAN KUMAR, M.Pharm.** Assistant professor and thank for his willingness to offer continuous guidance, support and encouragement, which are driving forces for me to complete this thesis. His vast knowledge, his attitude to research and skill of presentation has been an invaluable resource to me. He is an admirable professor and will always be a role model for me.

It is difficult to overstate my gratitude to **Dr. N. N. RAJENDRAN, M.Pharm., Ph.D.**, and Principal of our institution. His enthusiasm and integral view on research and his mission for providing 'only high-quality work and not less', has made a deep impression on me. I owe him lots of gratitude for having me shown this way of research.

It would be unwise if I forget to express my sincere thanks and gratitude to **Prof. R.NATARAJAN, M.Pharm., (Ph.D)**, **Mrs. R. SUBASHINI, M.Pharm., (Ph.D)**, **Mrs.M.RANGAPRIYA, M.Pharm., (Ph.D)** and **Ms. M.DHANALAKSHMI, M.Pharm.**, Department of Pharmaceutics for their immense support in all the aspects of my study.

I take this opportunity to tell my special thanks to **Miss. Latha & Mrs. P.Menaka, and Mr.K.Sundararajan** for their help and support in all my laboratory tests.

I owe my sincere thanks to my **Parents and Brother** who cared for my well-being and had spent their times in shaping my character, conduct and my life. Without their moral support I am nothing and I dedicate all my achievements at their feet.

Friends are treasures to me and it is very difficult to overstate my thanks to all my friends and colleagues **P.Adinarayana yadav, C.Prabhu, K. Shahul Hameed, N.Hari Babu., S.V.S.Subrahmanyam, M.Raviteja, K.Gangi Reddy, S.Varatha Kunan, T.Prakash.** It has been my happiest time to study, discuss, laugh and play with them all.

Also, I would like to thank The **Tamil Nadu Dr. M.G.R. Medical University** for providing a nice environment for learning.

I feel delighted to express my whole hearted gratitude to all those who gave their helping hands in completing my course and my project successfully.

RAJASEKHAR PASUPULETI

Reg.No:261210606

INDEX

CHAPTER NO.	CONTENTS	PAGE NO.
	Abstract	1
1	Introduction	2
2	Review of Literature	
2.1	Epidemiology of TB	6
2.2	Drug therapy in tuberculosis	7
2.3	TB drugs in development	8
2.4	Rifampicin and its bioavailability	9
2.5	Degradation of rifampicin	10
2.6	Nanoparticles as drug delivery system	11
2.7	Polymer as drug delivery system	13
2.8	Pharmaceutical approaches for the treatment of tuberculosis	14
2.9	Background of the review	18
3	Drug profile	19
3.1	Rifampicin	19
3.2	Isoniazid	24
3.3	Pyrazinamide	26
3.4	Etambutal	28
3.5	3-Formyl rifamycin SV	30
3.6	Polymer profile	31
3.6.1	PLGA	31
4	Aim and Objective of the study	33
5	Plan of work	34

6	Materials	
6.1	Chemicals	35
6.2	Equipments	36
7.0	Methodology	
7.1	Preformulation studies	37
7.2	Preparation of Calibration curve for Simultaneous estimation of rifampicin and 3FRSV by DW-spectrophotometric method.	37
7.3	Calibration curve for rifampicin and 3 FRSV.	38
7.4	<i>In-vitro</i> dissolution stability study of rifampicin in the presence and absence of FDC at pH 1.2 buffer.	39
7.5	<i>In-vitro</i> dissolution stability study of rifampicin with different concentration of plga in the presence of fdc at pH 1.2 buffer	40
7.6	Statistical analysis	40
7.7	Preparation of rifampicin loaded PLGA nanoparticles	40
7.8	In vitro Evaluation of nanoparticles	41
7.8.1	Drug and carrier interaction by fourier transform infra red spectroscopy	41
7.8.2	Particle size determination by scanning electron microscopy	41
7.8.3	Surface characterstics by zeta potential	42
7.8.4	Thermal analysis by differential scanning calorimetry(DSC)	42
7.8.5	Encapsulation efficiency and loading capacity of nanoparticles	42
7.8.6	Invitro release of rifampicin from the nanoparticles	42
7.8.7	Kinetics of drug release	43
7.9	In vivo evaluation	47
7.9.1	Animals	47
7.9.2	Animal dose	47
7.9.3	Procedure for collection of blood	47
7.9.4	Experimental procedure	48

7.9.5	Bioanalytical work	48
7.9.5.1	Chromatographic conditions	48
7.9.6	Pharmacokinetic parameters	50
8	Results	52
	In vitro evaluation	52
	Compatibility studies	
8.1	Drug and carrier interaction by FT-IR Spectroscopy	52
8.2	Differential Scanning Calorimetry(DSC)	57
8.3	Encapsulation efficiency and loading capacity	61
8.4	Morphology	62
8.5	Particle size	64
8.6	Zeta potential	64
8.7	Poly dispersive index	65
8.8	In vitro release of rifampicin nanoparticles	65
8.9	In vitro release kinetic data rifampicin loaded nanoparticles(diffusion)	98
8.10	Comparitive percentage drug degradation	125
8.11	Comparitive percentage formation of 3 FRSV	126
9	In vivo Evaluation	153
9.1	Pharmacokinetic calculations	153
9.2	Pharmacokinetic parameters of rifampicin	157
9.3	Pharmacokinetic parameters of 3FRSV	162
10	Discussion	167
11	Conclusion	179
12	Reference	174

ABSTRACT

The Present study aimed to improve the bioavailability of Rifampicin from fixed dose combination with Isoniazid, Pyrazinamide and Ethambutal by Incorporating Rifampicin Nanoparticles with fixed dose Combinations. Rifampicin Nanoparticles were Prepared With different Concentrations of PLGA as Polymer and it was evaluated for its physico chemical parameters such as FTIR ,DSC, Entrapment Efficiency, Loading Capacity, In vitro drug release and In vivo pharmacokinetics. The percentage formation of its metabolite (3FRSV) also studied.

1. INTRODUCTION

Tuberculosis (TB), widely occurring, is still one of the most deadly infectious diseases worldwide. Occurrence of tuberculosis along with AIDS has become of greater concern. Current treatments of tuberculosis are limited by severe adverse effects of the drugs during long-term therapy, potential bioavailability problems associated with drugs, and poor patient compliance. Tuberculosis infected with *Mycobacterium tuberculosis* currently infects approximately one third of the world's population. TB has been declared a public health emergency by the World Health organization (WHO). A control programme reaches the WHO targets of 70% case detection and 85% cure would reduce the incidence rate by 11% (range 8-12) per year and the death rate by 12% (9-13) per year. Without greater effort to control tuberculosis, the annual incidence of the disease is expected to increase by 41% (21-61) between 1998 and 2020 (from 7.4 million to 10.6 million cases per year). Achievement of WHO targets by 2010 would prevent 23% (15-30) or 48 million cases by 2020.¹

Rifampicin, Isoniazid, Pyrazinamide, and Ethambutol were earlier prescribed as separate formulations in TB control. The emergence of multidrug resistant TB has threatened the efforts of TB control. To overcome the treatment failure and increase the patient compliance, the world health organization (WHO) and International Union against Tuberculosis and Lung Disease (IUATLD) recommended the use of four drug fixed dose combination (FDC).

The anti-TB drugs have been categorized into two types. Namely, first line and second line drugs. First line drugs are rifampicin (RIF) and isoniazid (INH), pyranzinamide (PYZ), ethambutol (ETB) and streptomycin daily for 2 months which is known as intensive phase. A continuation phase of rifampicin and isoniazid for further 4 months, either daily or 3 times per week, to be administered. Second line drugs include capreomycin, anamycin, ethionamide, Para-amino salicylic acid, cyclosporine, thiacetazone, ciprofloxacin, levofloxacin, Ofloxacin, and sparfloxacin.²

Rifampicin (RIF) is a semi synthetic macrocyclic antibiotic derived from *streptomycesmediterranei*.³ key sterilizing component of highly effective short course antituberculous regimens and has a unique role in the killing of semi-dormant tubercle bacilli.⁴ Rifampicin (rifampicin) is a bactericidal for *Mycobacterium tuberculosis*.

It inhibits mycobacterial DNA-dependent RNA polymerase synthesis by blocking RNA transcription. Most strains of *M. tuberculosis* are inhibited in-vitro by rifampin concentrations of 0.5µg/ml. Rifampicin is known to include cytochrome P450 activity.

INH eradicates most of the rapidly replicating bacilli in the first 2 weeks of treatment, together with streptomycin and ETB. Thereafter, RIF and PYZ have an important role in the sterilization of lesions by eradicating organisms; these two drugs are crucial for successful 6-month treatment regimens. RIF kills low or non-replicating organisms and the high sterilizing effect of PYZ serves to act on semi dormant bacilli not affected by any other anti-TB agent in sites hostile to the penetration and action of the other drugs.^{6,7} INH and RIF, the two most potent anti-TB drugs, kill more than 99% of tubercular bacilli within 2 months of initiation of therapy.^{8,9} Using these drugs in conjunction with each other reduces anti-TB therapy from 18 months to 6 months.

After oral administration on an empty stomach, the absorption of rifampicin (rifampin) is rapid and practically complete. With a single 600mg dose, peak serum concentration of the order of 10microgram/ml generally occurs 2 hours after administration. Food and antacids can decrease the oral absorption of rifampicin.¹⁰ The half-life of rifampicin for this dose level is of the order of 2.5 hours.¹¹ It is 75% bound to plasma proteins and it is metabolized in the liver to an active metabolite, deacetylrifampin and undergoes enterohepatic recycling. A mean RIF maximal serum concentration (C_{max}) of 10.54 ± 3.18 µg/ml, the time at which it occurred (T_{max}) of 2.42 ± 1.32 h, and the area under the curve from time zero to infinity ($AUC_{0-\infty}$) of 57.15 ± 13.41 µg.h.ml⁻¹ on fasting conditions.¹² The previous studies indicate that rifampicin alone was degraded by 12.4% in an acidic medium in 1hr to 3-formylrifamycin and in the presence of isoniazid the degradation increased to 21.5% and also indicated that the degradation of rifampicin to 3-formylrifamycin is almost more than two times faster in the presence of isoniazid than that of rifampicin alone.¹³

Bioavailability of rifampicin is significantly impaired when it is administered along with isoniazid as a fixed dose combination, in comparison with administration of formulation containing only rifampicin. This lends confirmation to earlier in-vitro studies indicating isoniazid accelerates degradation of rifampicin into its insoluble,poorly absorbed derivative in acidic environment of stomach. There exists a qualitative correlation between acceleration of in-vitro

degradation of rifampicin in presence of isoniazid in acidic medium and decrease in the in-vivo bioavailability of rifampicin when administered as combination formulation with isoniazid.

It has been reported that reduced bioavailability of rifampicin from rifampicin-isoniazid fixed dose combination formulations may be one of the factors responsible for development of resistance to rifampicin. Thus, there is a need to develop stable formulations containing rifampicin-isoniazid combination to withstand the acidic environment of stomach.

Among the various polymers used in drug delivery research, PLGA (poly-D,L-lactide-co-glycolide) is one of the most successfully used biodegradable nanosystem for the development of nanomedicines since it undergoes hydrolysis in the body to produce the biodegradable metabolite monomers, lactic acid and glycolic acid. Since the body can effectively deal with these two monomers, there is very minimal systemic toxicity associated with this polymer.

Drugs do not deliver themselves. For a molecule to reach the target site from the site of administration in sufficient concentration, and to maintain therapeutic levels for a sufficient period of time, a delivery system is needed. The delivery system is as important as the therapeutic moiety itself. Controlled and novel drug delivery, which was only a dream or at best a possibility, is now a reality. During last decade and half, pharmaceutical and other scientists have carried out extensive and intensive investigation in the field of drug research. Among those, nanoparticulate drug delivery systems from biodegradable and biocompatible polymer are interesting options for controlled drug delivery and drug targeting. Poly (lactide-co-glycolide) has gained attention for preparation of wide variety of delivery systems containing several drugs due to their biodegradable and biocompatible properties and low toxicity. Because of their biodegradability and biocompatibility, Polylactic acid and its copolymers with glycolic acid (PLGA) are widely employed for the preparation of sustained release preparations³ and PLGA microparticles have successfully been employed as Antitubercular drug (ATD) carrier⁴⁻⁷. With injectable PLGA microparticle a sustained drug release has been observed for 6-7 weeks in mice⁴⁻⁵. The formulation was subsequently explored as an ATD-carrier in order to avoid the discomfort associated with subcutaneous injection. However, oral PLGA microparticle suffered from several drawbacks such as low drug encapsulation, high polymer composition, sustained drug release for 3-4 days⁶ and a partial therapeutic benefit. It is possible to circumvent these drawbacks by developing PLGA nanoparticles (PLGA-NP) encapsulated three front line antitubercular drugs, i.e. rifampicin (RIF), isoniazid (INH) and pyrazinamide (PZA) which

resulted in a reduced dosing frequency in a murine TB model. The administration routes of PLGA nano / micro particle may vary from parenteral, oral, dermatological, pulmonary and nasal to ocular. Recently, diclofenac sodium-loaded PLGA nanoparticles were developed for ocular use and found good biocompatibility with eye. Sparfloxacin loaded PLGA (50:50) nanoparticles were also studied extensively in various pharmacological aspects for their application in treatment of conjunctivitis and proved to have good stability and ocular tolerance. Tuberculosis (TB), a ubiquitous, high contagious chronic granulomatous bacterial infection caused by the *Mycobacterium tuberculosis* that infects over 8 million people worldwide and is responsible for 2 million deaths annually. Although an effective therapeutic regimen is available, patient noncompliance (because of the need to take antitubercular drugs (ATDs) daily or several times a week) results in treatment failure as well as the emergence of drug resistance. The study also reveals that fabrication of a polymeric once-daily oral multiparticulate fixed dose combination of the principal antitubercular drugs, which attains segregated delivery of rifampicin and isoniazid for improved rifampicin bioavailability, could be a step in the right direction in addressing issues of treatment failure due to patient noncompliance.

Patient compliance can be improved by the use of ATD formulations, which reduce the dosing frequency of the drugs. Thus the purpose of the present study was to prepare Rifampicin loaded PLGA nanoparticles for improving bioavailability of rifampicin PLGA nanoparticles from fixed dose combination with isoniazid, pyrazinamide and ethambutol.¹⁴

2. REVIEW OF LITERATURE

2.1. Epidemiology of TB

TB is an infection caused by *M. Tuberculosis*. The highest prevalence of tuberculosis infection and estimated annual risk of tuberculosis infection are in sub-Saharan Africa and Southeast Asia.¹⁵ *Mycobacterium africanum* consists of two phylogenetically distinct lineages within the Mycobacterium tuberculosis complex, known as M. africanum West African 1 and M. africanum West African 2. These lineages are restricted to West Africa, where they cause up to half of human pulmonary tuberculosis.¹⁶

The incidence of tuberculosis is stable and HIV-1 absent, a control programme reaches the WHO targets of 70% case detection and 85% cure would reduce the incidence rate by 11% (range 8-12) per year and the death rate by 12% (9-13) per year. Without greater effort to control tuberculosis, the annual incidence of the disease is expected to increase by 41% (21-61) between 1998 and 2020 (from 7.4 million to 10.6 million cases per year). Achievement of WHO targets by 2010 would prevent 23% (15-30) or 48 million cases by 2020.¹⁷

India is classified along with the sub-Saharan African countries to be among those with a high burden and the least prospects of a favourable time trend of the disease as of now (Group IV countries). The average prevalence of all forms of tuberculosis in India is estimated to be 5.05 per thousand, prevalence of smear-positive cases 2.27 per thousand and average annual incidence of smear-positive cases at 84 per 1,00,000 annually.¹⁸

The human immunodeficiency virus (HIV) epidemic is causing increases in the number of tuberculosis cases, particularly in Africa, although increases are also expected in Southeast Asia. In many industrialized countries, TB has recently failed to decline, and in eastern Europe and the former Soviet Union, cases and deaths are increasing. Drug resistance is a serious problem, especially in the United States.¹ TB remains a major cause of morbidity and mortality worldwide in the 21st Century. The WHO and other organizations have put vast resources into studying the disease, as well as implementing and monitoring treatment. There are large disparities between the rates of TB in children in resource poor countries and those in industrialised countries. Factors such as poverty, overcrowding and HIV infection have contributed greatly to the resurgence of childhood TB, particularly in Sub-Saharan Africa. The mortality rates from TB in children from resource-poor counties are unacceptably high. While

there are many challenges in the diagnosis and treatment of TB in children, perhaps the greatest challenge globally is to begin to identify the extent of disease in this forgotten group.¹⁹

TB remains prominent in international statistics of ill health mainly because it kills young adults. More than 80% of the burden of tuberculosis, as measured in terms of disability-adjusted life years (DALYs) lost, is due to premature death rather than illness. About 1.7 million people died of tuberculosis in 2004, including 264 000 patients who were co infected with HIV.²⁰

Effective control of tuberculosis (TB) requires an understanding of the changing epidemiology of the disease. The success in reducing the tuberculosis burden reflects several factors, including improved public health efforts, physician and patient education, infection control measures, and the use of directly observed therapy (DOT). Future efforts to curtail the incidence of TB will require vigilant public health efforts, improving education of patients and health care personnel, identifying mechanisms and routes of transmission, and assuring adequate treatment and prophylactic regimens among infected individuals.²¹

2.2. Drug therapy in TB

TB therapy is a multi-drug regimen given over a long period of time. Single agent TB therapy rapidly gives rise to drug-resistant organisms. Multi-drug treatment needs to be prolonged because mycobacterium tuberculosis it divides slowly and becoming drug insensitive. The advent of rifampicin and pyrazinamide allowed highly effective ‘short course’ TB Regimes usually a two-month intensive phase with rifampicin (R), isoniazid (H), pyrazinamide (Z) and ethambutol (E), followed by a four month continuation phase with RH (2RHZE/4RH).²²

INH and RIF, the two most potent anti-TB drugs, kill more than 99% of tubercular bacilli within 2 months of initiation of therapy. Using these drugs in conjunction with each other reduces anti-TB therapy from 18 months to 6 months.^{23,24}

INH eradicates most of the rapidly replicating bacilli in the first 2 weeks of treatment, together with streptomycin and ETB. Thereafter, RIF and PYZ have an important role in the sterilization of lesions by eradicating organisms; these two drugs are crucial for successful 6-month treatment regimens. RIF kills low or non-replicating organisms and the high sterilizing effect of PYZ serves to act on semi dormant bacilli not affected by any other anti-TB agent in sites hostile to the penetration and action of the other drugs.^{25,26}

2.3. TB drugs in development:

Pyrrole LL3858: Limited data are available regarding pyrrole LL3858. It is currently undergoing phase 1 clinical trials by Lupin Limited (India). Available data suggest that LL3858 has potency against standard and drug-sensitive TB strains in vitro.²⁷

Gatifloxacin: Gatifloxacin is a fluoroquinolone that inhibits DNA gyrase, thus inhibiting TB DNA replication and transcription. Gatifloxacin is currently undergoing phase 3 clinical trials. Gatifloxacin holds the potential to be the first TB agent to reduce pulmonary TB therapy to four-month duration. There are weak data to support its efficacy against MDR-TB.²⁸

R207910: R207910 is a diarylquinoline and is also known as Compound J and TMC207. It inhibits ATP synthase leading to ATP depletion and pH imbalance. Where it is undergoing phase 2a clinical trials in both drug sensitive and resistant disease. Murine studies suggest that R207910 has a good safety and tolerability profile and potent early bactericidal activity, matching isoniazid. It had a synergistic effect with pyrazinamide for MDR-TB; R207910/H/Z or R207910/R/Z combinations were more effective than amikacin/Z/moxifloxacin/ethionamide regimens.²⁹

OPC-67683: OPC-67683 is a nitroimidazo-oxazole that is similar in structure to PA-824. It inhibits cell wall biosynthesis. Otsuka Pharmaceuticals (Japan) are currently conducting phase 2 clinical trials. Preclinical studies in rodents and dogs suggest that OPC-67683 could be used in HIV/AIDS as it has no effect on CYP. It may have treatment-shortening potential as it synergises in vitro with rifampicin and pyrazinamide. OPC-67683 is effective against MDR-TB in vitro and displayed no cross-resistance to first line TB therapy. It also has potential to treat LTBI.³⁰

PA-824: PA-824 is a nitroimidazo-oxazine. It requires activation by M. tuberculosis F420 factor and inhibits synthesis of cell wall lipids as well as protein synthesis. The TB alliance is currently conducting phase 1 clinical trials of PA-824. Preliminary studies suggest that PA-824 will be active against MDR-TB and has no cross-resistance with other anti-tubercular drugs. Importantly, it is not metabolised by CYP and does not induce or inhibit CYP. It had similar bacteriostatic efficacy to rifampicin and was more efficient than isoniazid or moxifloxacin but less efficient than rifampicin.³¹

Moxifloxacin: Moxifloxacin is a fluoroquinolone and has a similar mechanism of action to gatifloxacin. It is undergoing phase 2 and 3 clinical trials. Moxifloxacin kills rifampicin-tolerant persisters in vitro, and it may help treat MDRTB if co-administered with ethionamide. It may thus shorten duration of TB therapy.³²

SQ-109: SQ-109 is an ethylenediamine and is derived from ethambutol. It is postulated to inhibit cell wall biosynthesis and has intracellular targets, which have not yet been elucidated. SQ-109 appears to be synergistic with isoniazid and rifampicin.³³

2.4. Rifampicin bioavailability

Rifampicin After oral administration on an empty stomach, the absorption of rifampicin (rifampin) is rapid and practically complete. With a single 600mg dose it undergoes first passage through the hepatoportal system, peak serum concentration of the order of 10microgram/ml generally occurs 2 hours after administration. The half-life of rifampicin for this dose level is of the order of 2.5 hours. On repeated administration, and most likely as a consequence of self-induced (autoinduction). Approximately 80% of rifampicin is transported in blood bound to plasma proteins, mainly albumin. Deacetyl rifampicin, the more polar metabolic derivative of rifampicin, behaves in the opposite way since its rate of transfer into bile is 4 times higher than that into urine. The rate of biotransformation of rifampicin into desacetyl rifampicin is of the same order of magnitude as that of biotransformation of the latter into a further metabolic derivative, which could be a glucuronide conjugate.³⁴

The absolute bioavailability of oral rifampin was determined in 20 pediatric patients. Intravenous doses of rifampin (mean 287 mg/m^2) were compared with P.O. doses (mean 324 mg/m^2). Pharmacokinetic analysis of the rifampin serum concentration data indicated that only 50 +/- 22% of a freshly prepared p.o. suspension were absorbed. The rifampicin elimination half-life following i.v. administration (2.25 +/- 0.64 h) was not different from that observed following p.o. dose administration (2.61 +/- 1.35 h). Peak rifampin concentrations were significantly higher following i.v. administration when corrected to a 300 mg/m^2 dose (27.4 vs. 9.1 [μ g/ml, respectively, $P < 0.0001$) than after P.o administration. The peak concentration following a p.o. dose occurred at 2.0 +/- 0.9 h. The ratios of desacetyl rifampicin to rifampin areas under the curves were similar for i.v. and p.o. routes of administration (0.23 vs. 0.19), suggesting linear

metabolism of rifampin to this metabolite. 3-formylrifamycin SV concentrations were lower than those of desacetyl rifampicin and were detectable in less than half of the patients.³⁵

The problem with rifampicin is its poor/variable bioavailability of rifampicin in anti-tubercular fixed-dose combination (FDC) products. They determined that rifampicin decomposition is enhanced by the presence of isoniazid in stomach after ingestion. 80–90% of rifampicin was dissolved in 0.1 M HCl within 10 min, and all samples showed an overlapping dissolution profile.³⁶

comparative bioavailability of rifampicin (RIF) after administration of a single component RIF (450 mg) capsule and rifampicin-isoniazid (RIF-INH) (450+300 mg) fixed dose combination (FDC) capsule formulations. Six healthy male volunteers participated in a single dose, two treatment, two period, cross-over study. A sensitive, specific and accurate HPTLC method was developed, validated and employed for estimation of RIF and its major active metabolite, 25-Desacetyl rifampicin (25-DAR) levels, in urine. Using the urinary excretion data various pharmacokinetic parameters: AUC_{0-24} , $AUC_{0-\infty}$ cumulative amount excreted in 24 h, peak excretion rate, etc. for both RIF and 25-DAR were calculated and compared statistically (ANOVA, 90% confidence interval for ratio). Significant decrease in the bioavailability of RIF from FDC capsules was observed. The present bioavailability study confirms our serious doubts about the stability of RIF in presence of INH in acidic environment of stomach, which probably is the main factor responsible for the reduced bioavailability of RIF from RIF-INH combination formulations. This study underlines the fact that there is an urgent need to reconsider the formulation of the FDC product in order to minimize or avoid the decomposition of RIF in gastrointestinal tract.³⁷

The problem of poor/variable bioavailability of rifampicin, which is shown in particular when the drugs are present in anti-tubercular fixed-dose combination (FDC) products. There is a potential of failure of therapy in patients. Some simple solutions offered by the knowledge of the cause were discussed and concluded that there is a need to have a multifaceted approach to handle the problem.³⁸

2.5. Degradation of rifampicin

Degradation of rifampicin in 0.1N HCl, and simulated gastric fluid (SGF) at 37°C in 45 min (USP dissolution test conditions) in the absence and presence of isoniazid has been documented. Rifampicin alone decomposes in the described conditions to an average extent of 6.33%, while the loss of rifampicin in the presence of isoniazid increases on an average to 16.32%.^{39,40}

The extent of decomposition of rifampicin in the presence of isoniazid in pH range of 1-3 at 37° C in 50 min, the mean stomach residence time. Its showed that rifampicin degraded in the presence of isoniazid to a higher extent at pH 2, the maximum pH in the fasting condition, under which antituberculosis fixed dose combination (FDC) products are administered. The extent of decomposition was also determined in marketed products, and the value range from 13-35% for rifampicin. This emphasizes that antituberculosis FDC formulations, which contain both drugs, should be designed in a manner that the interaction of the two drugs is prevented when the formulation are administered on an empty stomach.⁴⁰

Rifampicin is well absorbed from the stomach due to its solubility, which is maximum between pH 1-2. Isoniazid is poorly absorbed from the stomach, but is well absorbed from all three segments of the intestine. In combination, rifampicin disappearance was enhanced in the presence of isoniazid in the stomach and jejunum, but isoniazid disappearance was not influenced by rifampicin. The study shows higher in situ rifampicin disappearance in the presence of isoniazid, attributable to drug degradation due to catalysis by isoniazid. As the two drugs show regional specific permeability, FDCs without reduced rifampicin bioavailability resulting from its decomposition in the presence of isoniazid can be designed by segregating delivery of the two drugs by around 3-4 h. Rifampicin should be released in the stomach and isoniazid in the intestine.⁴¹

Rifampicin is better absorbed through the stomach and duodenum than through the distal regions of the intestine. Rifampicin alone exhibited decomposition of ~4% at pH 2, whereas it was negligible at pH 5.5 and 7. Rifampicin showed similar decomposition pattern even in the presence of Nucleotide/Nucleoside Reverse Transcriptase Inhibitors (NRTIs).⁴²

2.6. Nanoparticles as drug delivery systems

Over the last few decades, the applications of nanotechnology in medicine have been extensively explored in many medical areas, especially in drug delivery. Nanotechnology concerns the understanding and control of matters in the 1- 100 nm range, at which scale materials have unique physicochemical properties including ultra small size, large surface to mass ratio, high reactivity and unique interactions with biological systems. By loading drugs into nanoparticles through physical encapsulation, adsorption, or chemical conjugation, the pharmacokinetics and therapeutic index of the drugs can be significantly improved in contrast to the free drug counterparts.

Many advantages of nanoparticle-based drug delivery have been recognized, including improved serum solubility of the drugs, prolonging the systemic circulation lifetime, releasing drugs at a sustained and controlled manner, preferentially delivering drugs to the tissues and cells of interest, and concurrently delivering multiple therapeutic agents to the same cells for combination therapy. Moreover, drug-loaded nanoparticles can enter host cells through endocytosis and then release drug payloads to treat microbes-induced intracellular infections. As a result, a number of nanoparticle-based drug delivery systems have been approved for clinical uses to treat a variety of diseases and many other therapeutic nanoparticle formulations are currently under various stages of clinical tests.

Mechanisms of Nanoparticle - Based Antimicrobial Drug Delivery to Microorganisms

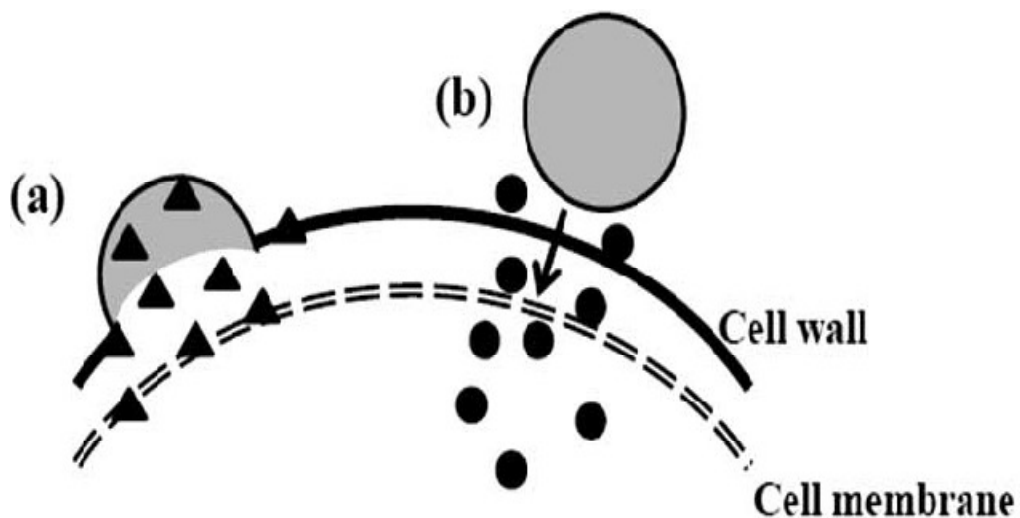


Fig. (a) nanoparticles fuse with microbial cell wall or membrane and release the carried drugs within the cell wall or membrane; **(b)** nanoparticles bind to cell wall and serve as a drug depot to continuously release drug molecules, which will diffuse into the interior of the microorganisms.⁴⁵

These nanocarriers are sub micron particles containing entrapped drugs intended for enteral or parenteral administration which might prevent or minimize the drug degradation and metabolism as well as cellular efflux. Nanoparticles also have a long shelf life, are made of safe materials, including synthetic biodegradable polymers, natural biopolymers, lipids and polysaccharides and have the potential for overcoming important mucosal barriers, such as intestinal, nasal and ocular barriers.⁴³

2.7. Polymers as drug delivery vehicle

A number of polymers have been investigated for formulating biodegradable nanoparticles, such as polylactide (PLA), polycaprolactone(PCL) and poly(lactide-co-glycolide) (PLGA). These are biocompatible and biodegradable polymers which have recently been the subject of extensive investigation. However, due to copolymer crystallization, low biodegradation rate or poor flexibility, the application of polymer nanoparticles is limited. For example, in case of homopolymer poly(L-lactide), due to its crystalline and low biodegradation rate, drug release from relevant drug delivery devices is mainly controlled by drug diffusion similar to that in non-degradable drug carriers. Biodegradation of polymeric biomaterials involves cleavage of hydrolytically or enzymatically sensitive bonds in a polymer, leading to polymer erosion. Depending on the mode of degradation, polymeric biomaterials can be further classified into hydrolytically degradable polymers and enzymatically degradable polymers. The most part of naturally occurring polymers undergo enzymatic degradation. Biodegradation of hydrolysable polymers proceeds in a diffuse manner, with amorphous regions degrading prior to the complete split of crystalline and cross-linked regions. Factors affecting biodegradation of polymers might be: chemical structure, chemical composition, distribution of repeat units in multimers, presence of ionic groups, presence of unexpected units or chain defects, Configuration structure, molecular weight, molecular weight distribution, morphology (amorphous/semicrystalline, microstructures, residual stresses), presence of low molecular-weight compounds, processing conditions ,annealing, sterilization process, storage history, shape, site of implantation, adsorbed and absorbed compounds (water, lipids, ions, etc.),

physicochemical factors (ion exchange, ionic strength pH), physical factors (shape and size changes, variations of diffusion coefficients, mechanical stresses, stress-and solvent-induced cracking, etc.), mechanism of hydrolysis (enzymes versus water).

Structure, properties and applications of nanoparticles are strongly affected by the properties of the polymer used in their formulation. For each application, one must evaluate the properties of the system (drug and particle) and determine the optimal formulation for a given drug delivery application. Polyesters based on polylactide (PLA), polyglycolide (PGA), polycaprolactone (PCL), and their copolymers have been extensively employed as systems for drug delivery. PLGA and PLA have been approved by the FDA for numerous clinical applications, such as sutures, bone plates, abdominal mesh, and extended-release pharmaceuticals.

Biomedical uses of PLA have been reported since the 1960s. Tissue response to such biodegradable materials is characterized by minimal localized inflammation and foreign body reaction that lessen with time. No toxic effects have been associated with the use of such polymers, biodegraded via a random, non-enzymatic process into homopolymers of lactic acid and glycolic acid, known products of cellular intermediary metabolism. PLGA degrades through hydrolysis of its ester linkages in the presence of water. It has been shown that the time required for the degradation of PLGA is related to the ratio of monomers used in its production: the higher the content of glycolide units, the lower the time required for degradation. An exception to this rule is copolymer with 50:50 ratios of monomers, which undergoes faster degradation (about two months) in both *in vitro* and *in vivo conditions*. Miller *et al.* have shown that PLGA 50:50 is the fastest degrading composition, with the degradation rate being decreased when either lactide or glycolide content of the copolymer was increased.⁴⁴

2.8. Pharmaceutical approaches for the treatment of TB

Chemotherapy of TB is complicated by the need of multidrug regimens that need to be administered over long periods. Poor patient compliance is the single most common reason for chemotherapy failure in TB.⁴⁶ To minimize toxicity and improve patient's compliance, extensive progressive efforts have been made to develop various implant, micro particulate, and various other carrier-based drug delivery systems to either target the site of *M. tuberculosis* infection or reduce the dosing frequency, which forms an important therapeutic strategy to improve patient outcomes.^{47,48} The systems under discussion employ either biodegradable polymers or systems

requiring removal after use, and can release the drug either by membrane or matrix-controlled diffusion.

Recent trends in controlled drug delivery have seen micro encapsulation of pharmaceutical substances in biodegradable polymers as an emerging technology. Carrier or delivery systems such as liposomes and microspheres have been developed for the sustained delivery of anti-TB drugs and have demonstrated better chemotherapeutic efficacy when investigated in animal models (e.g. mice)². Anti-TB drugs have been successfully entrapped and delivered in biodegradable polymers such as poly (DL-lactide-co-glycoside) (PLG), which are biocompatible and release drug in a controlled manner at therapeutic levels.⁴⁸

Dutt and Khuller (2001)⁴⁹ have entrapped INH and RIF in PLG polymers. When injected subcutaneously as a single dose, the micro particles, having a diameter ranging from 11.75 μm to 71.95 μm , provided sustained release of drugs over 6–7 weeks when tested in mice. The authors previously observed that particles with a size range $>10\text{ }\mu\text{m}$ remained at the site of injection forming a depot. The entrapped contents of the micro particles were gradually released by diffusion through the polymeric particles. Such depots can show release profiles extending over several months culminating in degradation of the entire polymeric device. However, these formulations have to be injected either subcutaneously or intravenously, and the pain and discomfort associated with these routes of administration, in general, is often not acceptable. Hence, there is a continuous need to develop an oral drug delivery system that is convenient for patients.⁴⁹

Amidst these concerns, Ain *et al* (2002)⁵⁰ reported the pharmacokinetics of PLG encapsulated anti-TB drugs; orally administered either individually or in combination in mice. A study conducted by Pandey *et al* (2003)⁵¹ reported the formulation of three frontline anti-TB drugs, i.e. RIF, INH and PYZ encapsulated in PLG nanoparticles. On oral administration of drug-loaded nanoparticles to *M. tuberculosis*-infected mice at every 10th day, no tubercle bacilli could be detected in the tissues after 5 oral doses of treatment. Therefore, oral nanoparticle-based anti-TB drug therapy can allow for a reduction in dosing frequency for better management of TB.

Osmotically regulated capsular multi-drug oral delivery system comprising asymmetric membrane coating- and dense semi permeable membrane coating-capsular systems for the simultaneous controlled administration of RIF and INH for the treatment of TB. This was in an

attempt to reduce the problems associated with multidrug therapy. The modified asymmetric system provided satisfactory sustained release of RIF and INH, with an initial burst release that may be sufficient to achieve minimum effective concentration in blood. Thereafter, the system provided the release of the drugs in a near zero order rate – an ideal release profile for controlled drug delivery. In turn, this would improve the safety profile of the drugs and enhance the activity duration of drug exhibiting short half-lives. The once daily system is optimal, and could potentially enhance patient compliance.⁴⁶

Further attempts to solve the problems inherent in multidrug therapy have included the development of biodegradable polymeric micro- or nanoparticulate carrier systems to target alveolar macrophages that harbour *M.tuberculosis*. In the case of pulmonary TB, delivering the drug directly to the site of infection through inhalation of an aerosolised delivery system has the inherent advantages of bypassing first-pass metabolism and maintaining local therapeutically effective concentrations with decreased systemic side effects.⁵² Because *M. tuberculosis* is known to infect alveolar macrophages and affect the pathogenesis of TB, there have been renewed interests in targeting of anti-TB drugs to these cells. Despite the success of these systems in targeting and providing sustained release of anti-TB drugs to alveolar macrophages, the methods used to generate particles in these studies vary in their capability for the production of reproducible particles with the optimal size for inhalation therapy (i.e. <5µm).

Barrow et al (1998)⁵³ formulated RIF-loaded microspheres using the method of solvent evaporation, aiming to maintain a size of 1 to 10-µm. Only the size distributions of two formulations were reported, being 3 to 4 µm and distribution demonstrated a Gaussian curve.

Dutt and Khuller (2001)⁴⁹ encapsulated INH and RIF into hardened PLG micro particles by a double emulsification solvent evaporation procedure, and these had a resultant volume mean diameter of 11.75 µm for INH microparticles and 11.64 µm for RIF microparticles. These are currently undergoing Phase I trials. Sharma et al (2001)⁵⁴ incorporated both INH and RIF into PLG microspheres using a combination of solvent extraction and evaporation, but these particles had a mean diameter of 6.214 µm and only 38% of the microspheres fell in the size range of 0.5–3 µm. Suarez et al (2001)⁵⁵ attained the airway delivery of RIF microparticle shaving volume median diameters of $2.76 \pm 1.57\mu\text{m}$. O'Hara and Hickey⁵⁶ succeeded in obtaining RIF loaded PLG particles with median diameters by volume of 2.76 µm and 3.45 µm by spray drying and solvent evaporation respectively. Zhou et al (2005)⁵¹ did achieve the formulation of spherical

micro particles between 1 and 3 μm in diameter. The microparticles, prepared by the precipitation with a compressed anti solvent process, were evaluated for their potential in targeting an ionizable prodrug of INH, isoniazid methane sulfonate (INHMS), for sustained delivery of INH to alveolar macrophages.

Most recently Zahoor et al (2006)⁵⁷ undertook pharmacokinetic and chemotherapeutic studies with aerosolized alginate nanoparticles encapsulating INH, RIF and PZA and RIF, INH, PYZ, ETB. The nanoparticles were prepared by cation-induced gelification of alginate and were 235.5 ± 0 nm in size, with drug encapsulation efficiencies of 70–90% for INH and PZA and 80–90% for RIF and 88–95% for EMB. The majority of particles (80.5%) were in the respirable range, with a mass median aerodynamic diameter of 1.1 ± 0.4 μm and geometric standard deviation of 1.71 ± 0.1 μm . The chemotherapeutic efficacy of three doses of drug-loaded alginate nanoparticles nebulised 15 days apart was comparable with 45 daily doses of oral free drugs. Thus, inhalable alginate nanoparticles could potentially serve as an ideal carrier for the controlled release of anti-TB drugs. Clinical trials are envisaged in the future for evaluation of this system before use in humans.

Pandey and Khuller⁵⁸ evaluated the chemotherapeutic potential of nebulised solid lipid nanoparticles (SLNs) incorporating RIF, INH and PYZ against experimental TB. SLNs are nanocrystalline suspensions in water, prepared from lipids, which are solid at room temperature. The SLNs, prepared by the emulsion solvent diffusion technique, possessed a favourable mass median aerodynamic diameter suitable for broncho alveolar drug delivery. Following a single nebulisation to guinea pigs, therapeutic drug concentrations were maintained in the plasma for 5 days and in the organs for 7 days whereas free drugs were cleared after 1–2 days.

Vyas⁵⁹ formulated aerosolized liposomes incorporating RIF via a cast-film method employing egg phosphatidylcholine- and cholesterol based liposomes. Liposomes coated with alveolar macrophage-specific ligands demonstrated preferential accumulation in alveolar macrophages, maintaining high concentrations of RIF in the lungs even after 24 hours.

In another approach to solve the predicament of poor patient compliance, depot-delivery of anti-TB drugs has been investigated. Studies have demonstrated that a single implant of INH in polylactic-co-glycolic acid (PLGA) copolymer could ensure sustained levels of free INH for a period of up to 8 weeks following implantation in rabbits⁴⁸.

2.9. Background of the study

The literature survey thus reveals the importance of fixed dose combination of Rifampicin, Isoniazid, Pyrazinamide and Ethambutol in the treatment of TB to overcome the drug resistance and to improve the patient compliances. Rifampicin appears to be the best choice for the treatment of TB however it has poor bioavailability from FDC formulation following oral administration due to degradation in the stomach. Rifampicin is well absorbed in the pH range 1-2 even though it undergoes degradation in the acidic medium and the degradation of rifampicin increases in the presence of Isoniazid, Pyrazinamide, Ethambutol and thus affects bioavailability of Rifampicin. Development of any method that can stabilize Rifampicin against degradation in the stomach will be therapeutically beneficial.

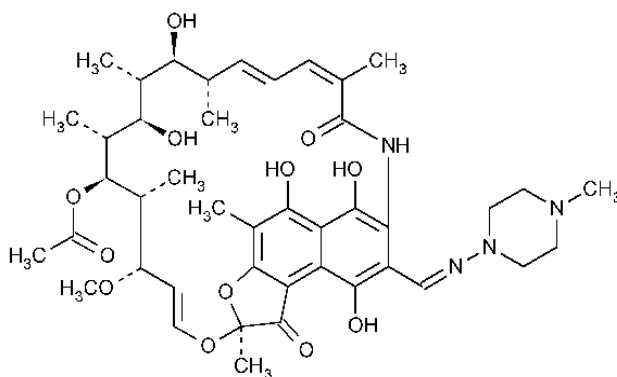
Since nanoparticles are known to cross the intestinal permeability barriers directly via transcellular/ paracellular pathways. It offers better delivery of the encapsulated drug into the circulation. In this case they are expected to penetrate inside the infected cell, Where TB is an intracellular infection. From the literature study it was found that PLGA is one of the most successfully used biodegradable nanosystem for the development of nanomedicine since it undergoes hydrolysis in the body to produce the biodegradable metabolite monomers lactic acid and glycolic acid. Based on this consideration the present study attempted to improve the bioavailability of rifampicin –PLGA nanoparticles from fixed dose combination with isoniazid, pyrazinamide and ethambutol.

3. DRUG PROFILE

3.1. Rifampicin:

Rifampicin is a bactericidal antibiotic drug of the rifamycin group. It is a semisynthetic compound derived from *Amycolatopsis rifamycinica* (formerly known as *Amycolatopsis mediterranei* and *Streptomyces mediterranei*).

Structure



Rifampicin

Empirical formula : C₄₃H₅₈N₄O₁₂

Molecular weight : 822.94.

Chemical name : 3-[[[(4-methyl-1-piperazinyl)imino]methyl]-5,6,9,17,19,21-Hexahydroxy-23-methoxy-2,4,12,16,18,20,22-heptamethyl-8-[N-(4-methyl-1-piperazinyl)formimidoyl]-2,7(epoxypentadeca[1,11,13]trienimino)naphtho[2,1-b]furan-1,11-(2H)-dione 21-acetate [13292-46-1].

Physical and Chemical Properties

Appearance : orange-red powder

Melting point : 183-188°C

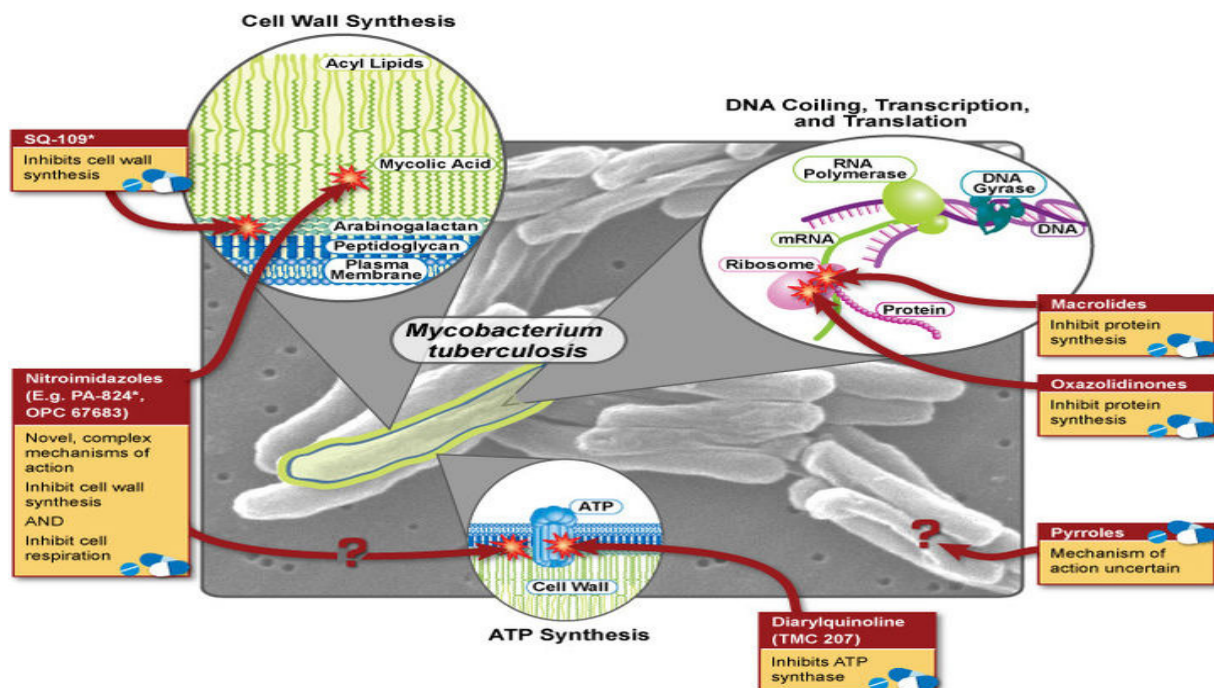
Solubility : Soluble in dilute acid solutions, slightly soluble in water.

Rifampicin: Mechanism of Action and Resistance⁶⁰

Rifampicin specifically inhibits bacterial RNA polymerase, the enzyme responsible for DNA transcription, by forming a stable drug-enzyme complex with a binding constant of 10^{-9} M

at 37°C. Various steps involved in transcription of bacteria is inhibited when rifampicin interferes with RNA polymerase. The various steps in the process of transcription of DNA to RNA are (1) binding of the enzyme to DNA; (2) binding of the first nucleoside tri-phosphate to the enzyme-DNA complex; (3) formation of the first phosphodiester bond, leading to a dinucleotide (chain initiation); (4) assembly of more nucleotides to form a polyribonucleotide (chain elongation); and (5) release of the completed RNA chain from the template (chain termination). More specifically, the β subunit of this complex enzyme is the site of action of drug. The corresponding mammalian enzymes are not affected by rifampicin.

Bacterial resistance to rifampicin is caused by mutations leading to a change in the structure of the β subunit of RNA polymerase. Such resistance is not an all-or nothing phenomenon; rather, a large number of RNA polymerases with various degrees of sensitivity to rifampicin have been found. No strict correlation exists between enzyme sensitivity and MIC values, since inhibition of RNA synthesis does not always show up to the same extent in the two different test systems used for the determination of these values.



Mechanism of action of rifampicin on mycobacterium tuberculosis

Formulations of rifampicin in market

Monocomponent products

Rifampicin capsules of 150 mg, 300 mg, 450 mg, 600 mg

Combination Products

Dipicin : Isoniazid 150 mg, Rifampicin 300 mg

Pyrina : Isoniazid 150 mg, Rifampicin 150 mg,
Pyrazinamide 500 mg

Rambuto: Isoniazid 200 mg, EthambutolHCl 400 mg,
Rifampicin 300 mg, Pyridoxine 25 mg

Rimactazid: Isoniazid 100 mg Rifampicin 150
Isoniazid 200 mg Rifampicin 225
Isoniazid 150 mg Rifampicin 300

Routes of entry

Oral	: This is the common route of entry.
Inhalation	: Not applicable.
Dermal	: Not applicable
Eye	: Use for ocular Chlamydia infection treatment
Parenteral	: Rifampicin may be given intravenously.

Pharmacokinetics

Absorption: Rifampicin is readily absorbed from the gastrointestinal tract (90%). Peak plasma concentration occurs at 1.5 to 4 hours after an oral dose. After a 450 mg oral dose, plasma levels reach 6 to 9 µg/ml while a 600 mg dose on an empty stomach yields 4 to 32 µg/ml (mean 7 µg/ml).

Distribution: It is widely distributed in body tissues and fluids. 89% of rifampicin in circulation is bound to plasma proteins.⁶¹ It is lipid soluble. When the meninges are inflamed, rifampicin enters the cerebrospinal fluid (4.0 µg/ml after a 600 mg oral dose). It reaches therapeutic levels in the lungs, bronchial secretions, pleural fluid, other cavity fluid, liver, bile, and urine.⁶² Rifampicin has a high degree of placental transfer with a foetal to maternal serum level ratio of

0.3. It is distributed into breastmilk.⁶³The apparent volume of distribution (VD) is 0.93 to 1.6 L/kg.⁶⁴

Biological half-life by route of exposure: T_{1/2} = three hours range (2 to 5 hours).

Metabolism: Approximately 85% of rifampicin is metabolized by the liver microsomal enzymes to its main and active metabolite - deacetyl rifampicin. Rifampicin undergoes enterohepatic recirculation but not the deacetylated form. Rifampicin increases its own rate of metabolism. Rifampicin may also be inactivated in other parts of the body. Formylrifampicin is a urinary metabolite that spontaneously forms in the urine.

Elimination by route of exposure: Rifampicin metabolite deacetyl rifampicin is excreted in the bile and also in the urine. Approximately 50% of the rifampicin dose is eliminated within 24 hours and 6 to 30% of the drug is excreted unchanged in the urine, while 15% is excreted as active metabolite. Approximately 43 to 60% of oral dose is excreted in the faeces.⁶²Intrinsic total body clearance is 3.5 (+/- 1.6) ml/min/kg, reduced in kidney failure.⁶¹ Renal clearance is 8.7 ml/min/kg. Rifampicin is excreted in breast milk (1 to 3 µg/ml).

Interactions

1. Food lowers peak blood levels because of interference with absorption of rifampicin.
2. Antacids containing aluminium hydroxide reduced the bioavailability of rifampicin.
3. Para-amino salicylic acid granules may delay rifampicin absorption. These two drugs should be given 8 to 12 hours apart.⁶²
4. Isoniazid and rifampicin interaction has led to hepatotoxicity.
5. Alcohol intake with rifampicin increases the risk for hepatotoxicity.
6. Rifampicin induces microsomal enzymes of the liver and therefore accelerates metabolism of some drugs, e.g. beta blockers, oral contraceptive pills etc.,
7. When rifampicin and oral contraceptives are used concomitantly, there is decreased effectiveness of oral contraceptives. It was reported that rifampicin may be the cause of some menstrual disorders when used with oral contraceptive pills.
8. Rifampicin can lower the plasma calciferol (Vitamin D) level because of induction of enzyme activity.

9. Barbiturates and salicylates decrease the activity of rifampicin.
10. Effects with clofazimine range from no effect to decrease in the rate of absorption of rifampicin, delay in the time it reaches peak plasma concentrations decrease in plasma rifampicin concentrations.

Adverse Effects

1. Severe gastrointestinal side-effects (e.g.pseudomembranouscolitis).
2. Hypersensitivity,shock shortness of breath, acute haemolyticaemia, renal failure (nephrotoxicity).
3. The other adverse effects are staining of body fluids, rash, chills and fever, nausea and vomiting, arthralgia, diarrhoea, and peripheral neuritis.
4. Ocular side effects as a consequent to rifampicin use occur in 5 to 15% of patients.
5. Angioneuroticoedema, urticaria, purpura, Stevens-Johnson syndrome, exfoliative dermatitis or pemphigoid lesions have been reported.
6. Local ophthalmic use of rifampicin has caused irritation of the eyes which manifests transiently as lacrimation, hyperaemia, oedema and ocular pain in Special risks

Toxicity

1. Thrombocytopenia
2. Hemolysis
3. Renal failure
4. Flu-like syndrome

3.2. ISONIAZID

Isoniazid was synthesized in 1912 at the German University of Prague by Meyer and Mally⁶⁵

Structure



Isoniazid

Empirical formulae : C₆H₇N

Molecular weight : 137.14

Chemical name : Isonicotinic acid hydrazide

Physical and chemical properties

Appearance : White crystalline powder

Melting point : 170 - 174

Dose : 5mg/kg body weight daily and 10 mg/kg body weight in thrice

Weakly treatment

Solubility : Freely soluble in water and sparingly soluble in alcohol⁶⁶

Mechanism of action

Isoniazid kills actively growing tuberculi bacilli by inhibiting the biosynthesis of mycolic acid which is the major component of cell wall of mycobacterium tuberculosis.⁶⁷ At therapeutic levels isoniazid is bacterial against actively growing intracellular and extracellular mycobacterium tuberculosis.

PHARMACOKINETICS

Absorption

90% of drug gets absorbed upon oral administration and the presence of food reduces the absorption. Time to attain peak plasma concentration is about 1 to 2 hours

Distribution

Isoniazid is widely distributed to all fluids and tissues including cerebrospinal fluid, pleural and ascetic fluids, skin, sputum, muscles and lungs. It crosses the placenta and distributed in to breast and milk. Protein binding is very low about 10%.

Volume of distribution : 0.57 to 0.76 L/kg

Biological Half life: 1-5hours

Metabolism

Metabolism occurs by liver, isoniazid is acetylated by liver in to active metabolites which are excreted in urine. Acetyl isoniazid is further hydrolyzed to isonicotinic acid and acetyl hydrazine. Non acetylated isoniazid is excreted unchanged in urine.

Elimination

5 to 30% of drugs get excreted by renal excretion. Slow acetylators excrete 25% to 66% of dose in urine as isoniazid and rapid acetylators excrete 5 to 37% of dose in urine.

Drug interactions⁶⁸

1. Concomitant use of acetaminophen and isoniazid cause nephrotoxicity
2. Alaprozolam administration with isoniazid cause elevated plasma concentrations of alaprozalam
3. Concomitant isoniazid therapy with BCG vaccine may inhibit efficacy of bcg vaccine
4. Antacids should not be administered with isoniazid
5. Administration of isoniazid with cycloserine cause increased CNS adverse effects

Adverse drug reactions

1. Peripheral neuropathy⁶⁹, seizures
2. Psychosis, optic neuropathy⁷⁰ and metabolic acidosis
3. Hypocalcemia, scaling and eczema
4. Memory loss, gynecomastia and vitamin B6 deficiency

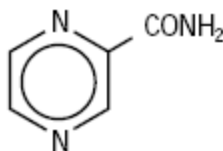
Use : Used in treatment of tuberculosis

Storage: Should protect from moist and light. Stored at 20⁰C to 25⁰C

3.3 PYRAZINAMIDE

The synthesis of pyrazonic acid, the active metabolites of pyrazinamide.

Structure



Pyrazinamide

Empirical formulae : C₅H₅N₃O

Molecular weight : 123.11

Chemical name : Pyrazine-2-carboximide

Physical and chemical properties

Appearance : White crystalline powder

Melting point : 190⁰c

Dose : Orally 15-30mg/kg once daily

Solubility : Sparingly soluble in water

Mechanism of action

Pyrazinamide is a synthetic purine analogue of nicotinamide and exhibits in vitro bactericidal activity only at acidic pH. Pyrazinamide as quite active agonis intracellular bacilli in the acidic environment of macrophages.because of its action agonist intracellular bacilli,heoraganism most likely to responsible relabse,it may play an important role in decreasing releases with tuberculosis lesions,it has been hybthesized that there may four different population of tubercle bacilli. Due to variables in their environment within the body, this four population may different in there metabolism and susceptibility to the antituberculosis drug. This group of organisms belived to be killed readily by isoniazid ,rifampicin,and streptomycin when used in bactericidal doses. The second group of bacilli is thought to have intermittent spurts of metabolic acivity,during which time rifampicin most cabable of killing time. The third group of bacilii is thought to be found in acidic environment such has with in macrophages. Pyarazinamide should be used only in combination with other antitubercular drug in the

treatment M tuberculosis; resistant developed rapidly (within 6 to 8 weeks) when pyrazinamide used alone.

PHARMACOKINETICS

Absorption: When given orally drug is completely absorbed from GIT, absorption is not influenced by food intake. After orally intake of 1500mg of pyrazinamide, peak level is obtained; the time taken to reach peak serum concentration is decreased by antacid concentration.

Distribution: Pyrazinamide has excellent penetration into cerebrospinal fluid ranging from 87 to 105 of corresponding serum concentration. Drug is distributed to all fluids. 31% drug binds to plasma proteins

Volume of distribution : 0.57 to 0.74 L/kg

Biological Half life: 9-10 hours

Metabolism: Pyrazinamide is hydrolysed in liver to its major active metabolites, pyrazonic acid is further hydroxylated to main excretory product 5-hydroxyl pyrazonic acid. Approximately 1% to 14% of drug is excreted as unchanged pyrazinamide.

Elimination: About 1% to 14% of drug is excreted as unchanged pyrazinamide in urine, remaining excreted as metabolites..

Drug interactions

1. Allopurinol increases plasma concentration of pyrazonic acid which is directly responsible for renal urate secretion
2. Pyrazinamide might antagonistically effect the action of medications that have uricosuric effect such as acetylsalicylic acid and probenecid.
3. A potentially serious interaction exists with zidovudine in combination therapy.

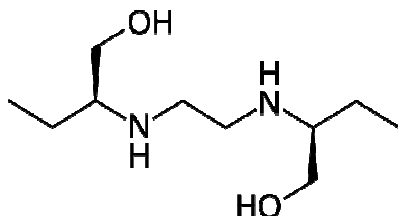
Use: Used in treatment of tuberculosis

Storage: Should be stored in well closed container at controlled room temperature at 15 to 30°C

3.4 ETHAMBUTOL

It is an oral human therapeutic agent specifically active against actively growing microorganisms

Structure



Etambutal

Empirical formula : C₁₀H₂₄N₂O₂

Molecular weight : 277.23

Chemical name : 2, 2(ethylene di amino) di-1- butanoldihydro chloride

Physical and chemical properties

Appearance : White crystalline powder

Melting point : 199⁰c to 204⁰c

Dose : Orally 15mg/kg once daily

Solubility : Sparingly soluble in water and alcohol.

Mechanism of action

Ethambutol diffuses into actively growing mycobacterium tuberculosis such as tubercle bacilli ethambutol. Appears to inhibit the synthesis of 1 or more metabolites, thus causing impairment of cell metabolism, arrest multiplication and causes cell death.

PHARMACOKINETICS

Absorption: Absorption is rapid. Food does not show any effect of absorption, following a dosage of 25mg/kg body weight, a peak serum concentration of 4 to 5 mg/ lit is achieved within 2 to 4 hrs after administration.

Distribution: Ethambutol is distributed to tissues and body fluids except cerebrospinal fluid. About 30% of the drug binds to plasma protein.

Volume of distribution: 1.6 lit/kg

Biological Half life: 3-4 hours

Elimination: Ethambutol gets eliminated by kidneys 50 to 90 % of drug excreted as unchanged form in urine. And 20 to 22 % get excreted in feces. 80% ethambutol is eliminated by glomerular filtration and tubular secretion.

Drug interactions

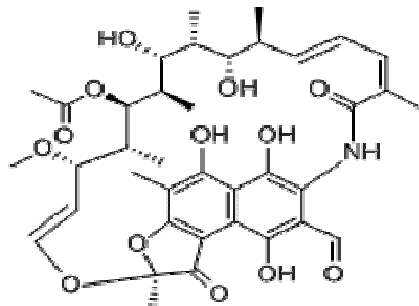
1. Magnesium antacid reduces ethambutolresorptin and lowers and delays repectively Cmax and Tmax.
2. Ethionamide and isoniazid combination increases ethambutolocular toxicity

Use: Used in treatment of tuberculosis

Storage: Should be storedin well closed container at controlled room temperature at 15 to 30⁰c.

3.5 3-Formyl Rifamycin Sv

Structure:



3-formyl rifamycin sv

Empirical formulae : $C_{38}H_{47}NO_{13}$

Molecular weight : 725.78

Chemical name : 3-formyl rifamycin sv

Synonyms: Rifamycin AF;3-formylrifamycin;3-formylrifampicinsv;Rifamycin, 3-formyl-;3-formyl rifamycin sv;11-dioxo-l-21-acetate;3-formylrifamycin sv, bp standard;3-formyl rifamycin sv(rifampicin intermediate)

Physical and chemical properties

Appearance : White crystalline powder

Melting point : 170 - 174

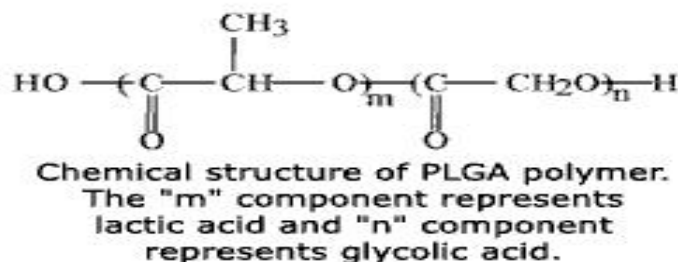
Dose : 5mg/kg body weight daily and 10 mg/kg body weight in
Thrice Weakly treatment

Solubility : Freely soluble in water and sparingly soluble in alcohol

3.6 POLYMER PROFILE

3.6.1 Name of the polymer: PLGA or poly (lactic-co-glycolic acid)

Structure



Typical properties

PLGA or poly (lactic-co-glycolic acid) is a copolymer which is used in a host of Food and Drug Administration (FDA) approved therapeutic devices, owing to its biodegradability and biocompatibility. Depending on the ratio of lactic to glycolide used for the polymerization, different forms of PLGA can be obtained. All PLGAs are amorphous rather than crystalline and show a glass transition temperature in the range of 40⁰c- 60⁰c. Unlike the homopolymers of lactic acid (polylactide) and glycolic acid (polyglycolide) which show poor solubilities, PLGA can be dissolved by a wide range of common solvents, including chlorinated solvents, tetrahydrofuran, acetone or ethyl acetate. The mechanical strength, swelling behavior, capacity to undergo hydrolysis and, subsequently, the biodegradation rate are directly influenced by the crystallinity of the PLGA polymer. The resultant crystallinity of the PLGA co- polymer is dependent on the type and the molar ratio of the individual monomer components (lactide and glycolide) in the copolymer chain. PLGA polymers containing 50:50 ratio of lactic and glycolic acids are hydrolyzed much faster than those containing a higher proportion of either of the two monomers. PGA is highly crystalline because it lacks the methyl side groups of the PLA. Lactic acid is more hydrophobic than glycolic acid and, therefore, lactide-rich PLGA co-polymers are less hydrophilic, absorb less water and, subsequently, degrade more slowly.

It has a glass transition temperature (T_g) of 45⁰c and an inherent viscosity of 0.5-0.8mPa. The T_gs of the PLGA co-polymers are above the physiological temperature of 37⁰c and hence they are normally glassy in nature. Thus, they have a fairly rigid chain structure, which gives them significant mechanical strength to be formulated as a degradable device. It has been reported that the T_gs of PLGA decrease with the decrease of lactic content in the co-polymer composition with decreasing M.W.

Biodegradation of PLGA

In both *in-vitro* and *in-vivo*, PLGA co-polymer undergoes degradation in an aqueous environment (hydrolytic degradation or biodegradation) through cleavage of its backbone ester linkages. The polymer chains undergo bulk degradation and the PLGA matrix. It has been recorded that the PLGA biodegradation occurs through random hydrolytic chain scissions of the swollen polymer. The carboxylic end groups present in the PLGA chains increase in number during the biodegradation process as the individual polymer chains are cleaved. These are known to catalyze the biodegradation process. It has also been reported that large fragments are degraded faster internally and amorphous regions degrade faster than crystalline regions. The biodegradation rates of the PLGA co-polymers are dependent on the molar ratio of the lactic and glycolic acids in the polymer chain, M.W. of the polymer and the degree of crystallinity.

Applications

The possibility to tailor the polymer degradation time by altering the ratio of the monomers used during synthesis has made PLGA a common choice in the production of a variety of biomedical devices such as : grafts, sutures, implants, prosthetic devices, micro and nanoparticles. They are also easy to formulate into various delivery systems for carrying a variety of drug classes, such as vaccines, peptides, proteins and micro molecules, which have been approved by the Food and Drug administration for drug delivery use. It has been used successfully in delivery of amoxicillin in treating listeriosis (treatment of *Listeria monocytogenes* infection). As an example, a commercially available drug delivery device using PLGA is Lupron Depot for the treatment of advanced prostate cancer.

4. AIM AND OBJECTIVE OF THE STUDY

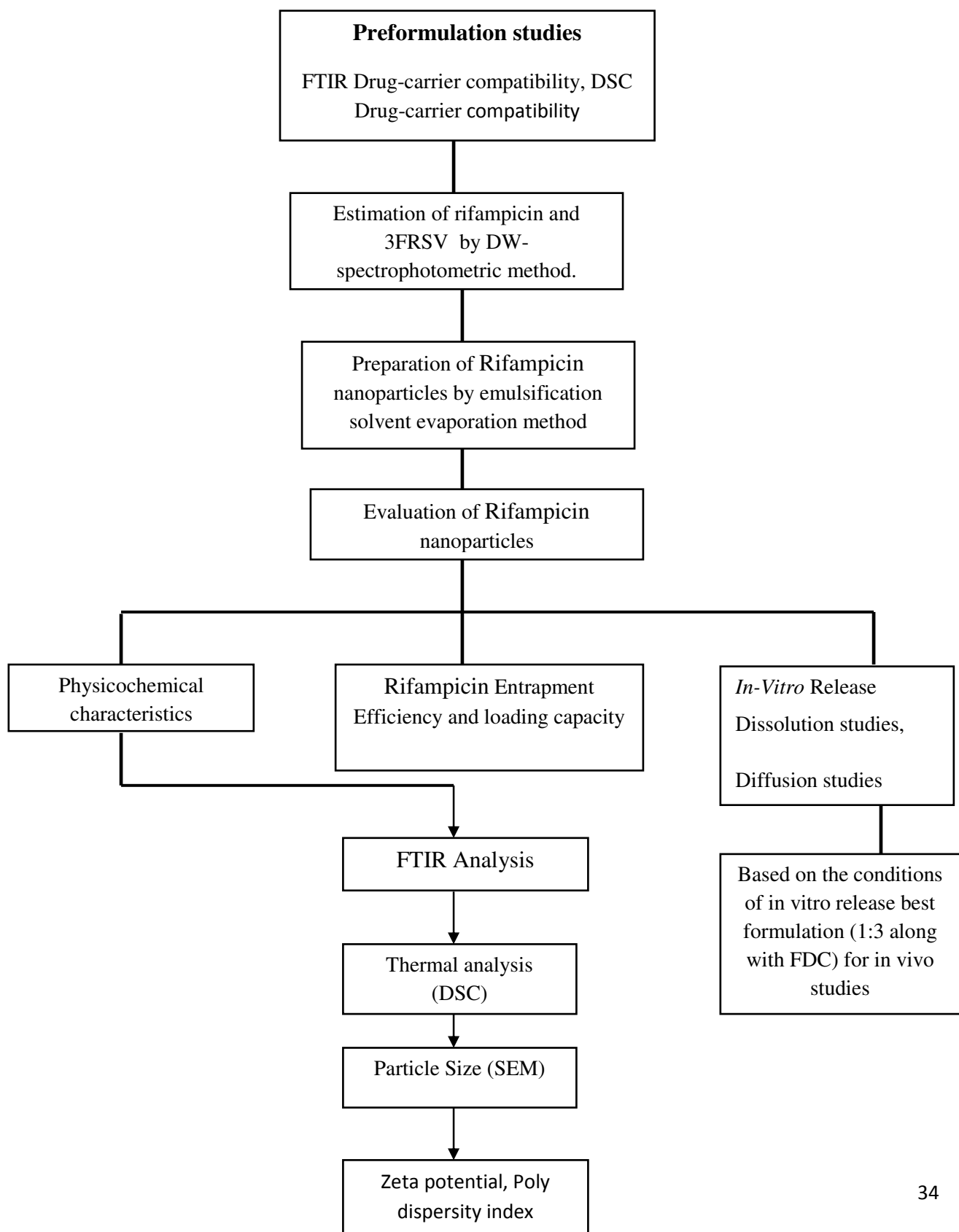
The present study aimed to improve the bioavailability of Rifampicin Nanoparticles from Fixed Dose Combination with Isoniazid, Pyrazinamide and Ethambutol.

The following parameters were examined

1. Pre-formulation studies.
 - a. Drug and carrier interaction by FT-IR spectroscopy.
 - b. Drug and carrier interaction by Differential Scanning Calorimetry(DSC)
2. Preparation of calibration curve for simultaneous estimation of Rifampicin and 3FRSV by DW-spectrophotometric method .
3. Preparation of Rifampicin loaded PLGA nanoparticles by emulsification solvent evaporation method.
4. Evaluation of Rifampicin loaded PLGA nanoparticles
5. Drug and carrier interaction by FT-IR spectroscopy.
 - a. Particle size determination by Scanning Electron Microscopy(SEM)
 - b. Surface characteristic by Zeta potential analyzer
 - c. Thermal analysis by Differential Scanning Calorimetry (DSC).
 - d. Rifampicin encapsulation efficiency and loading capacity of the nanoparticles.
 - e. *Invitro* release of Rifampicin from the nanoparticles.
 - f. Dissolution studies and Diffusion studies

Based on the conditions of in vitro release best sample was used for in vivo studies in animal model.

5. PLAN OF WORK



6. MATERIALS

The drugs chemicals and equipments were used in the present project work are given in tables. Drugs chemicals were of analytical grade and procured either gift samples or purchased.

6.1. Chemicals

Chemicals	Supplier/Manufacturer
Rifampicin	Themis lab, Mumbai
3FRSV	Themis lab, Mumbai
Isoniazid, Pyrazinamide and etambutal	Cadila health care ltd, ahmedabad
Chloroform	SRL chem, Mumbai
Methanol	SRL chem, Mumbai
Concentrated hydrochloric acid	Ranbaxy Ltd, Vijayawada
Anhydrous sodium sulphate	Samir tech chem, Mapurkur
Potassium dihydrogen phosphate	S.D fine chemicals, Bangalore
Dibasic sodium phosphate	Samir tech chem., Mapurkur
Acetonitrile(ACN)	Samir tech chem, Mapurkur
Disodium hydrogen phosphate	S.D fine chemicals, Bangalore
Eppendorf's tube	Redcross, Nellore
PLGA	Themis lab, Mumbai

6.2. Equipments

Equipments	Model/Company
Dialysis membrane 110	Himedia laboratory,mumbai
Auto pipettes	Tripette, Merck, Germany
Analytical balance	AG 135, Mettler Toledo
UV-Visible Spectrophotometer	Shimadzu UV-1800, Japan
DW-Spectrophotometer	Shimadzu 160A UV-Vis, japan
pH meter	MA 235, Mettler Toledo
High performance liquid chromatography	Shimadzu CLASS-VP, Japan

7.0. METHODS

7.1. preformulation studies^{58,59}

Before formulation of drug substances into a dosage form, it is essential that the drug and polymer should be chemically and physically characterized. Preformulation studies give the information needed to define the nature of the drug substance and provide a frame work for the drug combination with pharmaceutical excipients in the fabrication of a dosage form.

Fourier Transform Infra Red Spectroscopy (FTIR)

Compatibility study of drug with the polymer was determined by FTIR Spectroscopy using Perkin Elmer RX1. The pellets were prepared by gently mixing of 1mg sample with 200mg potassium bromide at high compaction pressure. The scanning range was 450 to 4000 cm^{-1} and the revolution was 4 cm^{-1} . The pellets thus prepared were examined and the spectra of drug and the polymer in the formulations were compared with that of pure drug or polymer spectra.

Differential Scanning Calorimetry (DSC)

Differential scanning calorimetric curve of pure rifampicin, poly lactic-co-glycolic acid (PLGA) polymer and mixture of drug and polymer measurement were carried out by using a thermal analysis instrument equipped with a liquid nitrogen sub ambient accessory. 2-6mg samples were accurately weighed in aluminum pans thematically sealed and heated at a rate of 10°C per min⁻¹ in a 30 to 300 °C temperature under nitrogen flow of 40 ml / min.

7.2. Preparation of calibration curve for simultaneous estimation of rifampicin and 3FRSV by DW-Spectrophotometric method³⁹

Procedure for preparation of pH 1.2 buffer

50ml of 0.2M KCl is mixed with 85ml of 0.2M HCl and make upto 200ml with water.

NOTE

0.2M KCl: 14.911gm of KCl was dissolved in H₂O and dilute with water and made upto 1000ml.

0.2M HCl: 17ml of HCl was mixed with 1000ml of H₂O.

Preparation of standard stock solution

RIF stock solution RIF powder (10mg) was accurately weighed and transferred to 10ml volumetric flask it was dissolved in 7ml of chloroform by sonication for 5min. The volume was adjusted to 10ml with chloroform. 1ml of this solution was further diluted to 10ml with chloroform to have the final concentration of 100mg/ml.

3-FRSV Stock solution 10mg was dissolved and diluted in chloroform as in case of RIF stock solution, to obtain the final concentration 100mg/ml.

Selection of wavelength for the estimation of rifampicin

Spectrum of pure 3-FRSV was scanned in the spectrum basic mode using the cursor function, the absorbance corresponding to 475 nm was noted from the spectrum then the cursor function was moved along with peak curve until the absorbance was equal to that of absorbance at 475nm was found. The wavelength obtained corresponding to this absorbance value was 507 nm. The absorbance of various dilution of 3-FRSV in chloroform was measured at 475 and 507nm the difference between the two absorbance values was calculated.

Selection of wave lengths for estimation of 3-FRSV

Spectrum of pure RIF was scanned in the spectrum basic mode using the cursor function; λ_1 and λ_2 were found as described above. The values obtained were 492nm (λ_1) (the wavelength of maximum absorbance for 3FRSV) and 475nm (λ_2), respectively.

7.3. Calibration curve of rifampicin and 3-FRSV

Appropriate aliquots from the stock solutions of RIF and 3FRSV were used to prepare four different sets of dilutions series A, B, C and D as follows.

Series A: This series comprised of mixtures of RIF and 3FRSV having fixed concentrations of 3FRSV (2 μ g/ml) and varying concentrations of RIF (5-50 μ g/ml). The solutions were prepared by pipetting out 0.2ml of 3FRSV stock solution (100 μ g/ml) and 0.5, 1.0, 1.5, 2, 2.5, 3.0, 3.5, 4.0, 4.5 and 5ml of the stock solution of RIF (100 μ g/ml) in to a series of 10ml volumetric flask and the volume was adjusted to the mark with chloroform.

Series B: This series comprised of mixtures of RIF and 3FRSV having fixed concentrations of RIF (50 μ g/ml) and varying concentrations of 3FRSV (2-10 μ g/ml) were prepared by pipetting out 5ml of RIF stock solution (100 μ g/ml) and 0.2, 0.4, 0.6, 0.8 and 1ml of the stock solution of the 3FRSV (100 μ g/ml) into 10ml volumetric flask and volume was adjusted to the mark with chloroform.

Series C: This series consisted of different concentration of RIF ranging from 5 to 50 μ g/ml prepared by appropriate dilution of aliquots of RIF stock solution, with chloroform, same as in the case of series A.

Series D: This series included solutions having concentrations of 3FRSV ranging from 2 to 10µg/ml prepared by diluting appropriate volumes of corresponding stock solution with chloroform as in the case of series B.

The absorbance of the solutions of series A and C were measured at 475.0(λ_1) and 507nm (λ_2) while absorbance of the solutions of seriesB and D where measured at 492(λ_1) and 457nm(λ_2). The difference in absorbance was plotted against concentration (µg/ml).

***In-vitro* dissolution stability study of rifampicin alone at pH 1.2 buffer**

A solution of 0.1NHCL (200ml) was placed in the vessel of the USP dissolution apparatus 2 (us pharmacopoeia XXIII, 1995) and the medium was equilibrated at $37\pm0.2^\circ\text{C}$ with stirring at 100rpm. RIF (150mg) was accurately weighed, dissolved in and diluted to 100ml with 0.1NHCL (37°C). The resulting solution was transferred immediately to the dissolution vessel at once and 5ml of specimen was withdrawn immediately from a zone midway between the surface of the dissolution medium and bottom of the vessel(0min sample). Spacimens were withdrawn at 15min intervals upto 60min. An aliquot, 1ml was extracted immediately with 5ml of chloroform using cyclomixer (3min). The aqueous phase was discarded and anhydrous sodium sulphate was added to chloroform layer to remove traces of water. The sample was analyzed for RIF and 3FRSV using DW-Spectrophotometric method.³⁹

***7.4. In-vitro* dissolution stability study of rifampicin in the presence of fdc at pH 1.2 buffer**

Solution of 200ml 0.1N HCl was placed in the vessel of the dissolution apparatus and the medium was equilibrated to $37\pm0.2^\circ\text{C}$ with stirring at 100 rpm. RIF (150mg) and INH (100mg) were accurately weighed, dissolved in and diluted to 100ml with 0.1N HCl (37°C), resulting solution was transferred immediately to the dissolution vessel and 5ml of specimen was withdrawn immediately from a zone midway between the surface of the dissolution medium and bottom of the vessel(0min sample). Spacimens were withdrawn at 15min intervals upto 60min and analyzed as follows.

Estimation of RIF and 3FRSV by DW-Spectrophotometric method

An aliquot, 1ml was extracted immediately with 5ml of chloroform using cyclomixer (3min). The aqueous phase was discarded and anhydrous sodium sulphate was added to chloroform layer to remove traces of water. The samples was analyzed for RIF and 3FRSV using DW-Spectrophotometric method.

7.5. *In-vitro* dissolution stability study of rifampicin with different concentration of plga in the presence of fdc at pH 1.2 buffer

Solution of 200ml 0.1N HCl was placed in the vessel of the dissolution apparatus and the medium was equilibrated to $37\pm 0.2^{\circ}\text{C}$ with stirring at 100 rpm. RIF (46.5mg), INH (24mg) PYZ(135.5mg),ETH(93mg)and plga(46.5mg) at varying strengths (1:1,1:2,1:3,1:1+fdc,1:2+fdc and 1:3+fdc) were accurately weighed, dissolved in and diluted to 100ml with 0.1N HCl (37°C), resulting solution was transferred immediately to the dissolution vessel and analyzed as described in 6.1.3.

7.6. Statistics

The values are expressed in mean \pm S.D. One way ANOVA followed by Tukey's multiple comparison Test was used to analyze the effect of different doses of silymarin when compared to control, with the help of Graph PadInstat software, version 3.01. $P<0.05$ was considered as significant.

7.7. Preparation of rifampicin loaded plga nanoparticles

Rifampicin loaded plga nanoparticles were prepared through single emulsion evaporation method. 160mg of PLGA and 40mg of were dissolved in 2ml of dichloromethane. This solution was added drop wise to an aqueous 20ml PVA (3%, w/v) solution under sonication for 20 min (in pulsed manner, 40% intensity) using a probe sonicator (Lapsonic® P, Sartorius Biotech GmbH, Germany) over an ice bath. The solvent was evaporated at room temperature (28°C) for 12h, under magnetic stirring. Loaded nanoparticles were isolated by 30 min centrifugation at 35,000 rpm. After centrifugation, the supernatant was recovered and assayed for untrapped drug and sediment was washed using the same amount of distilled water as of the supernatant and again centrifuged at 35,000 rpm for 20 min. The washing process was repeated 3 times. All the washings were collected and assayed for untrapped drug.

Rifampicin Plga Loaded Nanoparticles

Table:1

Formulation code	Drug	Polymer	Drug polymer ratio	Sonication time
F1	31mg/kg	31mg/kg	1:1	20mins
F2	31mg/kg	62mg/kg	1:2	20mins
F3	31mg/kg	93mg/kg	1:3	20mins
F4	31mg/kg	31mg/kg	1:1 along with FDC	20 mins
F5	31mg/kg	62mg/kg	1:2 along with FDC	20 mins
F6	31mg/kg	93mg/kg	1:3 along with FDC	20 mins

7.8. EVALUATION OF NANOPARTICLES

7.8.1. Drug and carrier interaction by Fourier Transform Infra Red Spectroscopy

Compatibility study of drug with the polymer was determined by FTIR Spectroscopy using Perkin Elmer RX1. The pellets were prepared by gently mixing of 1mg sample with 200mg potassium bromide at high compaction pressure. The scanning range was 450 to 4000 cm^{-1} and the revolution was 4 cm^{-1} .

7.8.2. Particle size determination by Scanning Electron Microscopy ⁶²

The size of the nanoparticles was analyzed by scanning electron microscope .The instrument used for this determination was JEOL MODEL JSM 6400 scanning electron microscope (SEM). The nanoparticles were mounted directly on the SEM stub, using double –sided, sticking tape and coated with platinum and scanned in a high vacuum chamber with a focused electron beam. Secondary electrons, emitted from the samples were detected and the image formed.

7.8.3. Surface Characteristics by Zeta Potential

The Zeta potential of nanoparticles was measured on a zeta potential analyzer Zetasizer 3000 HS Malvern instrument. The samples were diluted with pH 1.2 and placed in eletrophoretic cell and measured in the automatic mode.

7.8.4. Thermal Analysis by Differential Scanning Calorimetry (DSC)

Differential scanning calorimetric measurement of rifampicin plga nanoparticles was carried out by using a thermal analysis instrument equipped with a liquid nitrogen sub ambient accessory. 2-6mg samples were accurately weighed in aluminum pans thermatically sealed and heated at a rate of 10°C per min -1 in a 30 to 300°C temperature under nitrogen flow of 40 ml per min.

7.8.5. Encapsulation efficiency and Percentage yield of the nanoparticles⁶³

The Encapsulation efficiency and percentage yield of the nanoparticles were determined by the separation of nanoparticles from the aqueous medium containing nonassociated rifampicin by cold centrifugation at 12000g for 30 minutes. The amount of free rifampicin in the supernatant was measured by UV method at 475nm. The rifampicin encapsulation efficiency (EE) and percentage yield of the nanoparticles was calculated as follows.

$$\text{Encapsulation Efficiency} = \frac{\text{Total amount of Rifampicin} - \text{Free Rifampicin}}{\text{Weight of nanoparticles}} \times 100$$
$$\text{Percentage yield} = \frac{\text{Total amount of Rifampicin} - \text{Free Rifampicin}}{\text{Total amount of Rifampicin}} \times 100$$

7.8.6. *Invitro* release of rifampicin from the nanoparticles

Dissolution studies

The dissolution profiles of the plain drug and the nanoparticle formulations were determined in USP dissolution apparatus – II using 900ml of pH – 1.2 buffer for the 60 mins . The dissolution media were maintained at 37°±0.5°C with a paddle rotation speed at 50 rpm. The amount of drug used was equivalent to 2 mg. At specified time intervals (15, 30, 45 and 60 mins) 5ml of dissolution media were withdrawn and replaced with an equal volume of the fresh medium to maintain constant volume of the media. Samples were filtered through a0.22µm nylon

membrane filter (Millipore, Bedford, MA) and assayed for drug content spectrophotometrically at 475nm using UV/Vis double beam spectrophotometer after appropriate dilution with the corresponding media. Cumulative percentage of drug dissolved in the preparations was calculated using calibration equations. Dissolution tests were performed in triplicate for each formulation (n = 3).⁶⁴

Diffusion studies

The rifampicin loaded plga nanoparticles were separated from the aqueous suspension medium through ultracentrifugation. Nanoparticles equivalent to 2mg of rifampicin nanoparticles were redispersed in 10ml phosphate buffer solution pH-1.2 and placed in a dialysis membrane bag with a molecular cut-off of 5 kDa which acts as a donor compartment, tied and placed into 10 ml 1.2 phosphate buffer solution in a beaker which acts as a receptor compartment. The entire system was kept at 37°C with continuous magnetic stirring. At appropriate time intervals (15, 30, 45 and 60 mins) 1 ml of the release medium was removed and 1 ml fresh 1.2 phosphate buffer solution was added in to the system. The amount of rifampicin in the release medium was evaluated by UV-Visible Spectrophotometer at 475 nm.

7.8.7. Kinetics of drug release^{65, 66}

In order to understand the mechanism and kinetic of drug release, the drug release data of the in-vitro dissolution study were analyzed with various kinetic models like zero order, first order, Higuchi's, Peppas's and Coefficient of correlation (r) values were calculated for the linear curves by regression analysis of the above plots.

I) Fitting of Results into Different Kinetic Equations

The results of in vitro release profile obtained for all the formulations were plotted in modes of data treatment as follows: -

- a. Zero - order kinetic model - Cumulative % drug released versus time.
- b. First – order kinetic model - Log cumulative percent drug remaining versus time.
- c. Higuchi's model - Cumulative percent drug released versus square root of time.
- d. Korsmeyer equation / Peppas's model - Log cumulative percent drug released versus log time.

A) Zero order kinetics

Zero order release would be predicted by the following equation

$$A_t = A_0 - K_0 t$$

Where,

A_t = Drug release at time 't'.

A_0 = Initial drug concentration.

K_0 = Zero - order rate constant (hr^{-1}).

When the data plotted as cumulative percent drug release versus time, and the plot is linear, and then the data obeys Zero – order equal to K_0 .

B) First Order Kinetics

First – order release would be predicted by the following equation:-

$$\text{Log } C = \log C_0 - Kt / 2.303$$

Where, C = Amount of drug remained at time 't'.

C_0 = Initial amount of drug.

K = First – order rate constant (hr^{-1}).

When the data plotted as log cumulative percent drug remaining versus time yields a straight line, then the release follow first order kinetics. The constant 'K' can be obtained by multiplying 2.303 with the slope values.

C) Higuchi's model: Drug release from the matrix devices by diffusion has been described by following Higuchi's classical diffusion equation

$$Q = [D\varepsilon / \tau (2 A - \varepsilon C_s) C_s t]^{1/2}$$

Where,

Q = Amount of drug released at time 't'.

D = Diffusion coefficient of the drug in the matrix.

A = Total amount of drug in unit volume of matrix.

C_s = the solubility of the drug in the matrix.

ε = Porosity of the matrix.

τ = Tortuosity.

t = Time (hrs) at which 'q' amount of drug is released.

Above equation may be simplified if one assumes that 'D', 'C_s' and 'A' are constant. Then equation becomes

$$Q = Kt^{1/2}$$

When the data plotted according to equation i.e. cumulative drug release versus square root of time yields a straight line, indicating that the drug was released by diffusion mechanism. The slope is equal to 'K' (Higuchi's 1963).

D) Korsmeyer equation / Peppas's model

To study the mechanism of drug release from the sustained-release of acyclovir nanoparticles, the release data were also fitted to the well-known exponential equation (Korsmeyer equation/ peppa's law equation), which is often used to describe the drug release behavior from polymeric systems.

$$M_t / M_a = Kt^n$$

Where, M_t / M_a = the fraction of drug released at time 't'.

K = Constant incorporating the structural and geometrical characteristics of the drug / polymer system.

n = Diffusion exponent related to the mechanism of the release.

Above equation can be simplified by applying log on both sides,

And we get: - **Log M_t / M_a = Log K + n Log t**

When the data plotted as log of drug released versus log time, yields a straight line with a slope equal to 'n' and the 'K' can be obtained from y – intercept. For Fickian release 'n' = 0.5 while for anomalous (non - Fickian) transport 'n' ranges between 0.5 and 1.0.

Mechanism of Drug Release as per Korsmeyer Equation / Peppas's Model

S. No.	n Value	Drug release
1.	0.50	Fickian release
2.	$0.5 < n < 1.0$	Non – Fickian release
3.	1.0	Case II transport

E). Statistical analysis: The release data were subjected to ANOVA with Tukey-Kramer multiple comparison test.

7.9. IN-VIVO EVALUATION STUDIES

7.9.1 Animals: New Zealand white rabbits weighing 1.5 to 2.5kg were obtained from Swamy Vivekananda College of pharmacy animal house was used in this study. The animals were fed with cabbage and water. They were maintained in standard laboratory conditions 21 ± 2 °C and relative humidity of 55-60%. The animals are overnight fasted before the experiment. The study protocol was approved by the Institutional Animal Ethical Committee and the protocol number is SVCP/IAEC/M.Pharm/07/2013.

Requirements

Cotton

Surgical blade

26G needle

Blood collecting tubes (EDTA tubes)

Plasma sample collecting tubes

Sex Male

No. of animals 6

7.9.2 Animal dose

Rifampicin : 31mg/kg

Rifampicin nanoparticles: 31 mg/kg

Rifampicin nanoparticles + isoniazid + prrazinamide + etambutal
31mg/kg + 16mg/kg + 77mg/kg + 62mg/kg

7.9.3 Procedure for collection of blood

Collection of blood from marginal ear vein

The animal was placed in a restrainer. Hair of the ear was shaved smoothly with blade without disturbing the blood vessels. Ear was cleaned with 95% v/v alcohol on the collection site and rapid rubbing on the ear to dilate blood vessels which is easy to collect the blood. 2G needle was inserted in vein to collect the blood from marginal ear vein. After collecting blood, clean sterile cotton was kept on the collection site and finger pressure was applied to stop the bleeding.⁷¹

7.9.4 Experimental procedure: Rabbits were classified into 4 different groups each group consisting of 6 animals

GROUP I Rifampicin

GROUP II Rifampicin+ fdc

GROUP III Rifampicin+ plga nanoparticles

GROUP IV Rifampicin+plga nanoparticles+fdc

Procedure :After overnight fasting, Group1, Group 2, Group3,Group 4 animals received rifampic alone (31mg/kg), rifampicin (31mg/kg)+ isoniazid(16mg/kg)+pyrazinamide(77mg/kg)+ ethambutol(62mg/kg),rifampicin(31mg/kg)+PLGA(93mg/kg)and,rifampicin(31mg/kg)+PLGA(93mg/kg))+ isoniazid(16mg/kg) + pyrazinamide(77mg/kg) + ethambutol(62mg/kg) respectively through an intragastric tube. Blood samples (1 ml) were collected in heparinized tubes from the marginal ear vein at 0, 0.5, 1.5, 2, 2.5, 3, 3.5, 4, 5, 6, 8, 10, 12 and 24 h after drug administration and plasma was separated by using centrifugation and stored at -20°C. Samples were analyzed by validated high performance liquid chromatography (HPLC).⁴

7.9.5 Bioanalytical work

Extraction of RIF, 3FRSV from plasma

An aliquot of 500µl of plasma samples was pipetted into an eppendorf's tube of 1.5ml capacity. 500µl methanol was added, vortexed for 3 minute and centrifuged at 10,000 rpm for 15min. Then 300 µl of the supernatant was taken into another microcentrifuge tube and vacuum dried in centrivac. The residue obtained was reconstituted in 100µl of mobile phase. Plasma was filtered through 0.22 µm membranes (13 mm) and 20 µl volumes were injected. All the two analytes; RIF, 3FRSV were detected at 238nm⁷³

7.9.5.1 Chromatographic conditions⁷³

The parameters specified by USP for gradient HPLC analysis of RIF, 3FRSV are given in Table 1. The prescribed gradient program for analysis is given in Table 2. The analysis was done maintaining all the specified conditions

Table: 2 HPLC parameters for determination of R, H and Z by the proposed USP method

Parameter	Condition
Column	L1 (250×4.6 mm)
Particle size	5µm
Mobile phase	Buffer solution:1.4g of dibasic sodium Phosphate in 1 liter water (pH 6.8) Solution A=Buffer:ACN(96:4) Solution B=Buffer:ACN(45:55)
Flow rate	1.5ml\min
Detection wavelength	238nm
Column temperature	25 c
Injection volume	20µl

Table: 3 Gradient programs prescribed in the USP method

Time (min)	Solution A(%)	Solution B(%)	Elution
0	100	0	Equilibration
0-5	100	0	Isocratic
5-6	100-0	0-100	Linear gradient
6-15	0	100	Isocratic

Extraction efficiency

The extraction efficiency was calculated by comparing the peak heights of rifampicin spiked-pooled blank plasma samples with that of respective standard rifampicin samples

7.9.6. Pharmacokinetic parameters⁷⁴

The pharmacokinetic parameters were calculated for each rabbit of group I, group II, group III and group IV, by the semi logarithmic plot of plasma rifampicin concentration at various intervals. The following pharmacokinetic parameters were calculated:

- a. Elimination rate constant(K_e): The elimination rate constant was determined using the formula

$$1. K_e = -2.303 \times \text{slope of extrapolated curve}$$

- b. Elimination half life($t_{1/2}$): $t_{1/2}$ was calculated using the formula

$$t_{1/2} = 0.693/K_e$$

1. Absorption rate constant (K_a): This was determined by the method of residuals. The log linear portion of the decline phase was back extrapolated for each curve. The plasma concentration along this extrapolated line was C. the observed plasma concentration C was subtracted from the corresponding extrapolated value at each time point. The semi logarithmic plot of residuals (C-C) against time yields a straight line.

$$K_a = -2.303 \times \text{slope of residual line}$$

2. Absorption half life: It was calculated using the formula

$$T_{1/2(a)} = 0.693/K_a$$

3. Apparent volume of distribution(V_d): It was calculated using the formula

$$1. V_d = \frac{K_a F X_0}{(K_a - K_e) \text{ y intercept}}$$

4. Time to C_{max} (t_{max}): t_{max} was calculated using the formula

$$t_{max} = \frac{\ln K_a - \ln K_e}{K_a - K_e}$$

5. Maximum plasma concentration (C_{max}): C_{max} was calculated using the formula

$$C_{max} = \text{Y intercept} (e^{-K_e \cdot T_{max}} - e^{-K_a \cdot T_{max}})$$

6. Area under curve (AUC₀₋₁₂): AUC₀₋₁₂ was calculated using the formula

$$AUC = \frac{F X_0}{V_d \cdot K_e}$$

7. AUC_{0-∞} was calculated using the formula

$$AUC_{0-\infty} = \frac{C_0}{K_e}$$

Statistics

The values are expressed in mean ± SEM. One way ANOVA followed by Tukey's multiple comparison Test was used to analyse the effect of different doses of silymarin when compared to control, with the help of Graph PadInstat software, version 3.01. P<0.05 was considered as significant.

8. RESULTS

COMPATIBILITY STUDIES:

8.1. Drug and carrier interaction by FT-IR Spectroscopy

FT-IR spectra of rifampicin, PLGA in physical mixture of rifampicin and plga and rifampicin loaded plga nanoparticles are shown in tables 8, 9, 10 and 11 and figures 4, 5, 6 and 7. Rifampicin showed characteristic peaks at 2885.6 cm^{-1} (C-H-alkyl stretching), 1699.34 cm^{-1} (C=O-aromatic ketones), 1651.34 cm^{-1} (COOH unsaturated carboxylic acid stretching), 3043.77 cm^{-1} (O-H carboxylic acid-stretching). All these characteristic peaks present in rifampicin physical mixture observed in nanoparticles and thus confirming drug and polymer were compatible.

Sl.no	IRSpectrum	Peaks(cm^{-1})	Groups	Stretching /Deformation
1	Rifampicin	2885.6	C-H(alkyl)	Stretching
		1699.34	C=O(aromaticketone)	Stretching
		1651.12	COOH(unsaturated carboxylicacid)	Stretching
		3043.77	O-H(Carboxylicacid)	Stretching

IR SPECTRUM OF RIFAMPICIN

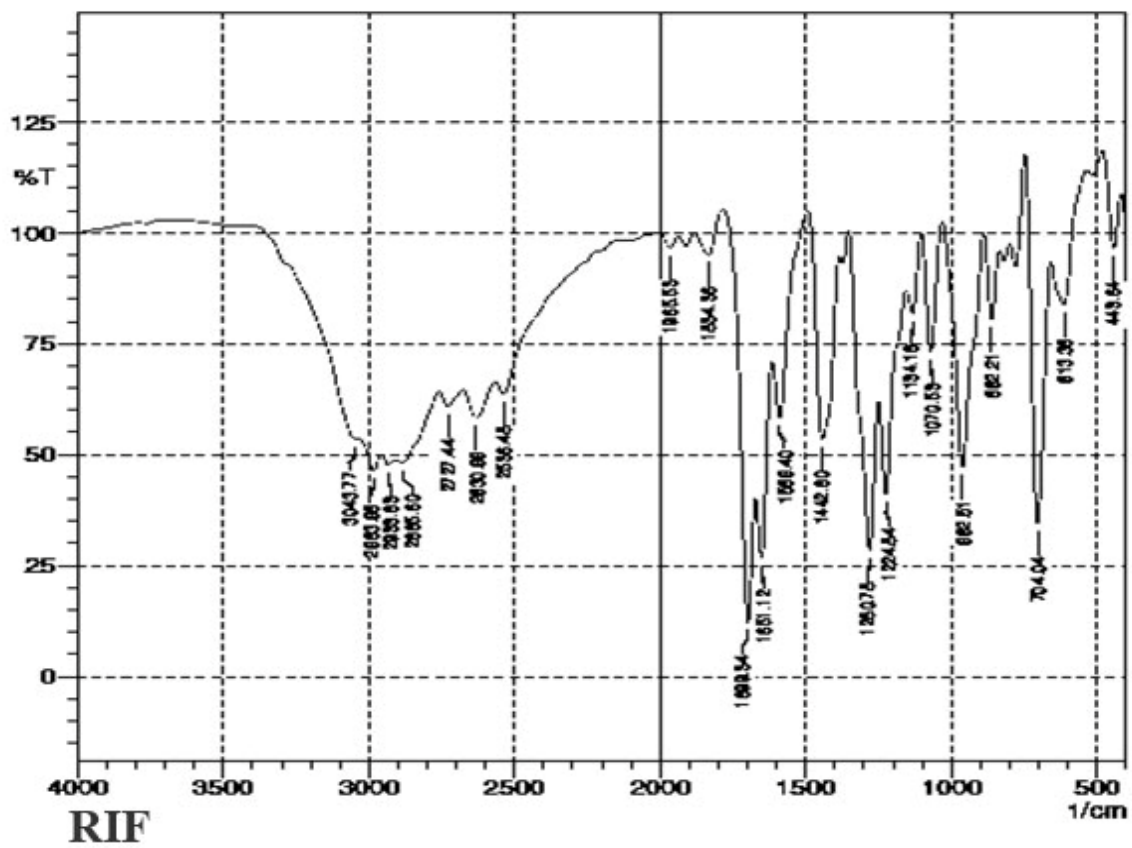


Fig :1 IR SPECTRUM OF RIFAMPICIN

2	Blank nanoparticles of plga	2872.1	C-H(alkyl)	Stretching
		1653.05	C=O(aromaticketone)	Stretching
		1629.6	COOH(unsaturated carboxylicacid)	Stretching
		3084.28	O-H(Carboxylicacid)	Stretching

IR SPECTRUM OF BLANK NANOPARTICLES USING PLGA

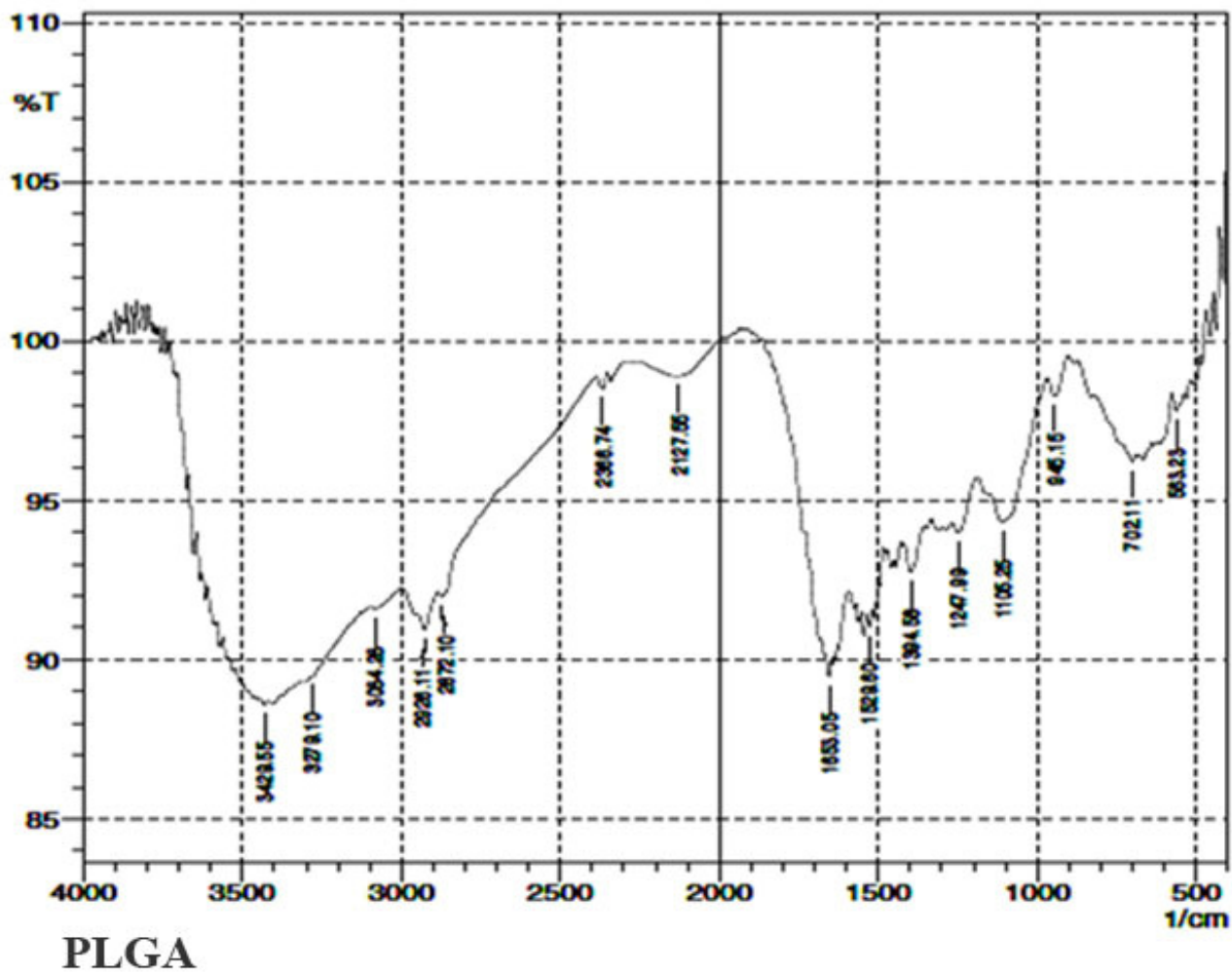


Fig: 2 IR SPECTRUMS OF BLANK NANOPARTICLES USING PLGA

3	Physical mixture of Rifampicin and plga	2891.39	C-H(alkyl)	Stretching
		1697.41	C=O(aromaticketone)	Stretching
		1651.12	COOH(unsaturated carboxylicacid)	Stretching
		3045.7	O-H(Carboxylicacid)	Stretching

IR SPECTRUM OF PHYSICAL MIXTURE OF RIFAMPICIN WITH PLGA

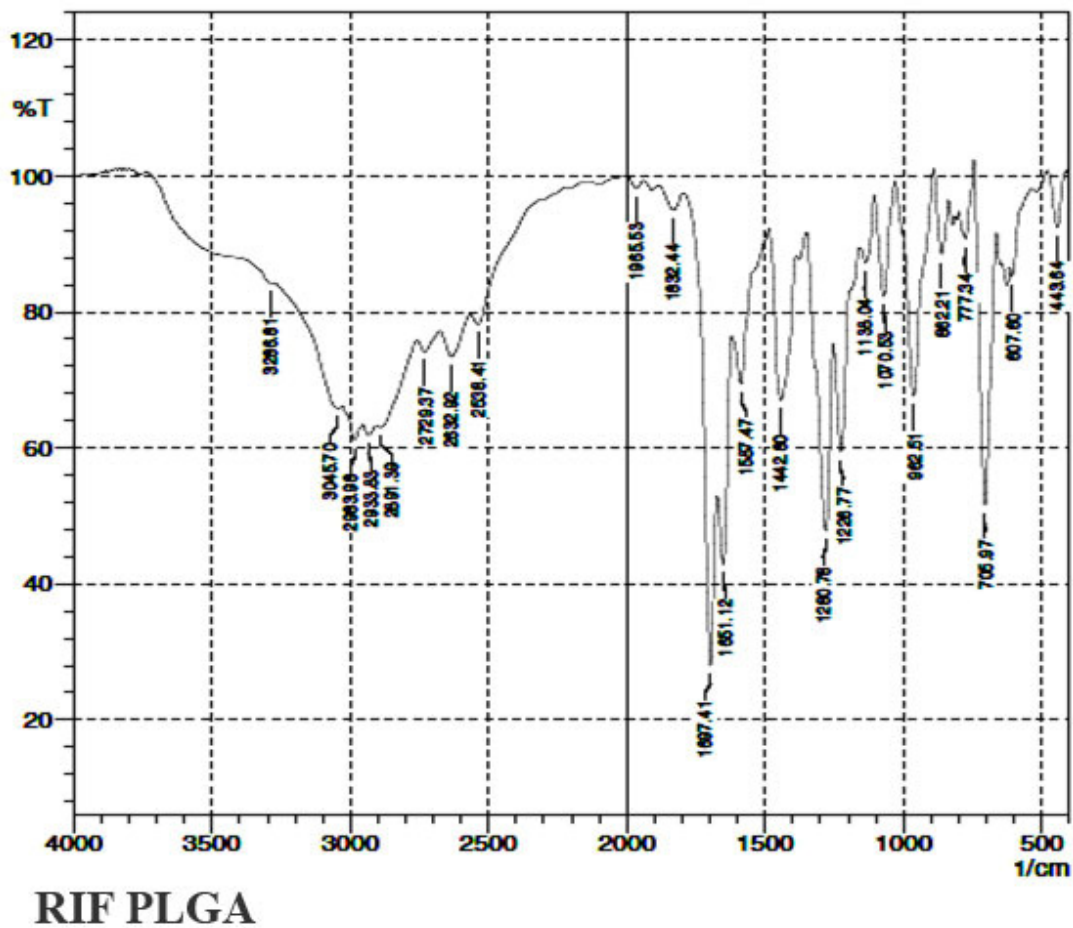


Fig:3 IR SPECTRUM OF PHYSICAL MIXTURE OF RIFAMPICIN WITH PLGA

4	Rifampicin nanoparticles of Plga	2856.67	C-H(alkyl)	Stretching
		1654.98	C=O(aromaticketone)	Stretching
		1645.03	COOH(unsaturated carboxylicacid)	Stretching
		2926.11	O-H(Carboxylicacid)	Stretching

IR SPECTRUM OF RIFAMPICIN NANOPARTICLES

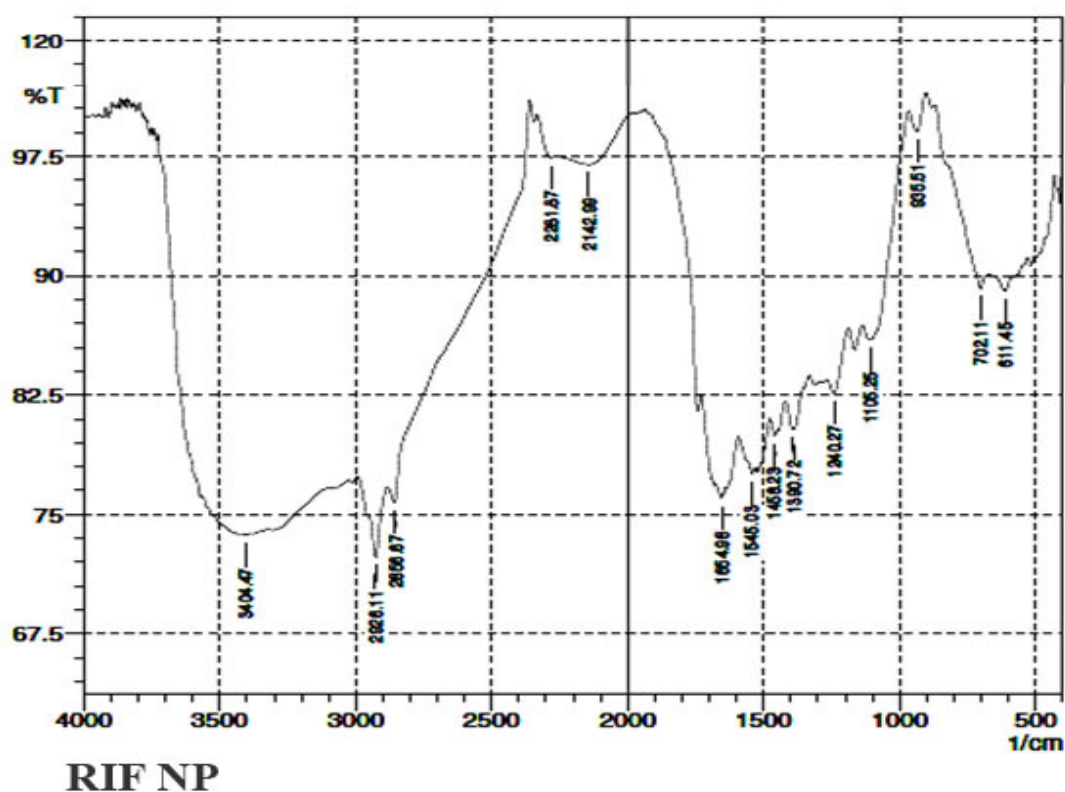
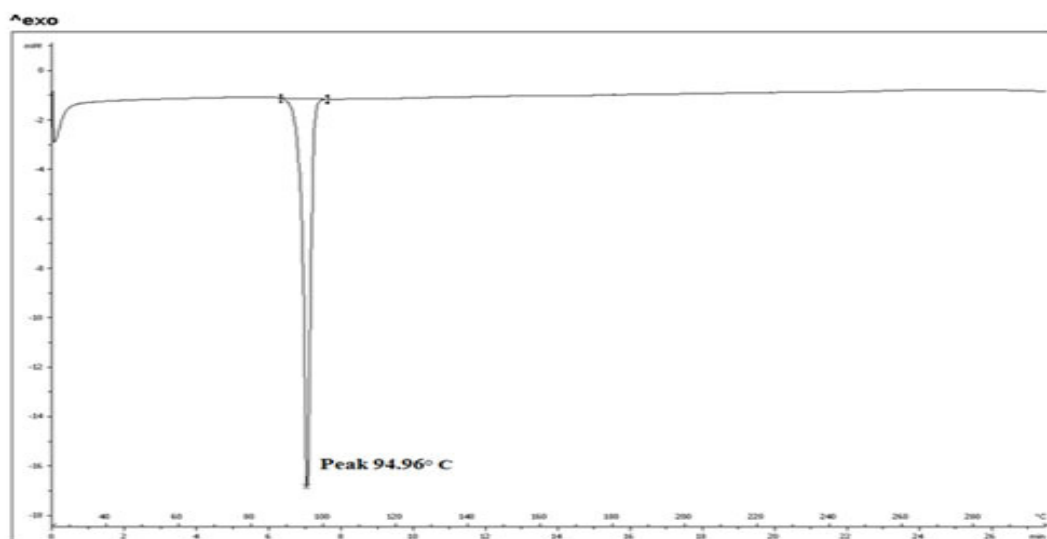


Fig:4 IR SPECTRUM OF RIFAMPICIN NANOPARTICLES

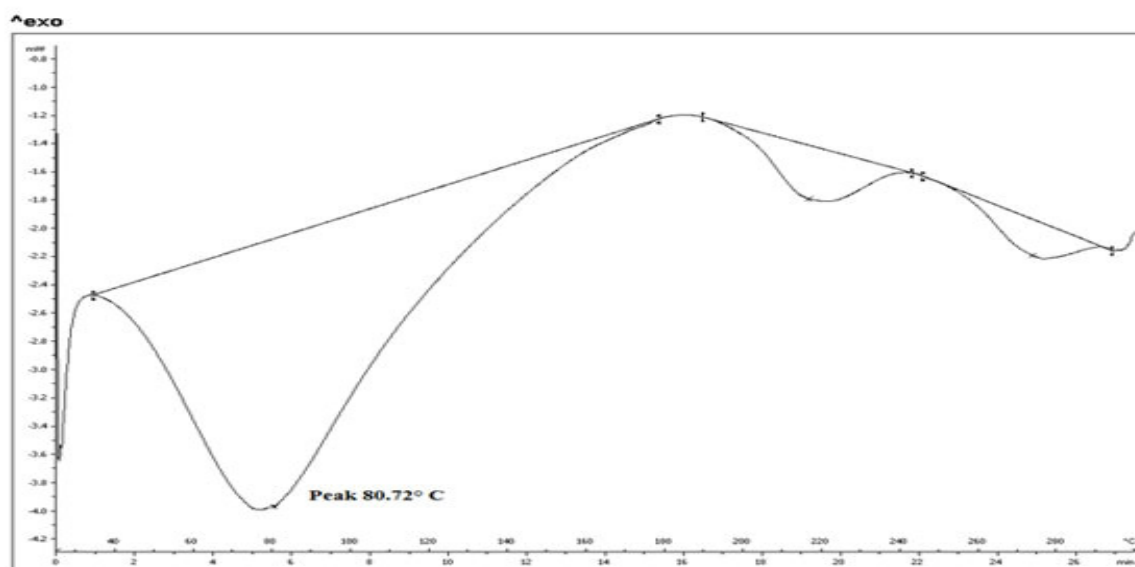
8.2. B. Differential scanning calorimetry (DSC)

In order to confirm the physical state of rifampicin in the nanoparticles, DSC of the RIF, physical mixture of RIF and polymer, RIF nanoparticles and blank nanoparticles, was carried out and the results are shown in figures 8,9,10,11,12 and 13. The DSC thermogram of RIF showed a sharp endothermic peak at 94.96°C, its melting point. The physical mixture of RIF and polymer, showed the same thermal behavior 93.04°C as the individual component, indicating that there was no interaction between the RIF and the polymer in the solid state. The DSC thermogram of blank nanoparticles showed a single endothermic peak at 80.72°C, the melting point of PLGA. The nanoparticles of F1, F2, F3, F5 and F6, showed endothermic peak at 68.75°C, 81.59°C and 92.05°C respectively, which are the characteristic peaks of PLGA shifted from 80.72°C, and there was no evidence for presence of the characteristic peaks of RIF at 94.96°C in F1, F2, F3, F4, F5 and F6. The change in thermogram indicates that RIF existed in an amorphous form completely whereas the PLGA partially changes to amorphous state.



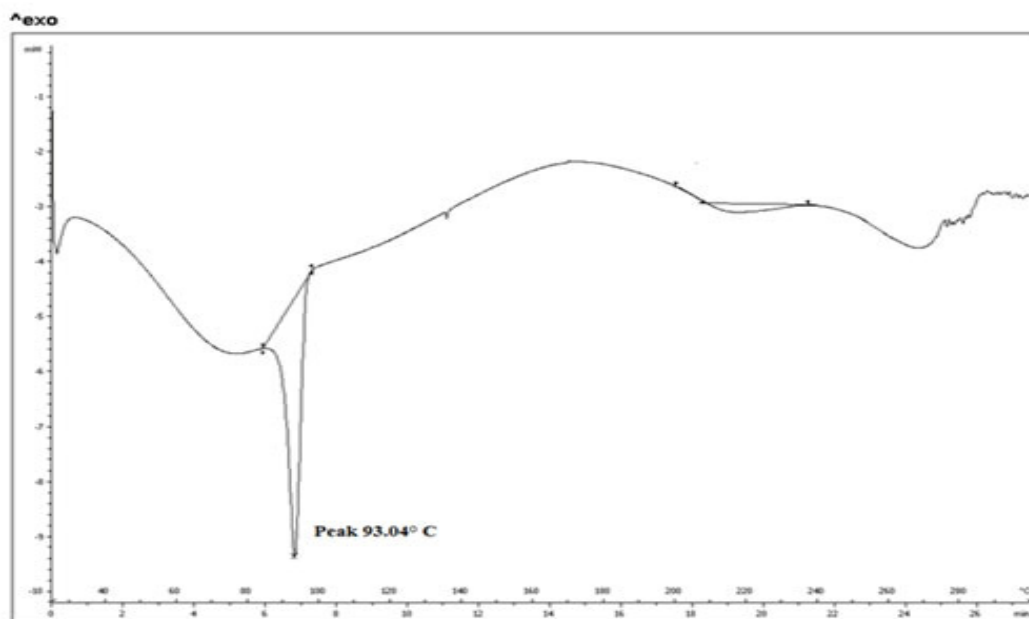
RIF

Fig:5 DSC thermogram of rifampicin



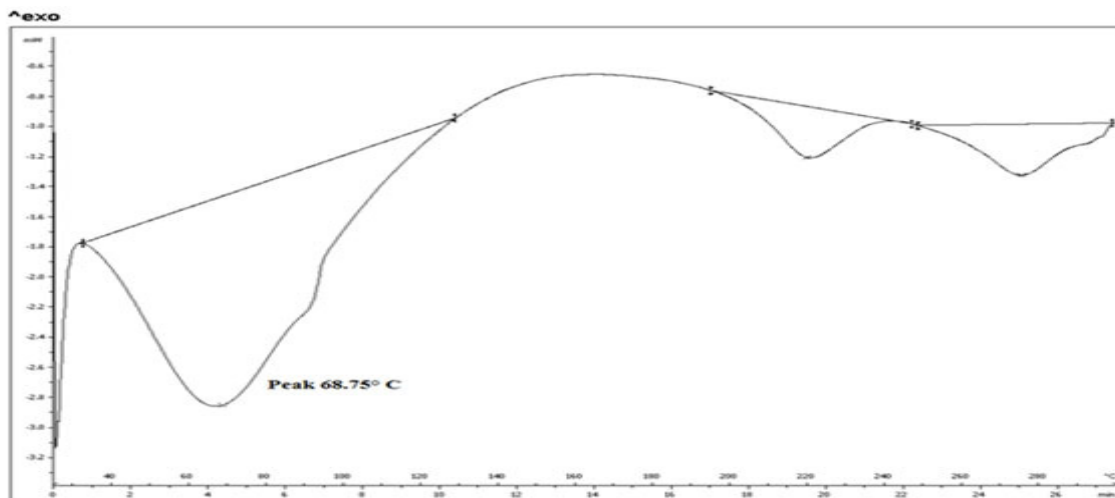
PLGA

Fig:6 DSC thermogram of blank nanoparticles using Plga



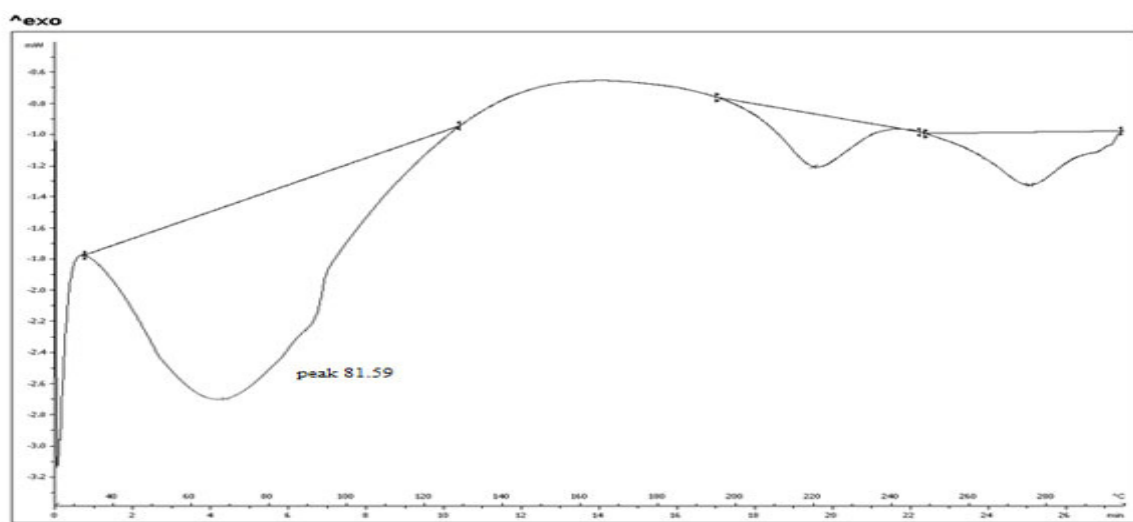
RIF PLGA

Fig:7 DSC thermogram of physical mixture of Rifampicin and plga



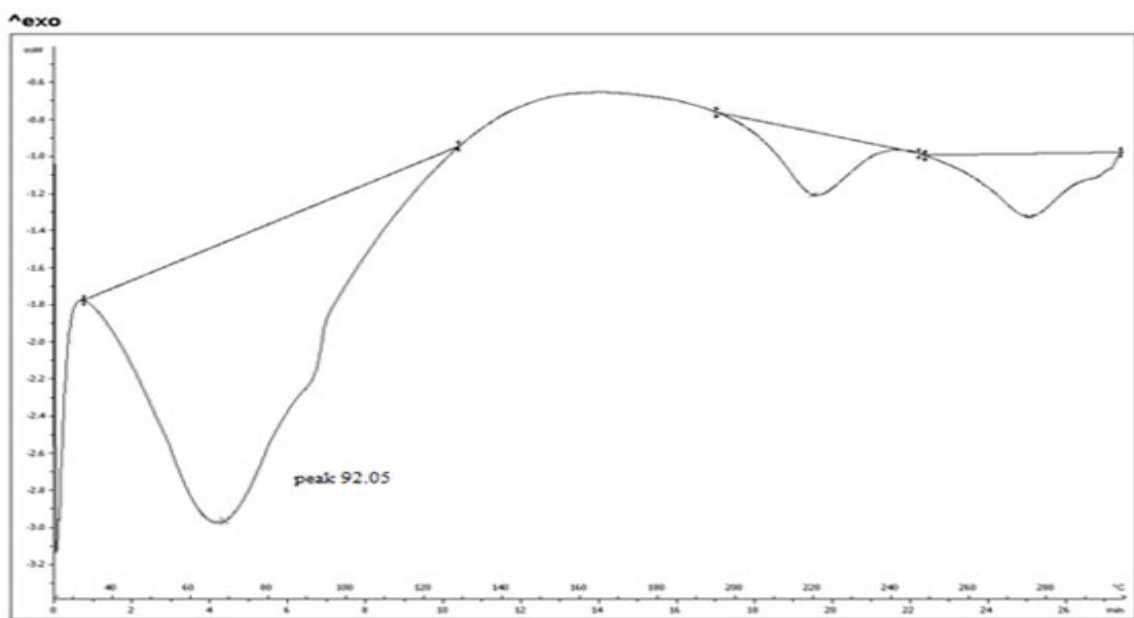
RIF NP 1

Fig:8 DSC thermogram of Rifampicin nanoparticles using plga



RIF NP 2

Fig:9 DSC thermogram of Rifampicin nanoparticles using plga



RIF NP 3

Fig:10 DSC thermogram of Rifampicin nanoparticles using plga

8.3. Encapsulation efficiency and percentage yield:

The entrapment efficiency of F1,F2 ,F3,F4,F5and F6 were 58.54%, 68.44% ,71.32 73.12%,75.41and 76.11 respectively. Similarly the percentage yield increases in the concentration of plga increases. The percentage yield of F1, F2, F3, F4, F5 and F6 were 50.91, 60.46, 67.31, 83.86, 85.22and 87.44respectively. Table 12 shows the results of encapsulation efficiency and percentage yield of the rifampicin nanoparticles.

Formulation Code	Drug polymer ratio (mg)	Encapsulation Efficiency (%)	Percentage yield (%)
F1	1:1	58.54	50.91
F2	1:2	68.44	66.46
F3	1:3	71.32	67.31
F4	1:1along with FDC	73.12	83.36
F5	1:2 along with FDC	75.41	85.22
F6	1:3 along with FDC	76.11	87.44

Table:8 encapsulation efficiency and percentage yield of the nanoparticles

8.4. Morphology:

The SEM of nanoparticles are shown in figures, The particles was formed smooth and spherical in shape at the drug:polymer ratio 1:1 in F1 and remained in the same characteristic at higher concentration of the polymer as seen in F2,F3,F4,F5 and F6 formulations.

SEM IMAGES:

Fig:11 (F)



Fig:12 (F0)

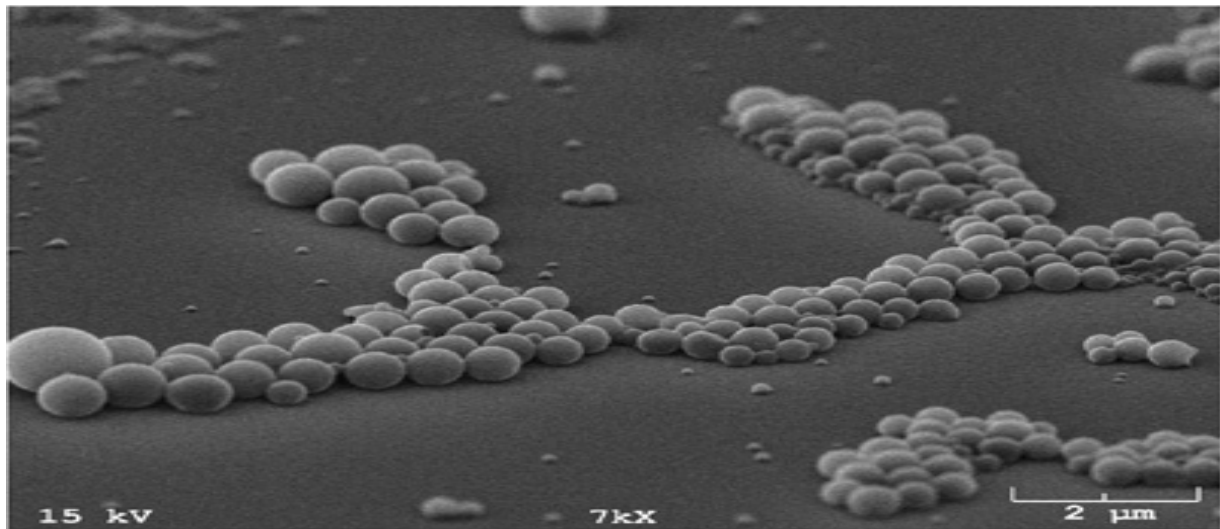
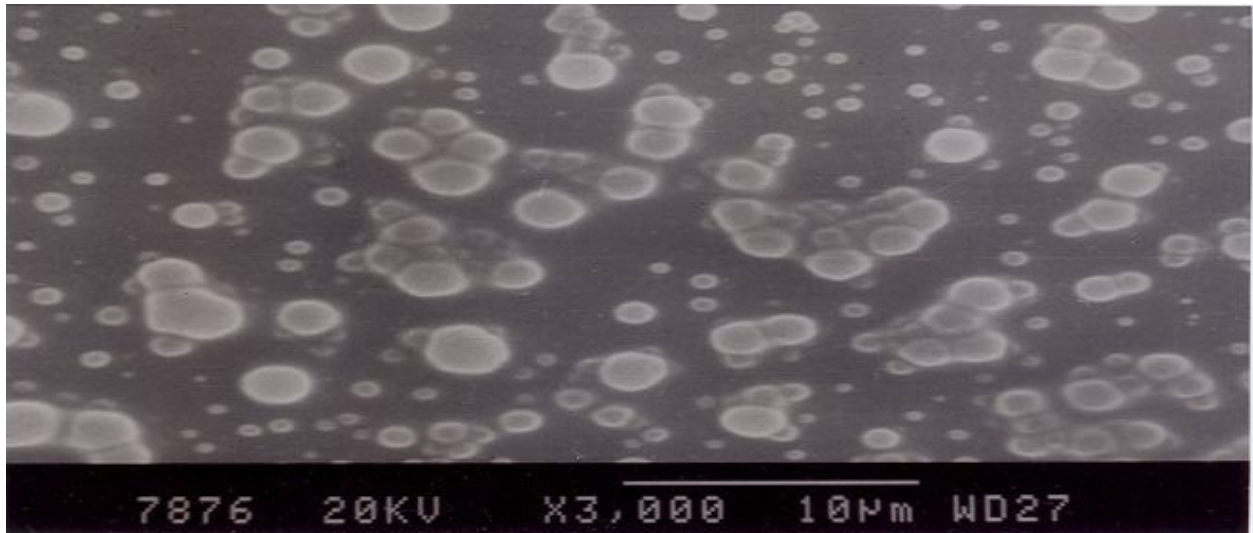


Fig:13 (F3)



8.5. PARTICAL SIZE:

The mean particle size of F1, F2,F3,F4,F5 and F6 formulations ,obtained by zetasizer analysis were 298,495,596, 698 859,892nm (table 13) respectively. The particle size of nanoparticles was found increases with increase in the polymer concentration.

Table:9 Particle size, Zeta potential and PDI of Rifampicin loaded nanoparticles

Formulation code	Drug polymer ratio (mg)	Particle size	Zeta potential(mv)	PDI
F1	1:1	298±0.25nm	-0.27±1.2mV	0.195±0.35
F2	1:2	495±0.12nm	-0.22±2.8mV	0.238±0.39
F3	1:3	596±0.52nm	-0.20±2.8mV	0.325±0.51
F4	1:1 (along with Fdc)	698±0.52nm	-0.18±1.8mV	0.325±0.35
F5	1:2(along with Fdc)	859±0.25nm	-0.16±1.4 mV	0.435±0.39
F6	1:3(along with Fdc)	892±0.12nm	-0.14±1.2 mV	0.541±0.35

8.6. Zeta potential:

The zeta performed of F1, F2, F3, F4, F5 and F6 formulations are shown in table 13. The zeta potential of nanoparticles ranges from -0.14 to -0.27 the least zeta potential with F6 and the ahighest value with F1. The zeta potential decreases with increase in the concentration of the polymer.

8.7. Polymer dispersive index:

The PDI of F1, F2, F3, F4, F5 and F6 are shown in table. The PDI of all these formulations easily formed to be less than 0.5 indicating homogenous dispersion of the drug. The results are showed in table 13.

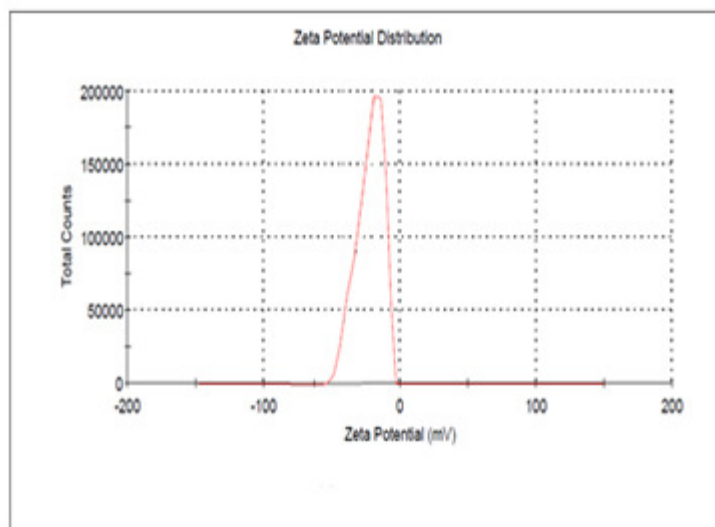


Fig:14 Rifampicin zeta

8.8. In vitro release of rifampicin nanoparticles

The diffusion profile of F1,F2, F3,F4,F5and F6 are presented in tables. The present drug diffused at every time point interval significantly dispersed between F1,F2 F3,F4,F5,F6. The diffusion rate with F5 and F6 was slower compared to F1.

Table :10 In Vitro Release Data For Pure Rifampicin(F):

Time	Trail 1	Trail 2	Trail 3	Cumulative % drug release
0	0	0	0	0
15	30	32.5	35.1	32.4 ± 2.554
30	41	42.5	40.1	41.2 ± 1.212
45	48	47.6	45.1	46.9 ± 1.572
60	56	56.4	59.4	57.2 ± 1.858

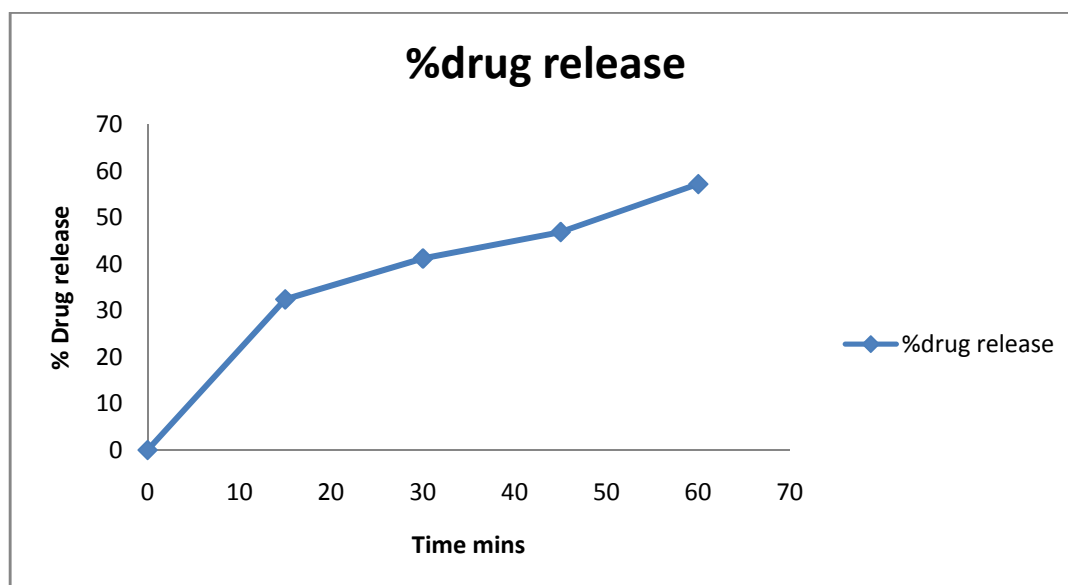


Fig:15 Percentage Drug release

Table :11 Kinetic release data for pure rifampicin (F)

Time in mints	Square root of time	Log time	Cumulative % drug release	Log cumulative % drug release	Cumulative % drug remaining	Log cumulative % drug remaining
0	0	0	0	0	100	2
15	3.872	1.176	32.4	1.510	67.6	1.829
30	5.477	1.477	41.2	1.614	58.8	1.769
45	6.708	1.653	46.9	1.671	53.1	1.725
60	7.745	1.778	57.2	1.757	42.8	1.631

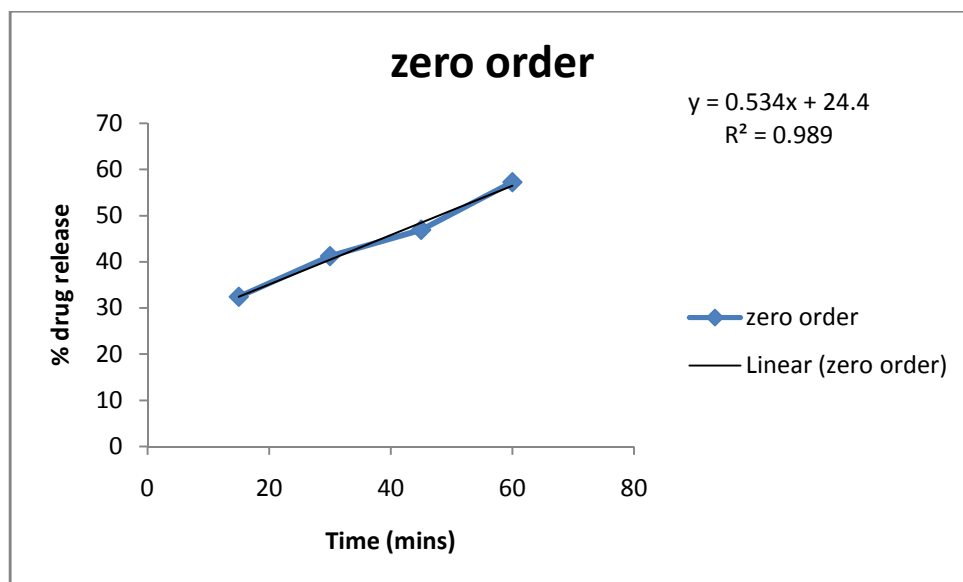


Fig: 15(a)

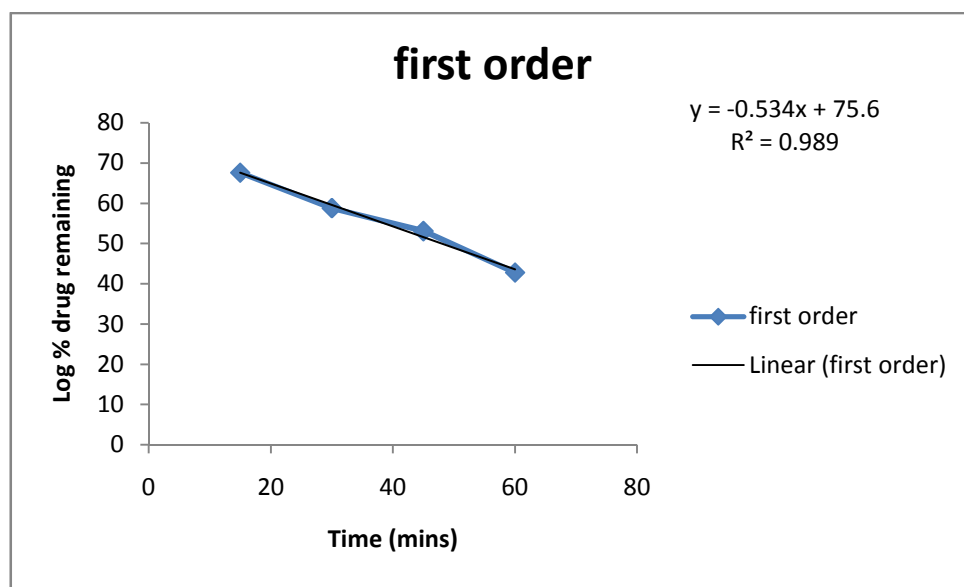


Fig:15(b)

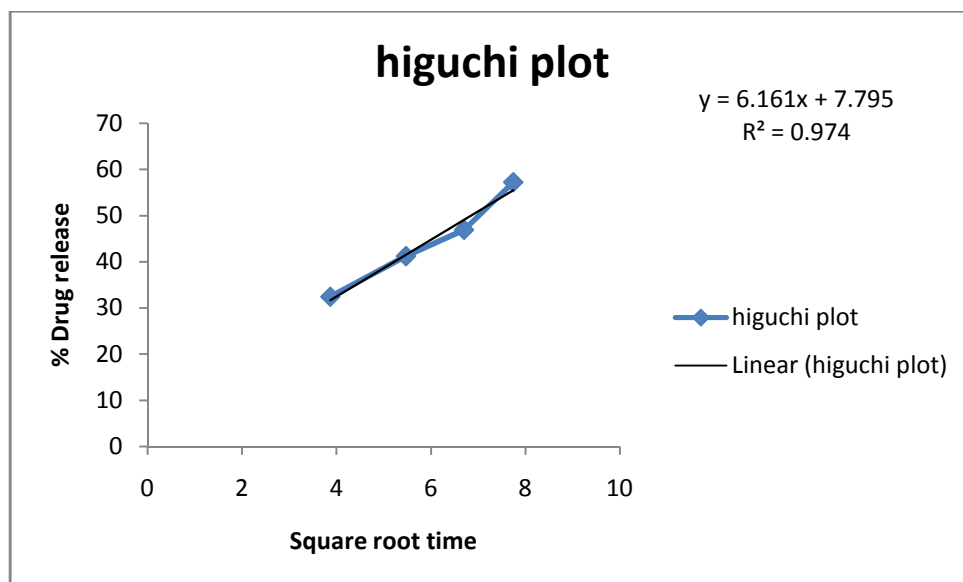


Fig:15(c)

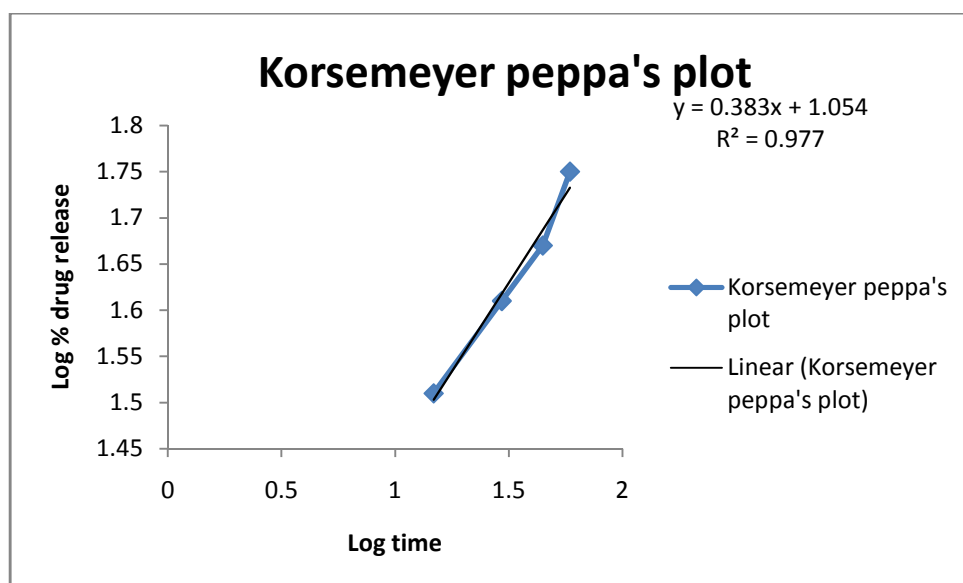


Fig:15(d)

Table: 12 In *vitro* release data for rifampicin in rifampicin along with FDC(F₀):

Time	Trail 1	Trail 2	Trail 3	Cumulative % drug release
0	0	0	0	0
15	14	13.9	14.3	14 ± 0.2082
30	18	18.5	19	18.5 ± 0.5
45	21	22	20.5	21.1 ± 0.7638
60	26	25.3	26.7	26 ± 0.7

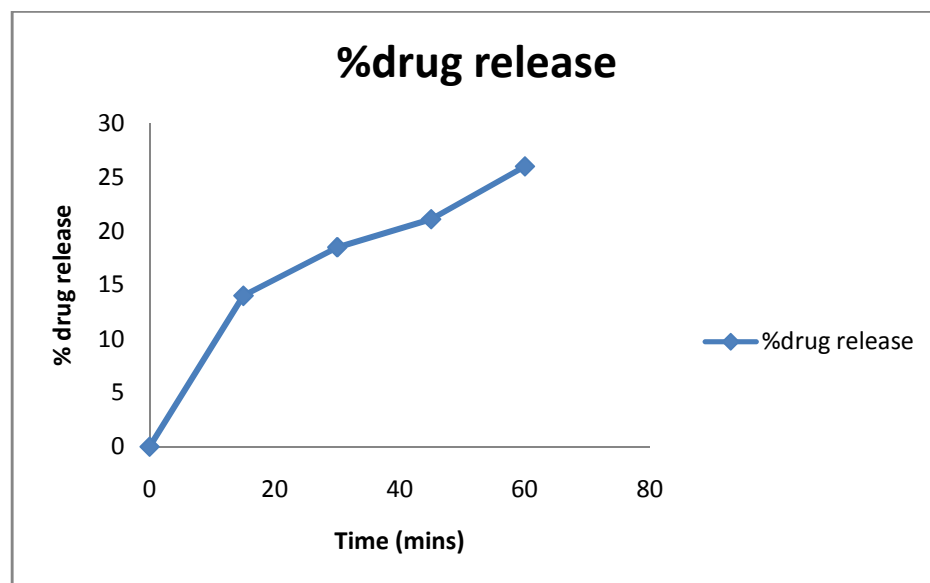


Fig:16 Percentage Drug release

Table: 13 Kinetic release data for pure rifampicin (F₀)

Time in mints	Square root of time	Log time	Cumulative % drug release	Log cumulative % drug release	Cumulative % drug remaining	Log cumulative % drug remaining
0	0	0	0	0	100	2
15	3.872	1.176	14	1.146	86	1.934
30	5.477	1.477	18.5	1.267	81.5	1.911
45	6.708	1.653	21.1	1.324	78.9	1.897
60	7.745	1.778	26	1.414	74	1.869

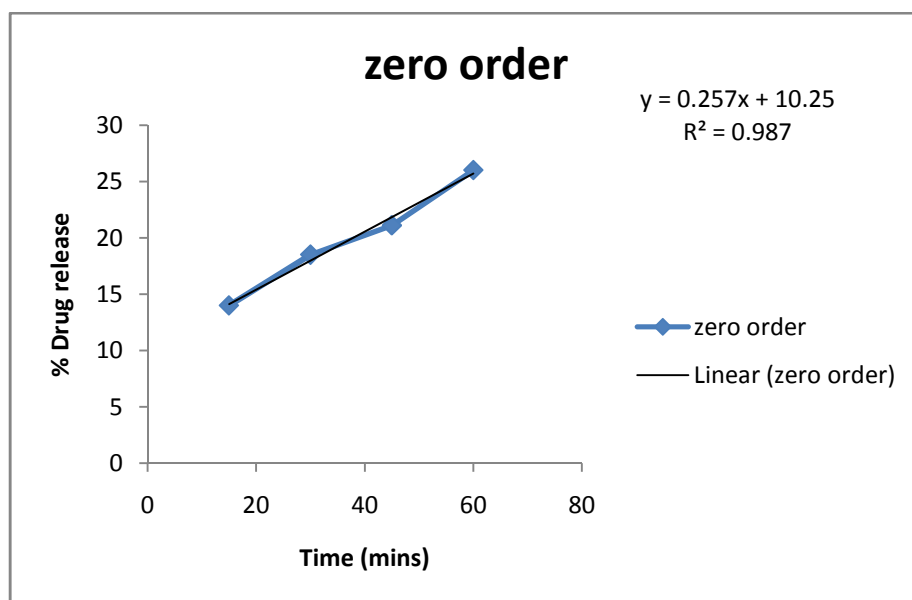


Fig:16(a)

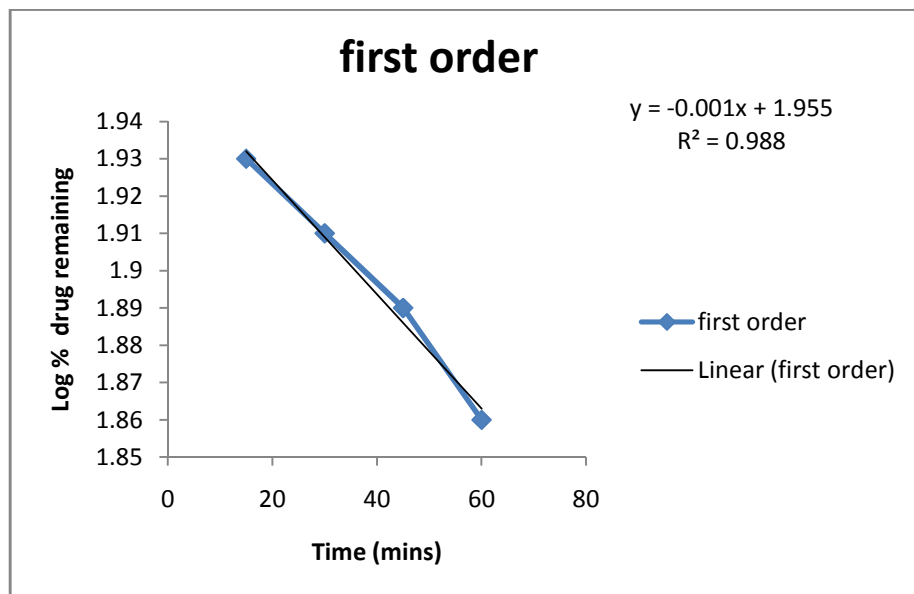


Fig:16(b)

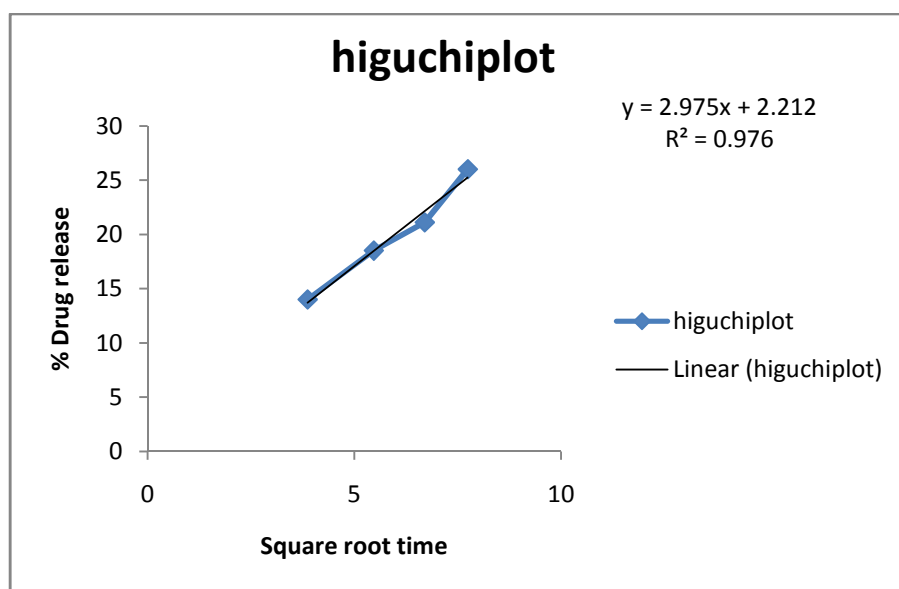


Fig:16(c)

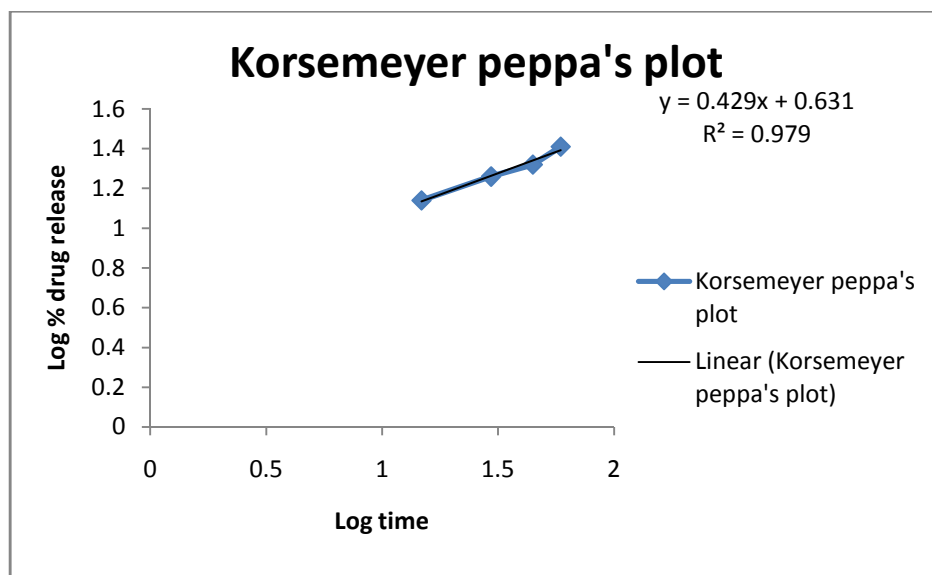


Fig:16(d)

Table :14 In vitro release data for rifampicin in rifampicin + PLGA 1:1 (F₁):

Time	Trail 1	Trail 2	Trail 3	Cumulative % drug release
0	0	0	0	0
15	15	14.9	15.3	15 ± 0.2082
30	24	24.6	23.9	24.1 ± 0.3786
45	26	26.2	25	26.4 ± 0.5292
60	35	34.8	35.2	35 ± 1.332

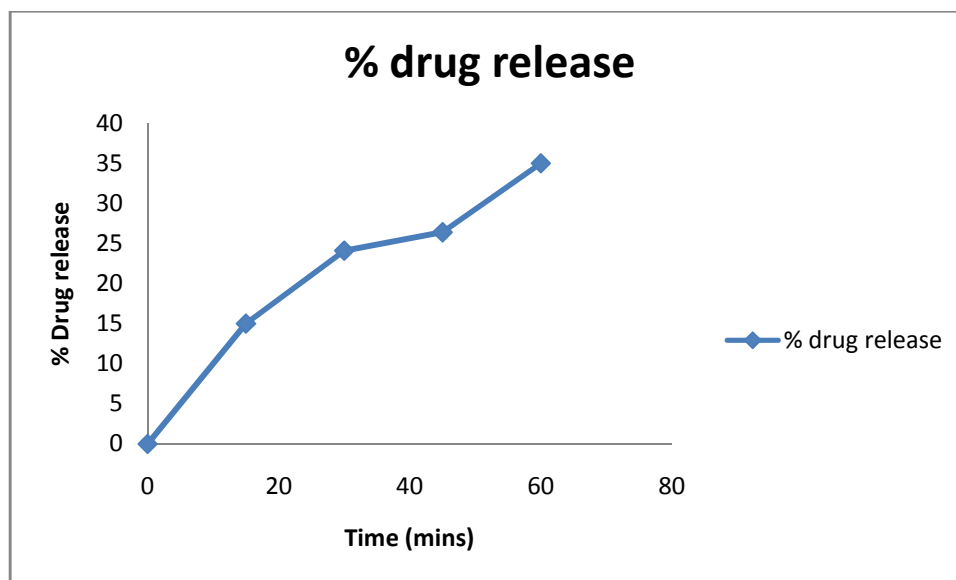


Fig: 17 Percentage Drug release

Table :15 Kinetic release data for rifampicin in rifampicin + PLGA 1:1 (F₁)

Time in mints	Square root of time	Log time	Cumulative % drug release	Log cumulative % drug release	Cumulative % drug remaining	Log cumulative % drug remaining
0	0	0	0	0	100	2
15	3.872	1.176	15	1.176	85	1.929
30	5.477	1.477	24.1	1.382	75.9	1.880
45	6.708	1.653	26.4	1.421	73.6	1.866
60	7.745	1.778	35	1.544	65	1.812

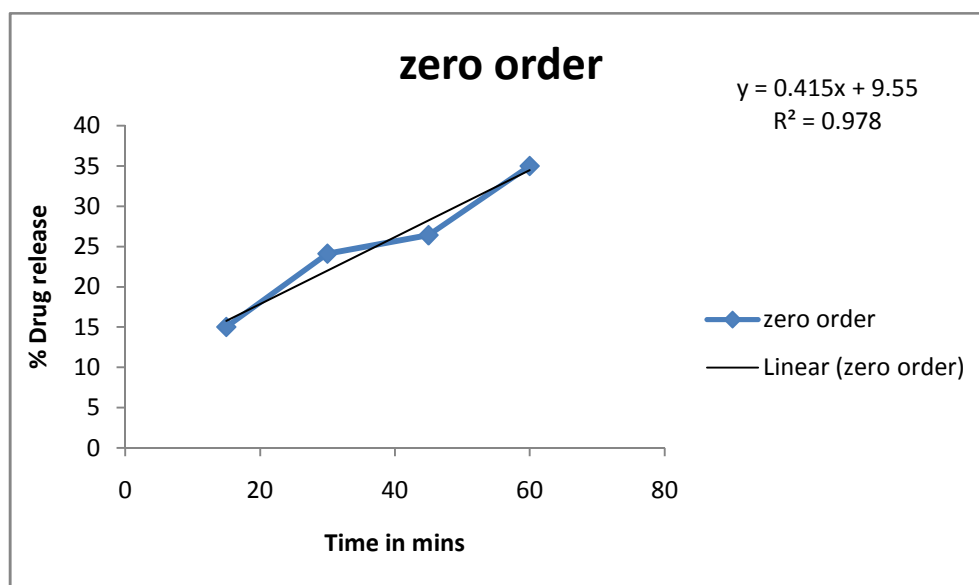


Fig:17(a)

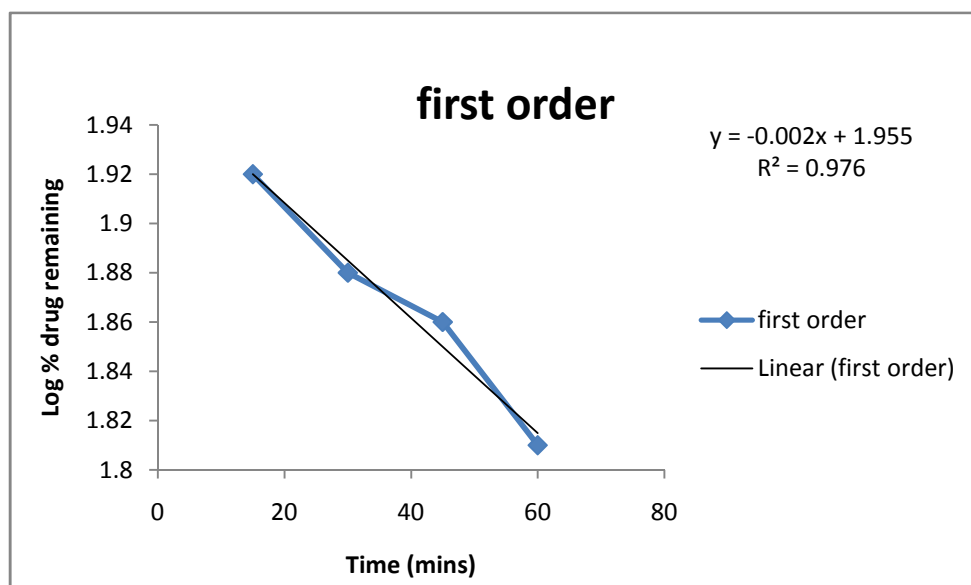


Fig: 17(b)

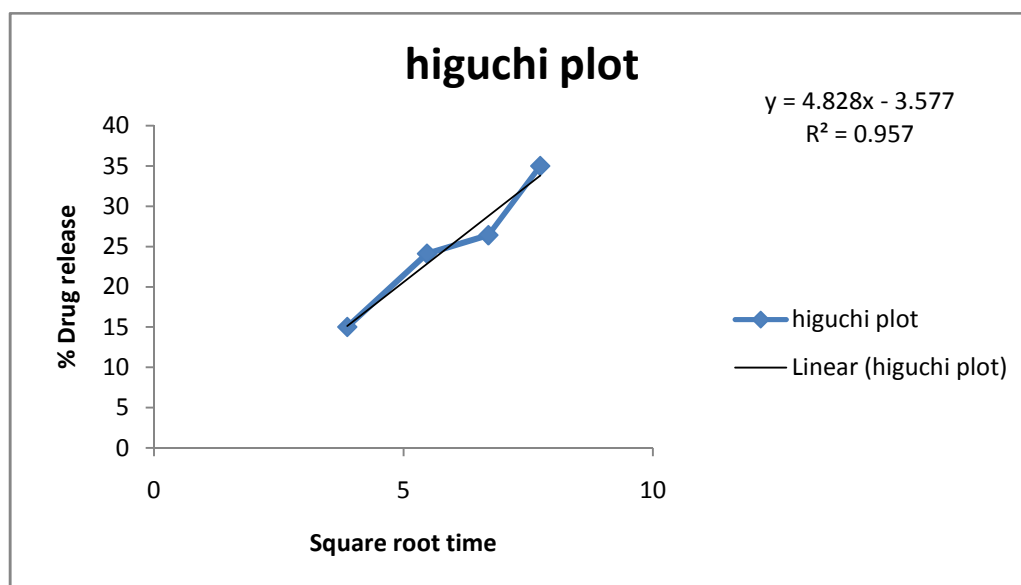


Fig:17(c)

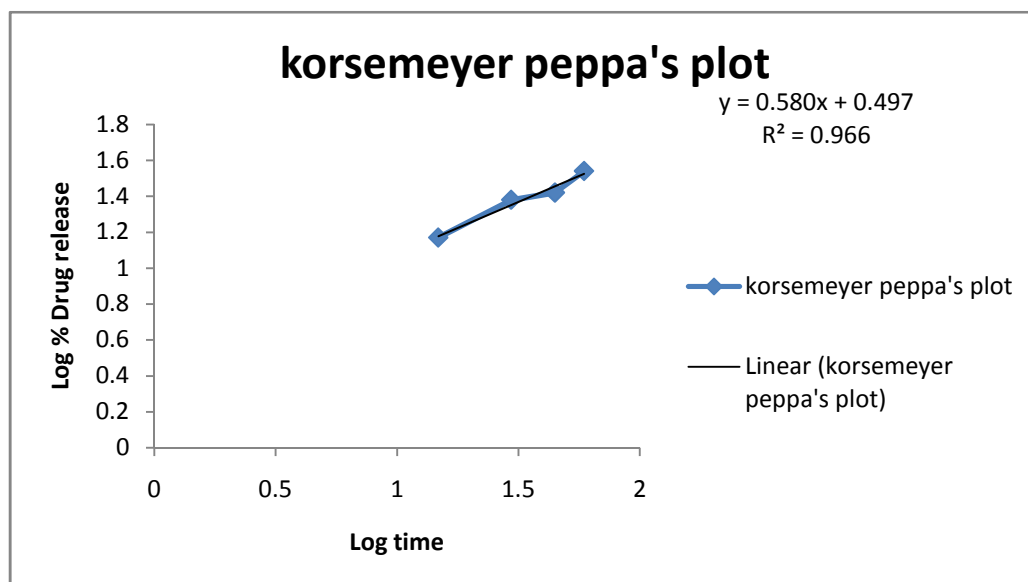


Fig:17(d)

Table :16 In *vitro* release data for rifampicin in rifampicin + PLGA 1:2 (F₂):

Time	Trail 1	Trail 2	Trail 3	Cumulative % drug release
0	0	0	0	0
15	13	13.3	12.7	13 ± 0.3
30	15	16.2	15.3	15.5 ± 0.625
45	19	20	19.4	19.8 ± 0.721
60	31	31.3	32	31.4 ± 0.513

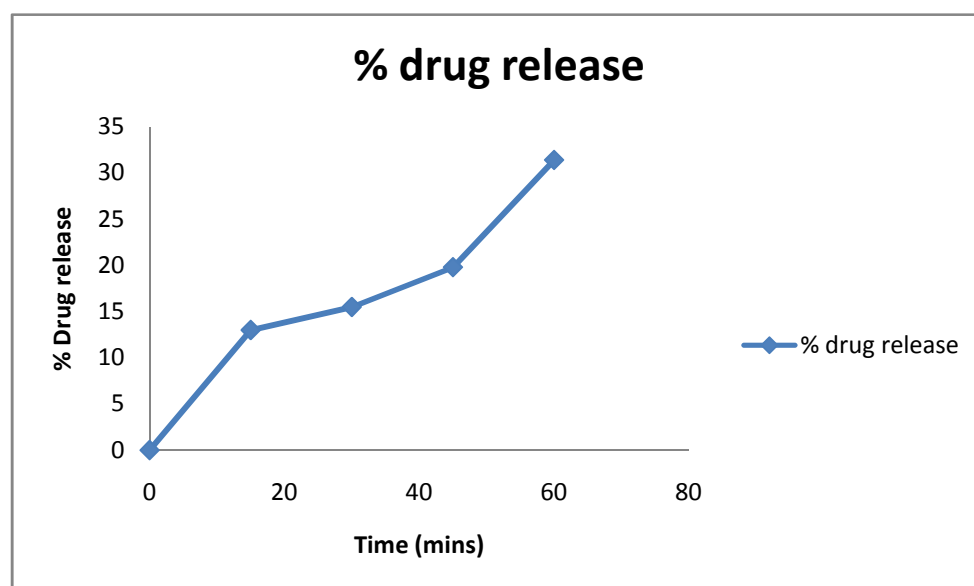


Fig:22 Percentage Drug release

Table :18 Kinetic release data for rifampicin in rifampicin + PLGA 1:2 (F₂)

Time in mints	Square root of time	Log time	Cumulative % drug release	Log cumulative % drug release	Cumulative % drug remaining	Log cumulative % drug remaining
0	0	0	0	0	100	2
15	3.872	1.176	13	1.113	87	1.939
30	5.477	1.477	15.5	1.190	84.5	1.926
45	6.708	1.653	19.8	1.296	80.2	1.904
60	7.745	1.778	31.4	1.496	68.6	1.836

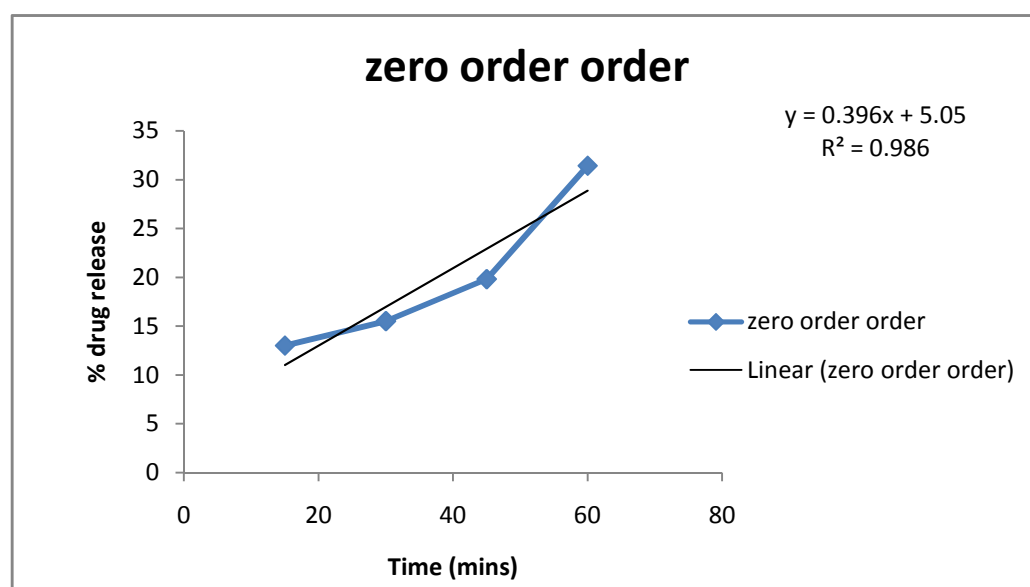


Fig:18(a)

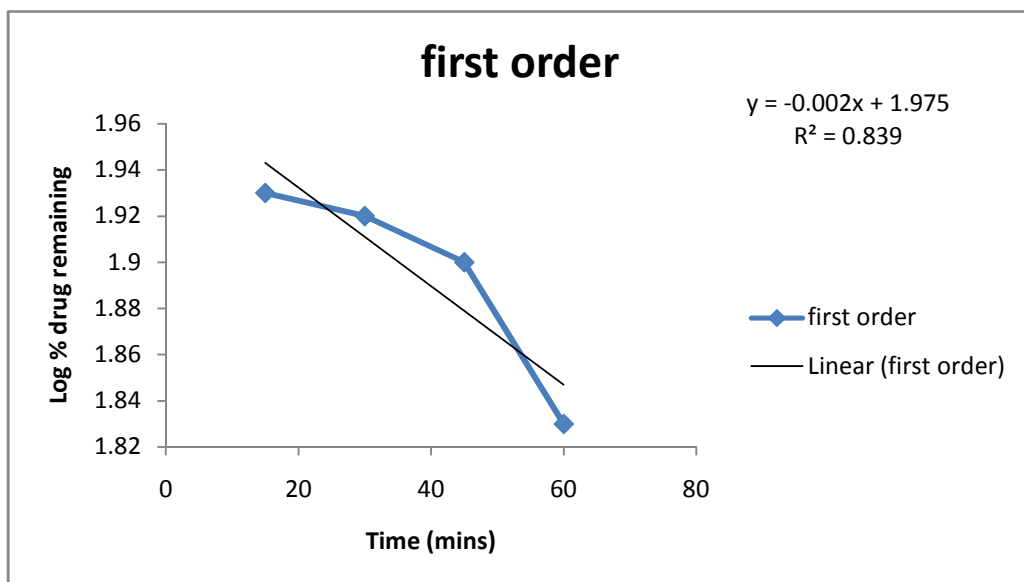


Fig:18(b)

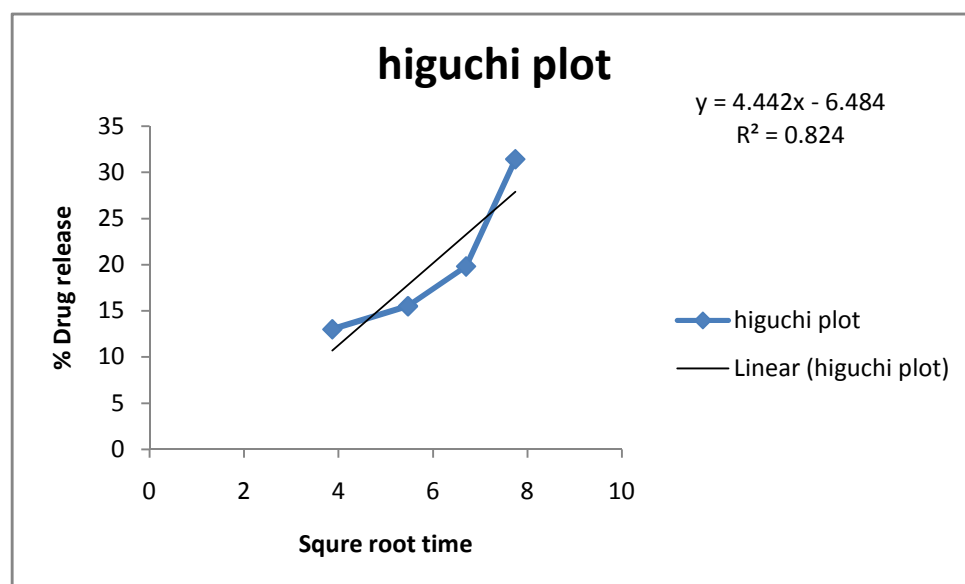


Fig:18(c)

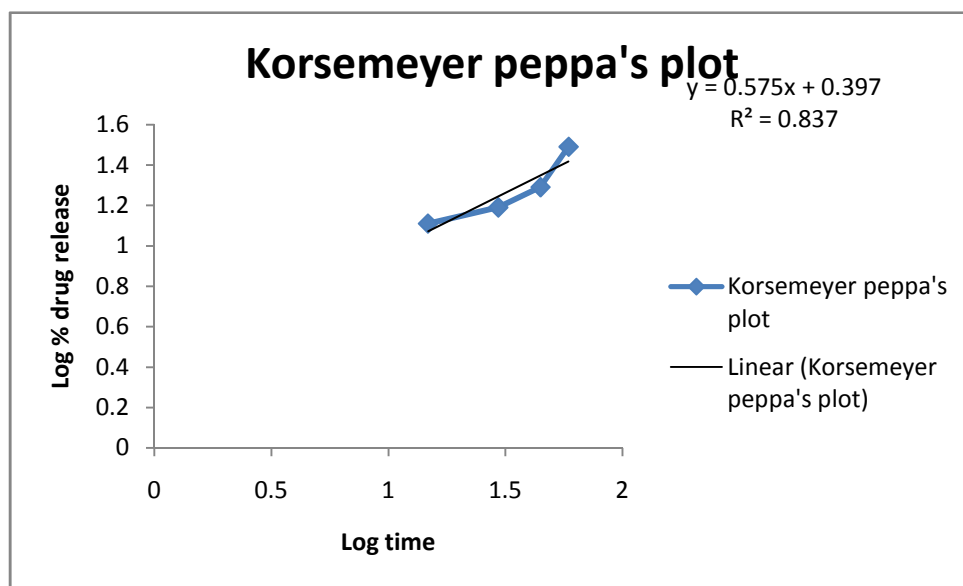


Fig:18(d)

Table :18 In *vitro* release data for rifampicin in rifampicin + PLGA 1:3 (F₃):

Time	Trail 1	Trail 2	Trail 3	Cumulative % drug release
0	0	0	0	0
15	10	10.3	9.7	10 ± 0.3
30	13.4	13.2	14	13.4 ± 0.5292
45	18	18.7	17.8	18 ± 0.4726
60	28	28.3	29.2	28 ± 0.4726

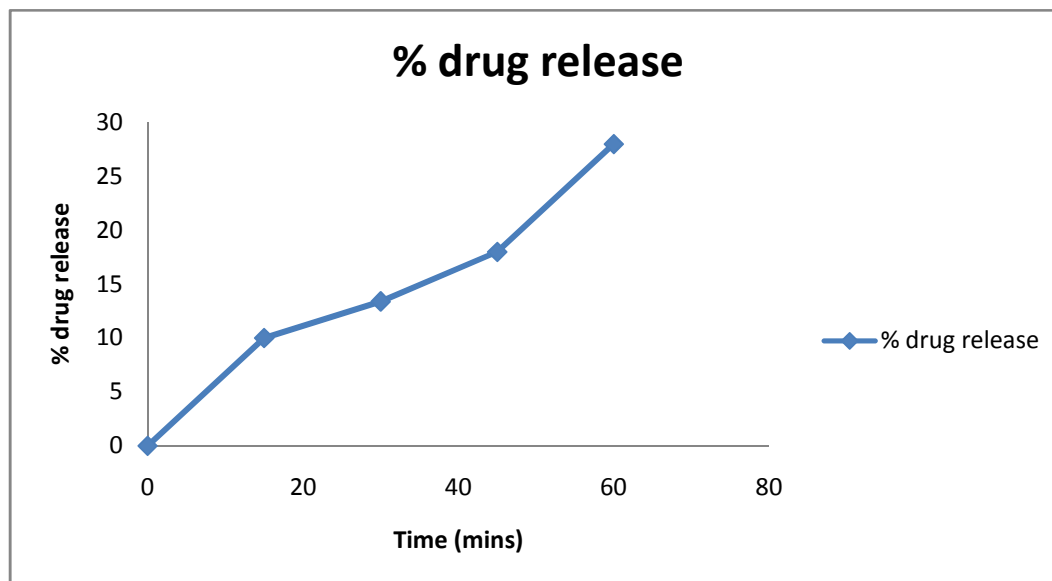


Fig:19 Percentage Drug release

Table :19 Kinetic release data for rifampicin in rifampicin + PLGA 1:3 (F₃)

Time in mints	Square root of time	Log time	Cumulative % drug release	Log cumulative % drug release	Cumulative % drug remaining	Log cumulative % drug remaining
0	0	0	0	0	100	2
15	3.872	1.176	10	1	90	1.954
30	5.477	1.477	13.4	1.127	86.6	1.937
45	6.708	1.653	18	1.255	82	1.913
60	7.745	1.778	28	1.447	72	1.857

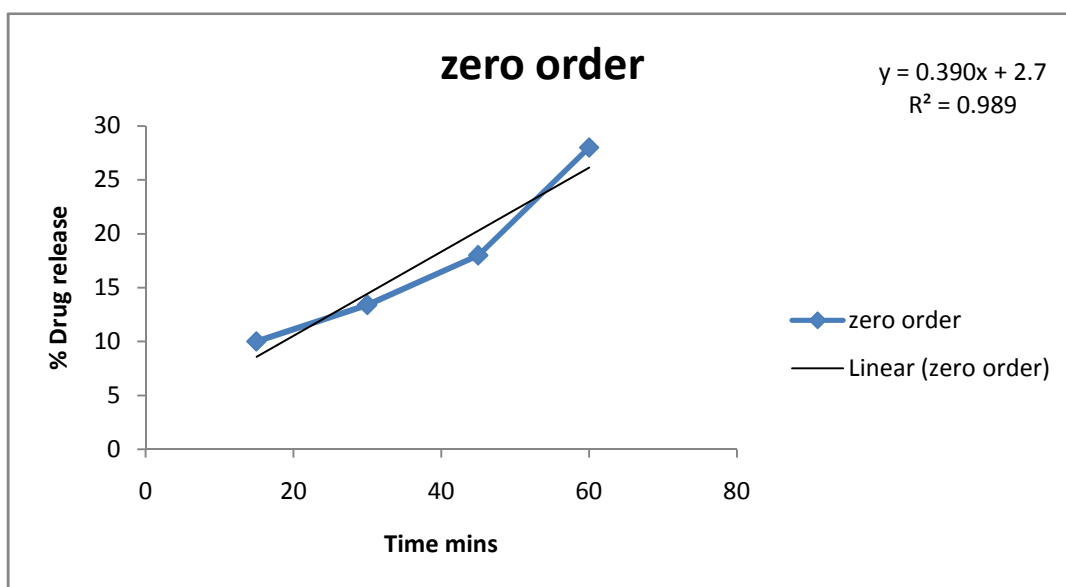


Fig:19(a)

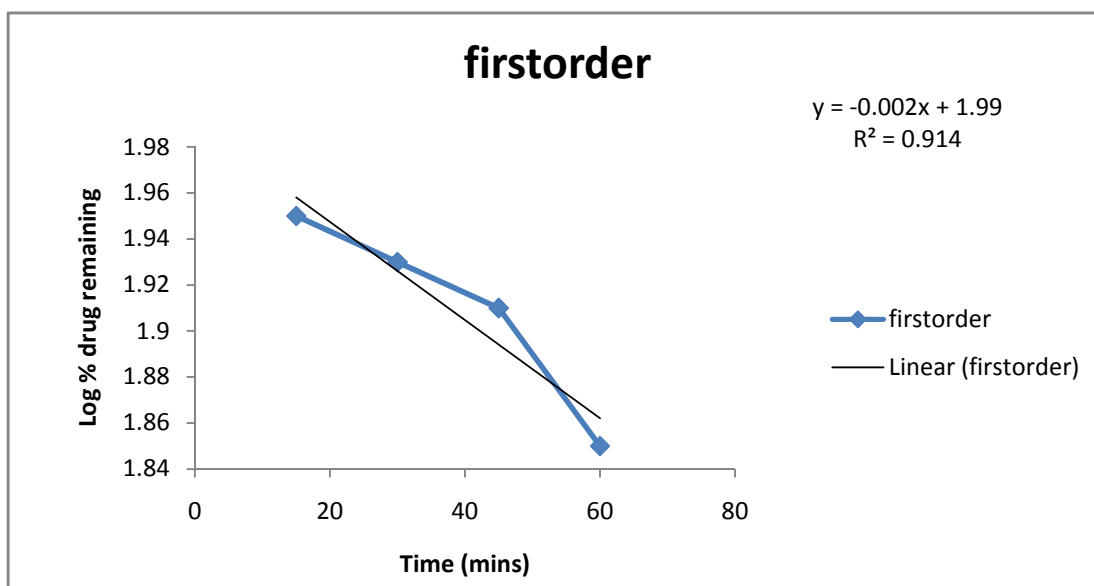


Fig:19(b)

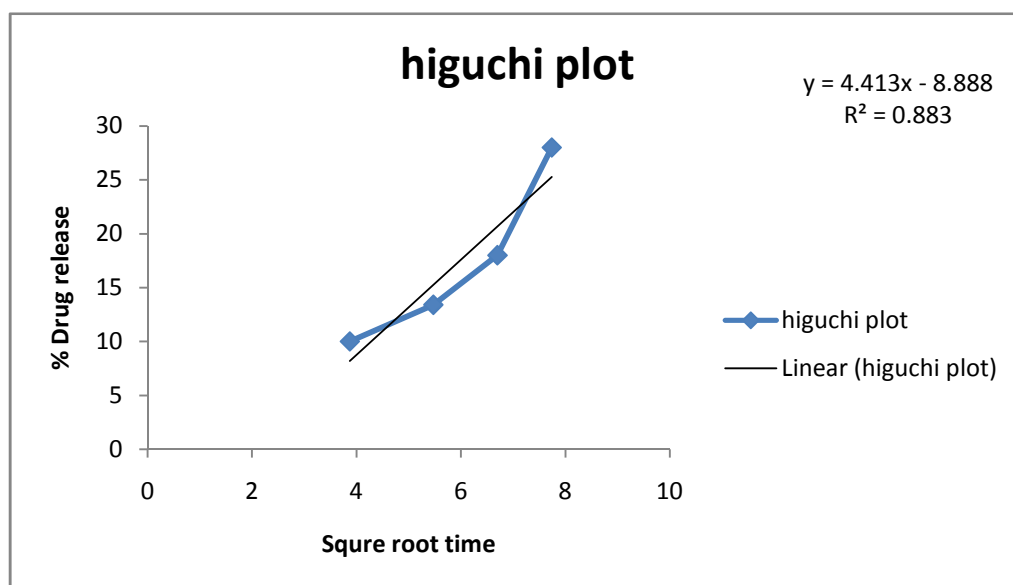


Fig:19(c)

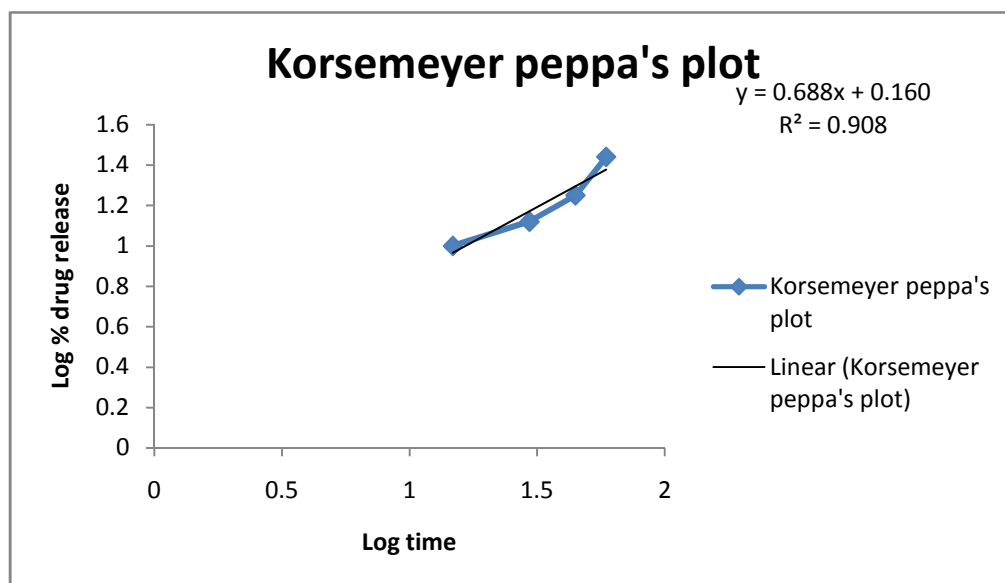


Fig:19(d)

Table :20 In *vitro* release data for rifampicin in rifampicin + PLGA 1:1 along with FDC (F₄):

Time	Trail 1	Trail 2	Trail 3	Cumulative % drug release
0	0	0	0	0
15	8	8.7	9.5	8.5 ± 0.513
30	11	11.3	12	11.4 ± 0.513
45	17	15.1	16.7	16.9 ± 0.208
60	22.4	22.3	23	22.4 ± 0.513

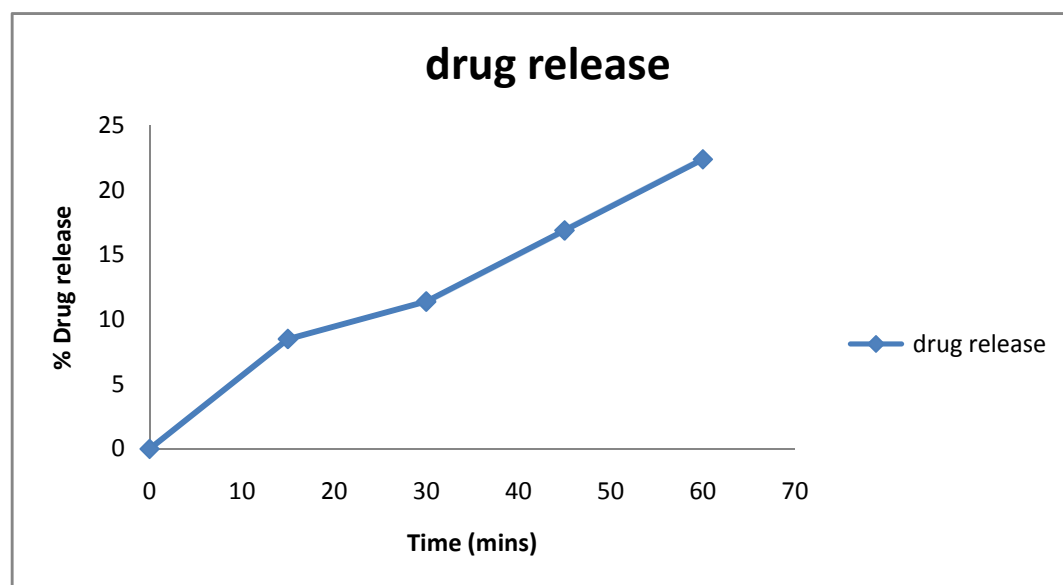


Fig: 20 Percentage Drug release

Table: 21 Kinetic release data for rifampicin in rifampicin + PLGA 1:1 along with FDC (F₄)

Time in mints	Square root of time	Log time	Cumulative % drug release	Log cumulative % drug release	Cumulative % drug remaining	Log cumulative % drug remaining
0	0	0	0	0	100	2
15	3.872	1.176	8.5	0.929	91.5	1.961
30	5.477	1.477	11.4	1.056	88.6	1.947
45	6.708	1.653	16.9	1.227	83.1	1.919
60	7.745	1.778	22.4	1.350	77.6	1.889

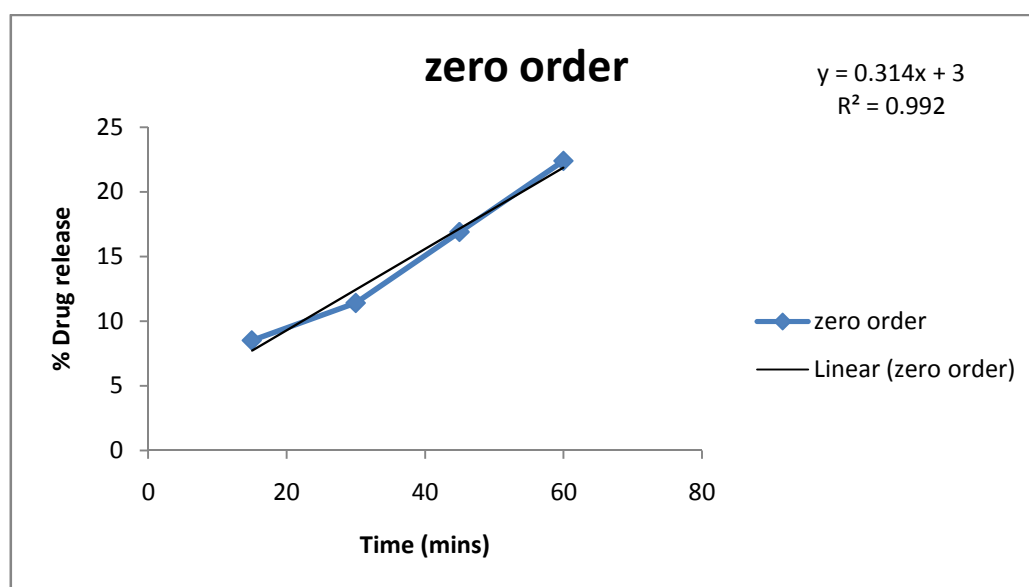


Fig: 20(a)

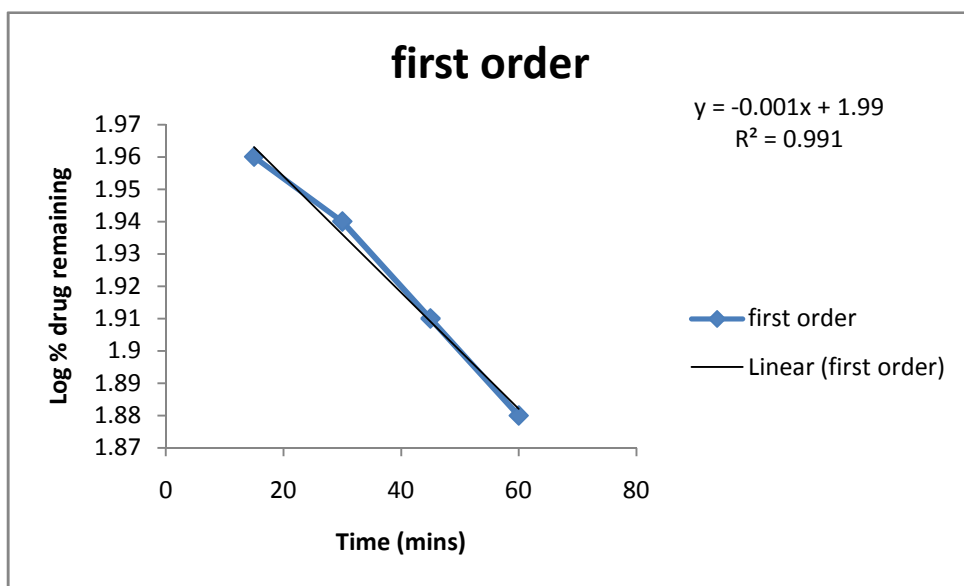


Fig: 20(b)

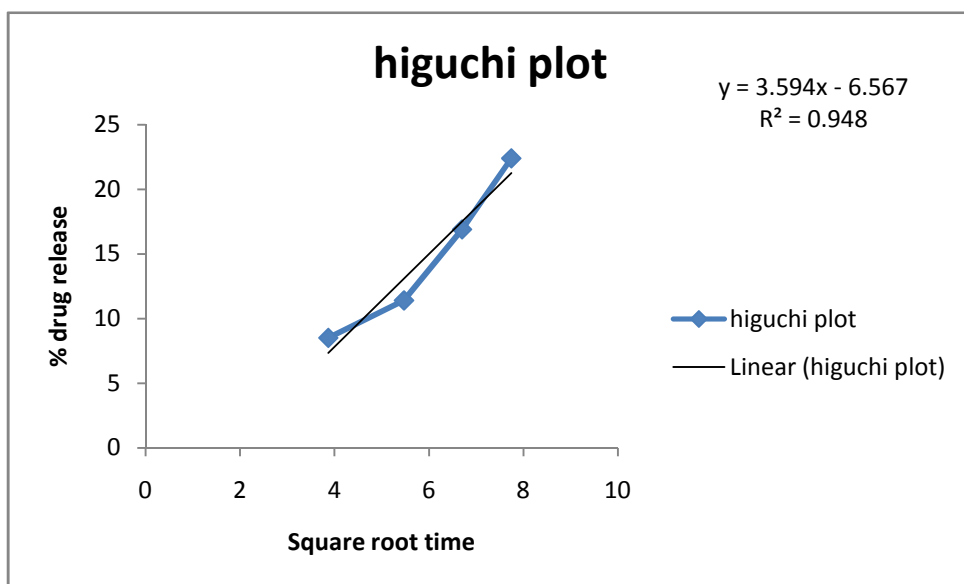


Fig: 20(c)

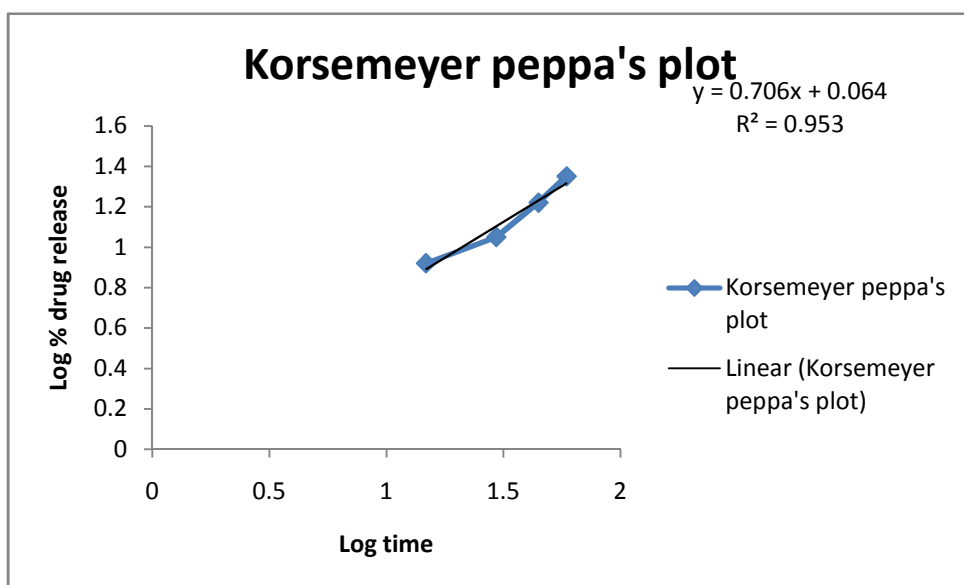


Fig: 20(d)

Table: 22 In *vitro* release data for rifampicin in rifampicin + PLGA 1:2 along with FDC (F₅):

Time	Trail 1	Trail 2	Trail 3	Cumulative % drug release
0	0	0	0	0
15	6.5	6.3	5.7	6.5 ± 0.513
30	9.9	9.7	8.8	9.4 ± 0.513
45	13	14.1	15	14.9 ± 0.208
60	19.4	20	21.3	20.4 ± 0.513

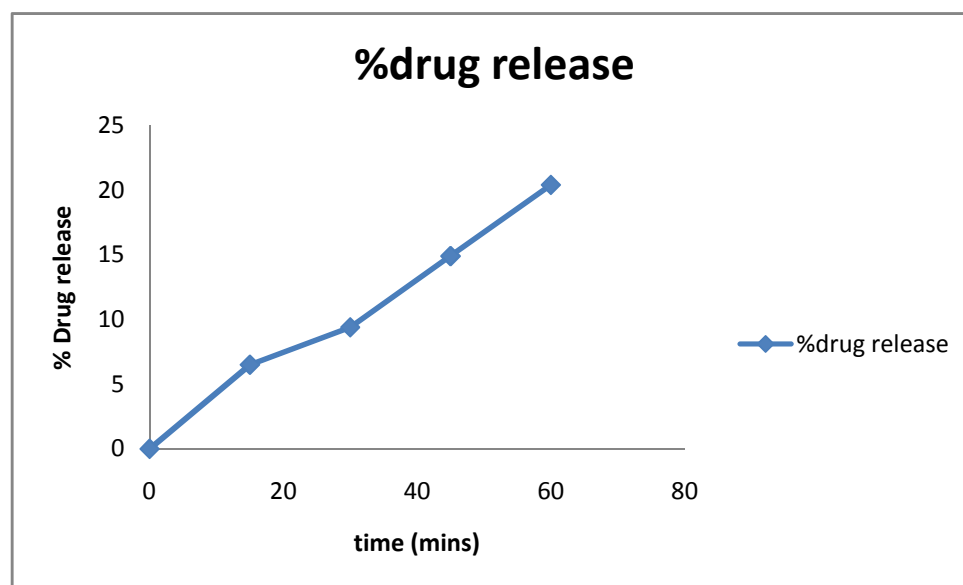


Fig: 21 Percentage Drug release

Table: 23 Kinetic release data for rifampicin in rifampicin + PLGA 1:2 along with FDC (F₅)

Time in mints	Square root of time	Log time	Cumulative % drug release	Log cumulative % drug release	Cumulative % drug remaining	Log cumulative % drug remaining
0	0	0	0	0	100	2
15	3.872	1.176	6.5	0.812	93.5	1.970
30	5.477	1.477	9.4	0.973	90.6	1.957
45	6.708	1.653	14.9	1.173	85.1	1.929
60	7.745	1.778	20.4	1.309	79.6	1.900

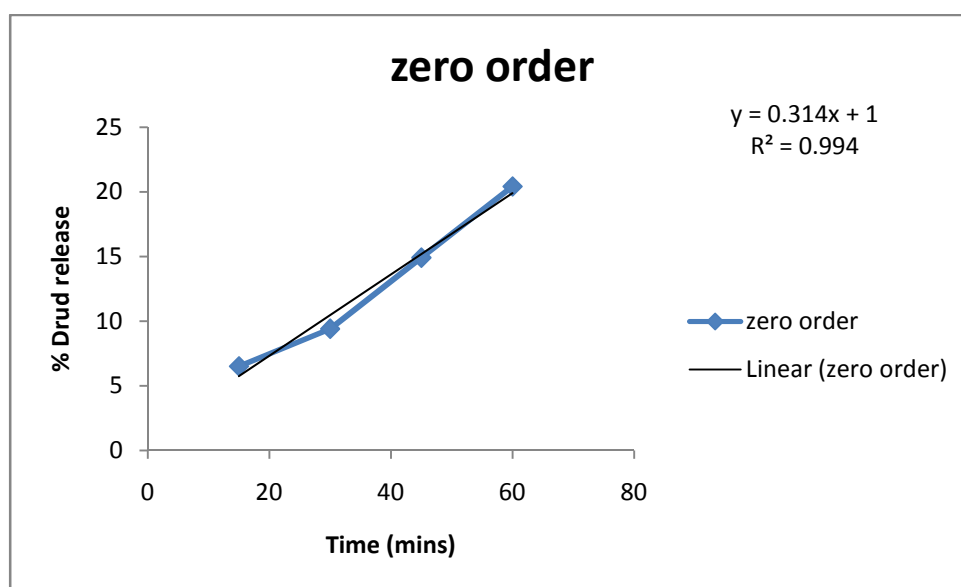


Fig: 21 (a)

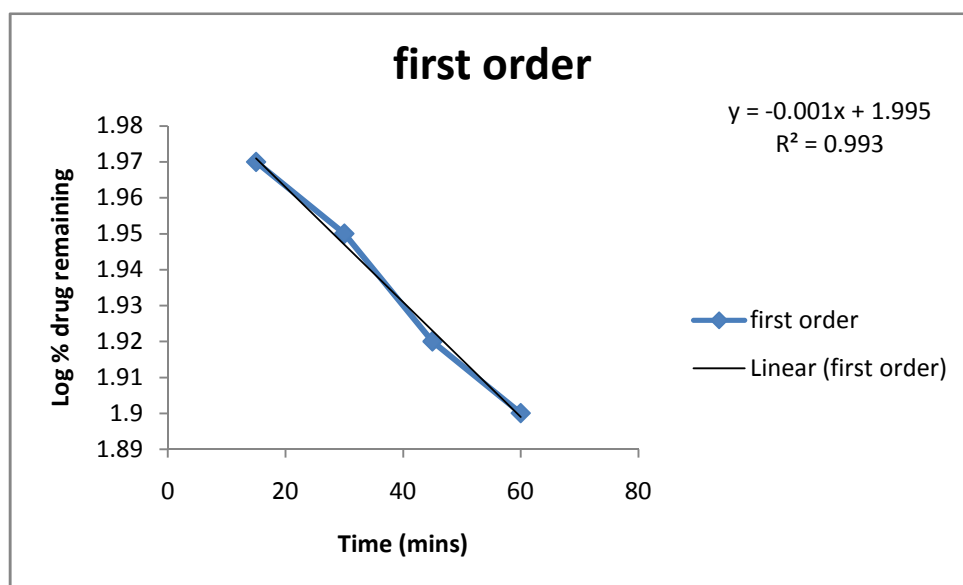


Fig: 21 (b)

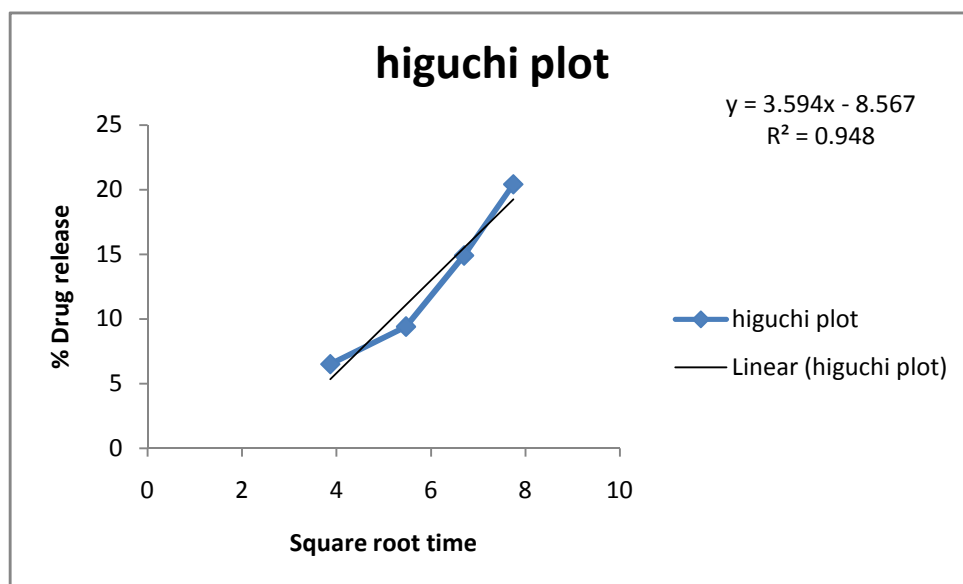


Fig:21 (c)

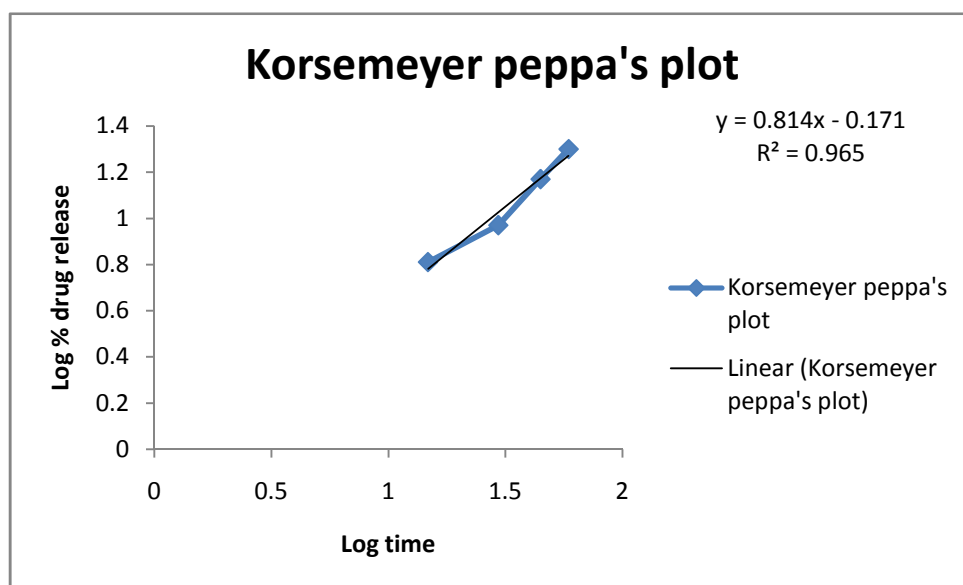


Fig:21 (d)

Table :24 In *vitro* release data for rifampicin in rifampicin + PLGA 1:3 along with FDC (F₆):

Time	Trail 1	Trail 2	Trail 3	Cumulative % drug release
0	0	0	0	0
15	4	9	5.7	4.5 ± 0.513
30	10	10.3	9	9.3 ± 0.513
45	13	13.6	14	13.2 ± 0.208
60	17	16.7	17.8	17.2 ± 0.513

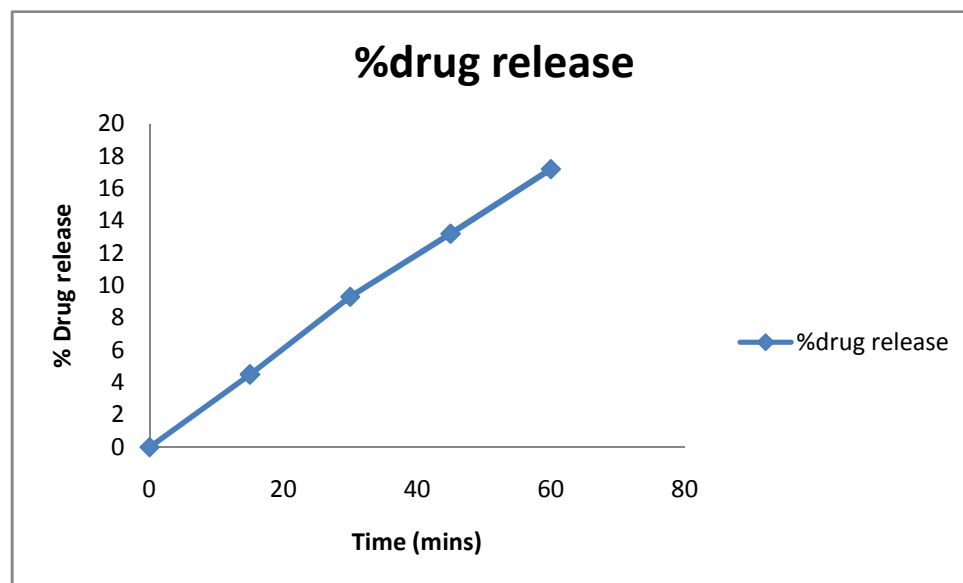


Fig: 22 Percentage Drug release

Table :25 Kinetic release data for rifampicin in rifampicin + PLGA 1:3 along with FDC (F₆)

Time in mints	Square root of time	Log time	Cumulative % drug release	Log cumulative % drug release	Cumulative % drug remaining	Log cumulative % drug remaining
0	0	0	0	0	100	2
15	3.872	1.176	4.5	0.653	95.5	1.980
30	5.477	1.477	7.4	0.869	92.6	1.966
45	6.708	1.653	11.9	1.075	88.1	1.944
60	7.745	1.778	18.4	1.264	81.6	1.911

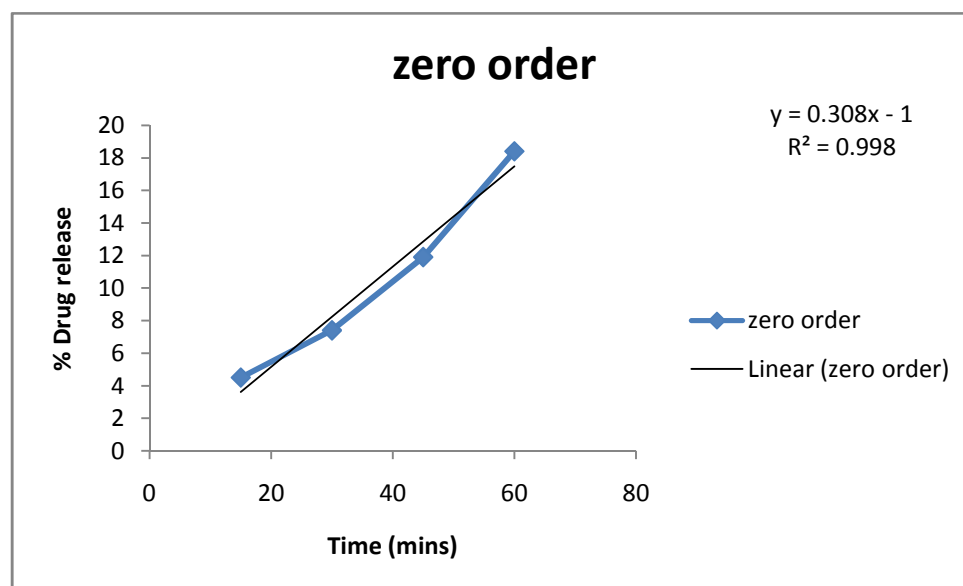


Fig: 22 (a)

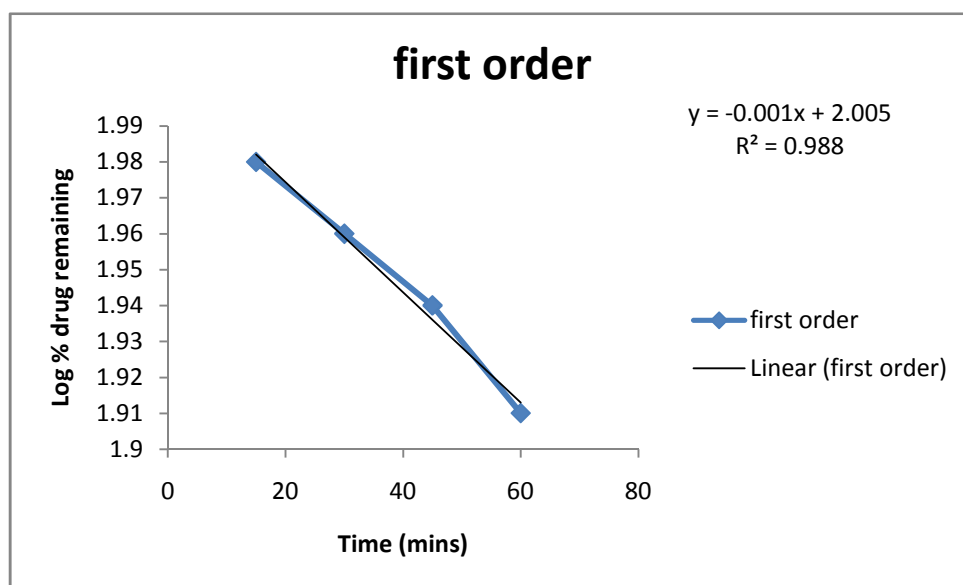


Fig:22 (b)

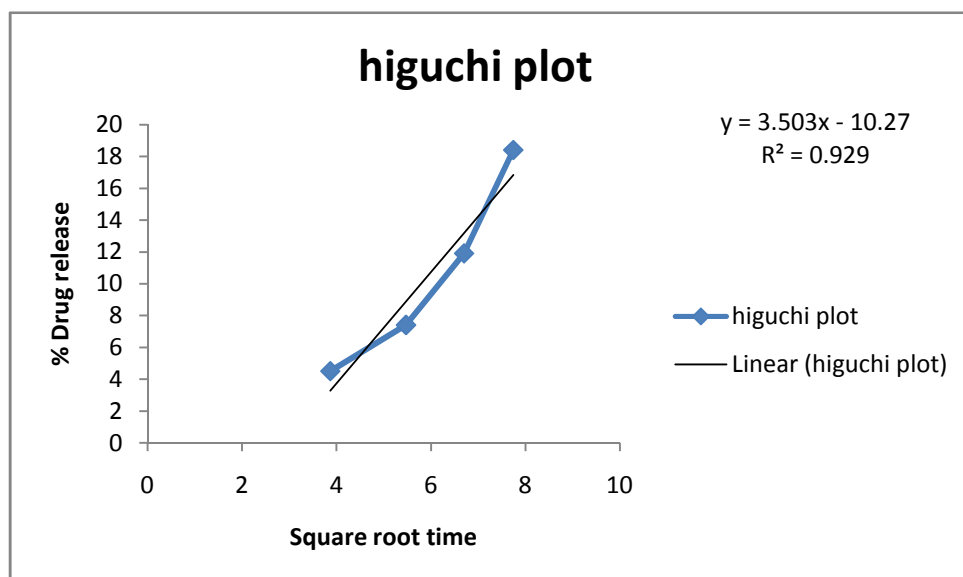


Fig:22 (c)

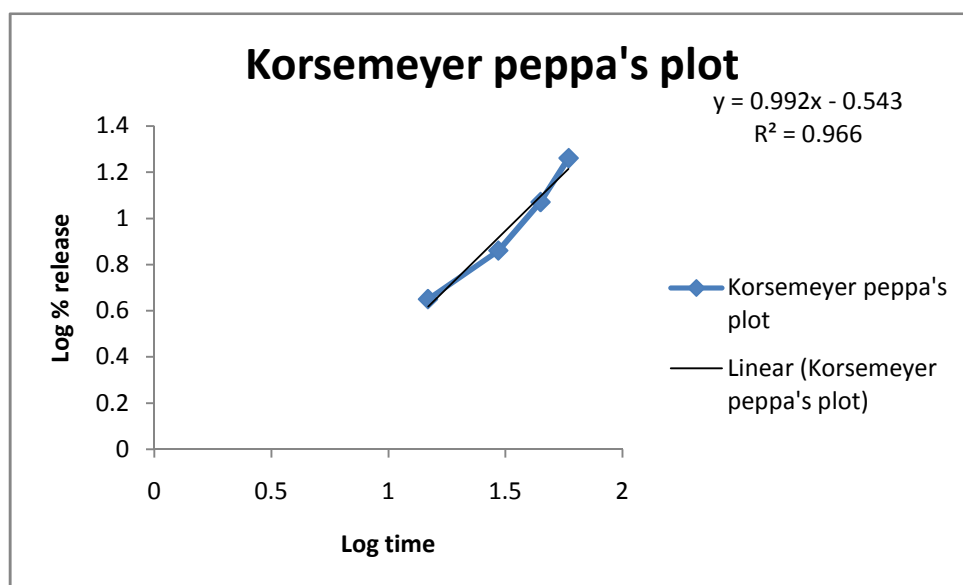


Fig:22 (d)

Table: 26 COMPARITIVE % DRUG RELEASE

Time	RIF ALONE	RIF+FD C	RIF+PLGA 1:1	RIF+PLG A 1:2	RIF+PLGA 1:3	RIF+PLGA 1:1+FDC	RIF+PLG A 1:2+FDC	RIF+PLG A 1:3+FDC
0	0	0	0	0	0	0	0	0
15	32.4±2.554	14±0.208	15±0.208	13±0.3	10±0.3	8.5±0.513	6.5±0.513	4.5±0.513
30	41.2±1.212	18.5±0.5	24.1±0.378	15.5±0.624	13.4±0.529	11.4±0.513	9.4±0.513	9.3±0.513
45	46.9±1.572	21.1±0.763	26.4±0.529	19.8±0.721	18±0.472	16.9±0.208	14.9±0.208	13.2±0.108
60	57.2±1.858	26±0.7	35±1.332	31.4±0.513	28±0.472	22.4±0.513	20.4±0.513	17.2±0.513

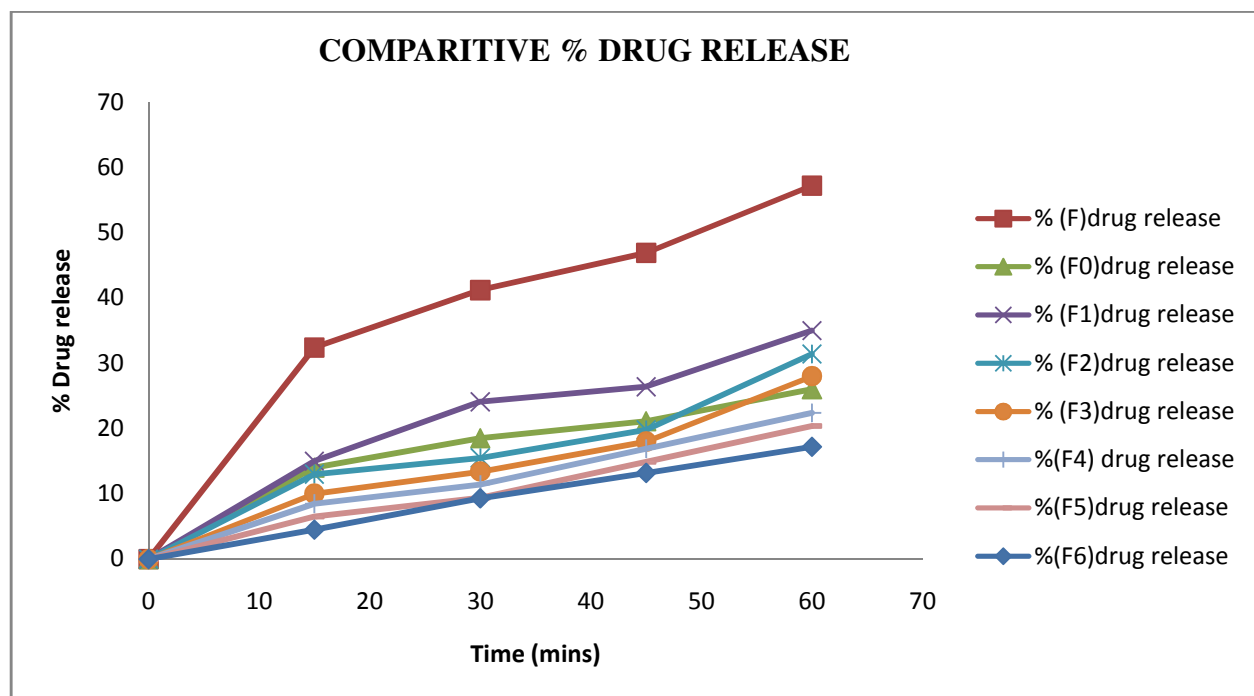


Fig: 23

8.9. Table :27 In vitro release kinetic data Rifampicin loaded nanoparticles (DIFFUSION)

Formulation code	First order “R²”value	Zero order “R²”value	Higuchi plot “R²”value	Peppas plot “R²”value	n value
F1	0.959	0.978	0.957	0.966	0.580
F2	0.888	0.986	0.824	0.837	0.575
F3	0.935	0.989	0.883	0.908	0.688
F4	0.982	0.992	0.948	0.953	0.706
F5	0.982	0.994	0.948	0.965	0.814
F6	0.970	0.998	0.929	0.966	0.992

K₀. Zero order rates constant

K₁ - First order rate constant

R – Coefficient of correlation

N – Diffusion exponent

The regression co-efficient values are zero order plots were compared. It was observed that the “R” value of zero order plot were in the range of 0.976 to 0.988 from all the six formulations. The “R” values of first order plot were in the range of 0.959 to 0.970 based on the highest regression values (R), the best fit model for F1, F2, F3, F4 and F6. Followed zero order release. The “R” value of the linear regression for korsmeyer plot were found in the range of 0.966 to 0.966 for all the formulation indicating that the data fit into the korsmeyer plot model well, and the drug release was found to be predominately controlled by swelling process.

When the slope n values of formulation F1, F2, F3, F4, F5 and F6 in korsmeyer equation ($F1=0.966$, $F2=0.837$, $F3=0.908$, $F4=0.953$, $F5=0.965$ and $F6=0.966$) were compared, it was observed that increasing polymer concentration in the nanoparticle led to increase in the slope value from 0.580 to 0.992 indicating that the drug release by Non –Fickian release. ($n < 1.0$) Non –Fickian release mechanism which involves swelling controlled release of the drug.

Turkey – Kramer multiple comparison test: t_{90}

The release data were subject to ANOVA with Turkey- Kramer comparison test F2 showed release pattern as compared F1 ($p < 0.05$). Similar release behavior was observed between F3 and F1 ($p < 0.001$) and between F4 and F1 ($p < 0.05$). Similarly the release behavior was observed between F5 and F1 ($p < 0.05$). Similar release behavior was observed between F6 and F1 ($p < 0.001$). F3 showed release pattern as compared F2 ($p < 0.05$). Similar release behavior was observed between F3 and F2 ($p < 0.001$) and between F4 and F2 ($p < 0.05$). Similarly the release behavior was observed between F5 and F2 ($p < 0.05$). Similar release behavior was observed between F6 and F2 ($p < 0.001$). F4 showed release pattern as compared F3 ($p < 0.05$). Similar release behavior was observed between F4 and F3 ($p < 0.001$) and between F5 and F3 ($p < 0.05$). Similar release behavior was observed between F6 and F3 ($p < 0.001$). F5 showed release pattern as compared F4 ($p < 0.05$). Similar release behavior was observed between F5 and F4 ($p < 0.05$). Similar release behavior was observed between F6 and F4 ($p < 0.001$). Similar release behavior was observed between F5 and F6 ($p < 0.001$). The result suggest that the slow drug release characteristics appear to be influenced by polymer concentration

Table: 28 Turkey – Kramer multiple comparison test: t_{90}

Comparision	“p” value
F1 Vs F2	P< 0.05
F1 Vs F3	P< 0.001
F1 Vs F4	P< 0.05
F1VsF5	P< 0.05
F1VsF6	P< 0.001
F2VsF3	P< 0.05
F2VsF4	P< 0.05
F2VsF5	P< 0.05
F2VsF6	P< 0.001
F3VsF4	P< 0.05
F3VsF5	P< 0.05
F3VsF6	P< 0.001
F4VsF5	P< 0.05
F4VsF6	P< 0.001
F5VsF6	P< 0.001

The “P” value is <0.0001, considered extremely significant. Variation among column means is significantly greater than expected by chance.

Dissolution stability of rifampicin alone at pH 1.2 buffers

The result of dissolution stability study of the RIF alone was shown in Tables 29,30 and 31 and figures 24 and 25. The degradation of RIF was increased gradually over the time period between 0-60min. The percent degradation of RIF was found to be increased from 2.42, 7.51, 10.19 and 13.35 in the time period of 15, 30, 45, and 60min respectively. The percent formation of 3FRSV was shown as 2.35, 7.29, 9.89 and 12.96 at 15, 30, 45 and 60min respectively.

Table :29 Percent degradation of rifampicin alone in pH 1.2 buffer(F)

TIME (min)	Percent degradation of RIF			MEAN \pm S.D
	TRIAL1	TRIAL2	TRIAL3	
0	-	-	-	-
15	2.55	2.42	2.29	2.42 \pm 0.130
30	8.67	7.51	6.66	7.51 \pm 1.009
45	11.40	9.12	10.17	10.19 \pm 1.141
60	13.38	12.34	11.26	13.35 \pm 1.060

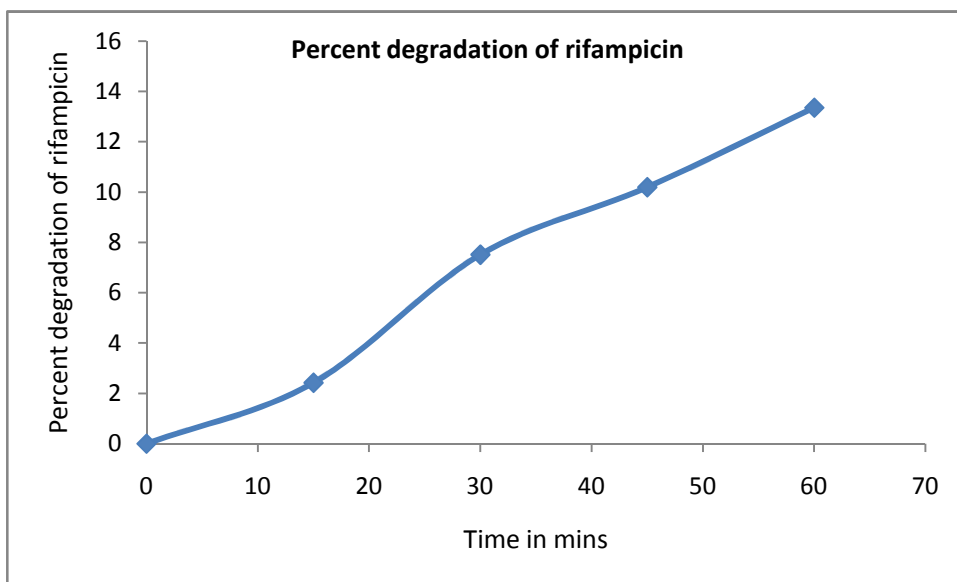


Fig:24 Percent degradation of rifampicin alone in pH 1.2 buffer

Table :30 Percent formation of metabolite (3FRSV) of rifampicin in RIF alone at pH 1.2 buffer(F)

TIME (min)	Percent formation of 3FRSV			MEAN \pm S.D
	TRIAL1	TRIAL2	TRIAL3	
0	0	0	0	0 \pm 0.00000
15	2.25	2.45	2.35	2.35 \pm 0.10000
30	7.20	7.29	7.38	7.29 \pm 0.09000
45	9.89	9.87	9.90	9.89 \pm 0.01528
60	12.91	13.00	12.97	12.96 \pm 0.04583

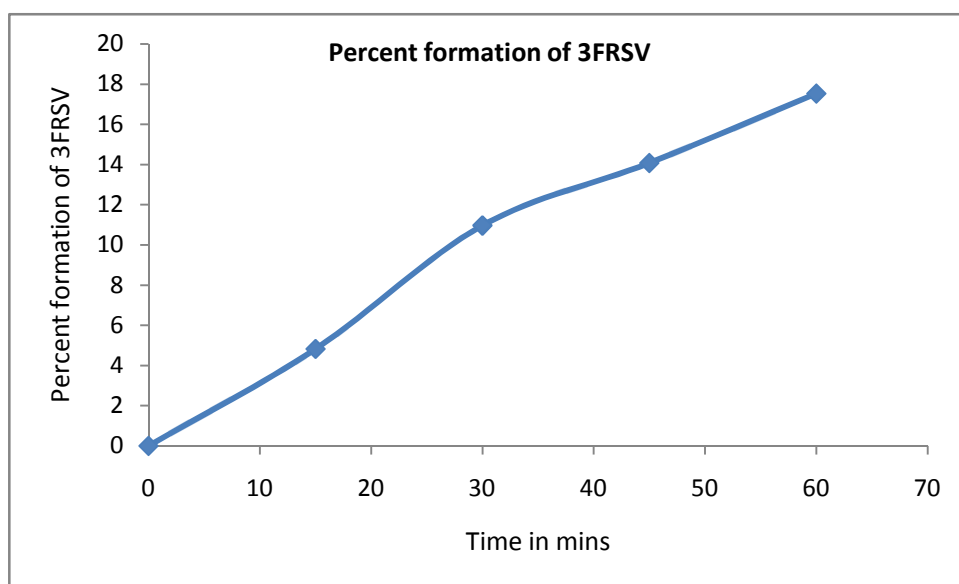


Fig:25 Percent formation of metabolite (3FRSV) of rifampicin in RIF alone at pH 1.2 buffer

Table :31 Comparison of %degradation of rifampicin and % formation of 3FRSV in rifampicin alone(F)

TIME(min)	%Degradation of RIF	%Formation of 3FRSV
0	0	0
15	2.42	2.35
30	7.51	7.29
45	10.19	9.89
60	13.35	12.96

Dissolution stability study of rifampicin in presence of FDCat pH 1.2 buffer

The results of dissolution stability study of RIF in the presence of FDC were shown in tables 32,33 and 34. figures 26 and27 . The percent degradation of RIF in the presence of FDC was gradually increased from 7.96, 13.07, 16.95 and 21.40 in the time period of 15, 30, 45 and 60min respectively. Where, the concentration of RIF in the media was decreased from 97.45 to 76.58 (µg/ml). However, the percent degradation of RIF in the presence of FDC increased when compared to percentage degradation of RIF alone and this increase was statistically significant ($P<0.05$). The percent formation of 3FRSV was found to be 7.77, 12.74, 16.52 and 20.96. Hence the percentage formation of 3FRSV in the presence of FDC was also significantly ($P<0.05$) increased when compared with RIF alone.

Table :32 Percent degradation of rifampicin in presence of FDCat pH 1.2buffer(F₀)

TIME (min)	Percent degradation of RIF			MEAN \pm S.D
	TRIAL1	TRIAL2	TRIAL3	
0	-	-	-	-
15	7.97	8.94	8.02	7.97 \pm 0.5462
30	13.08	13.02	13.12	13.07 \pm 0.0503
45	16.94	16.95	16.96	16.95 \pm 0.01
60	21.45	21.43	21.41	21.40 \pm 0.02

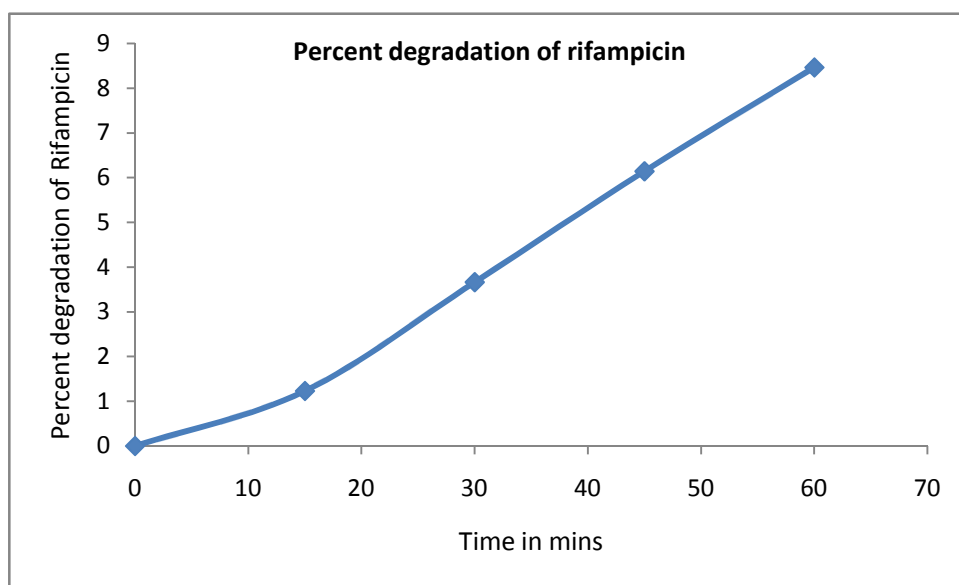


Fig:26 Percent degradation of rifampicin in presence of FDCat pH 1.2buffer

Table: 33 Percent formation of metabolite (3FRSV) of rifampicin in RIF+FDC mixture (F₀)

TIME (min)	Percent formation of 3FRSV			MEAN \pm S.D
	TRIAL1	TRIAL2	TRIAL3	
0	0	0	0	0
15	7.70	7.80	7.81	7.77 \pm 0.060830
30	12.70	12.72	12.78	12.74 \pm 0.041630
45	16.50	16.58	16.48	16.52 \pm 0.052920
60	20.80	20.82	20.96	20.86 \pm 0.087180

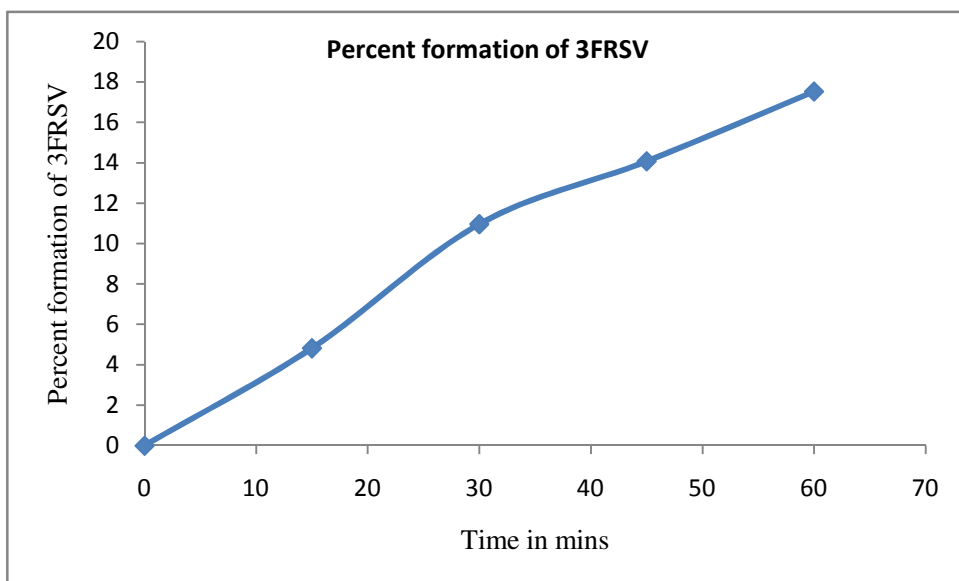


Fig:27 . Percent formation of metabolite (3FRSV) of rifampicin in RIF+FDC mixture

Table: 34 Comparison of %degradation of rifampicin and % formation of 3FRSV in RIF+FDC mixture

TIME	%Degradation of RIF	%Formation of 3FRSV
0	-	-
15	7.97	7.77
30	13.07	12.74
45	16.95	16.52
60	21.40	20.86

Dissolution stability study of rifampicin with PLGA 1:1 ratio at ph 1.2

The results of dissolution stability study of RIF with plga 1:1 ratio. The percentage degradation of RIF was increased gradually from, 1.92, 6.51, 8.19 and 11.35 in the time period of 15, 30, 45 and 60 mins respectively. Hence, it was indicated that the percentage degradation of RIF caused by plga 1:1 was reversed significantly ($P < 0.05$). The percentage formation of 3FRSV was also decreased significantly ($P < 0.05$) when compared with percentage formation of 3FRSV in RIF+PLGA 1:1 ratio mixture. The concentrations of 3FRSV were found to be 1.42, 5.51, 7.19 and 10.96. Addition of plga 1:1 did not cause much change in the degradation of FDC (Table 35, 36 and 37 and Figure 28 and 29.)

Table: 35 Percent degradation of rifampicin in rifampicin +plga1:1 ratio at pH 1.2buffer (F₁)

TIME (min)	Percent degradation of RIF			MEAN \pm S.D
	TRIAL1	TRIAL2	TRIAL3	
0	-	-	-	-
15	1.91	1.89	1.92	1.98 \pm 0.130
30	6.50	6.49	6.50	5.12 \pm 1.009
45	8.16	8.19	8.19	8.19 \pm 1.141
60	11.30	11.35	11.35	11.35 \pm 1.060

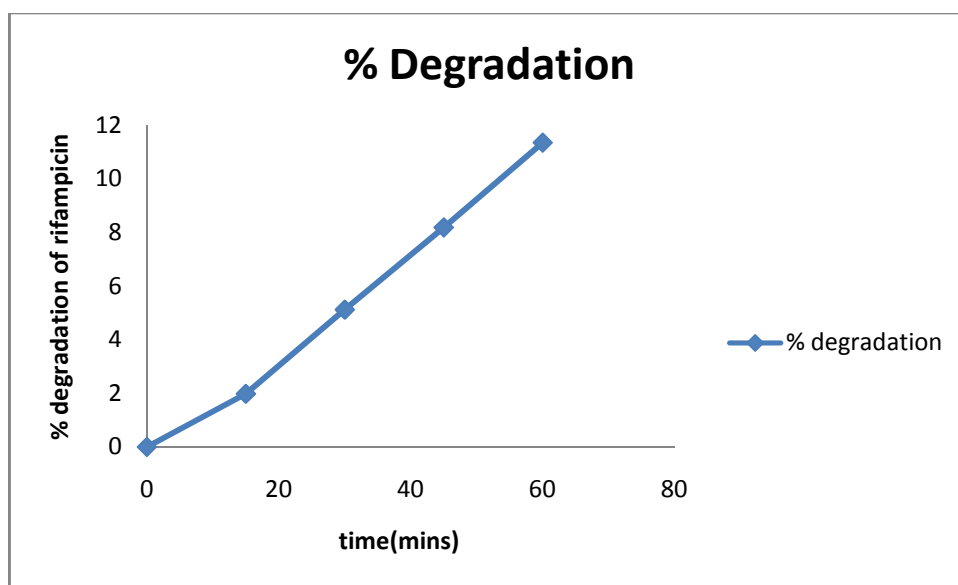


Fig:28

Table :36 Percent formation of metabolite (3FRSV) of rifampicin in RIF+PLGA1:1ratio mixture(F₁)

TIME (min)	Percent formation of 3FRSV			MEAN \pm S.D
	TRIAL1	TRIAL2	TRIAL3	
0	0	0	0	0
15	1.40	1.42	1.42	1.42 \pm 0.130
30	5.50	5.50	5.51	4.12 \pm 1.009
45	7.19	7.20	7.19	7.19 \pm 1.141
60	10.96	10.95	10.96	10.96 \pm 0.04583

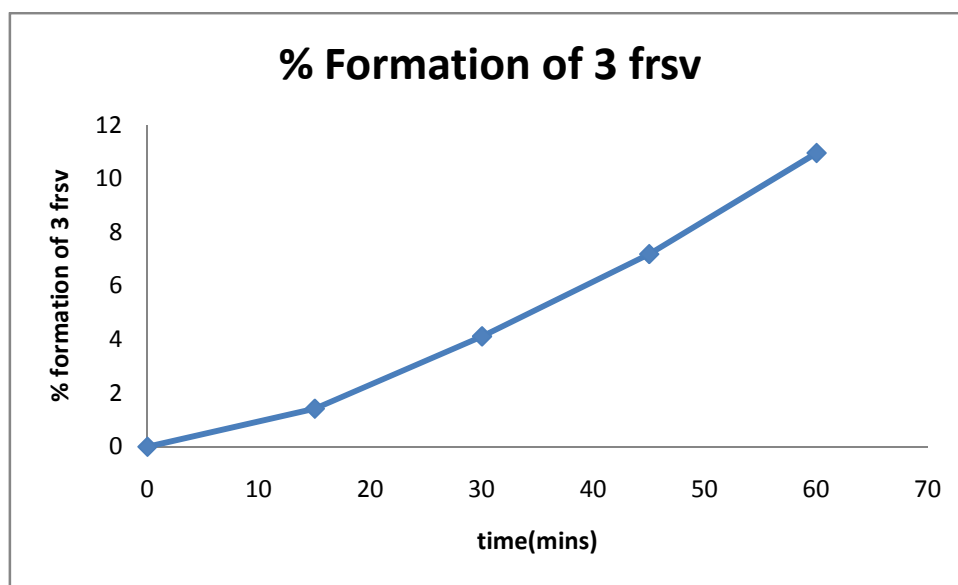


Fig:29

Table: 37 Comparison of %degradation of rifampicin and % formation of 3FRSV in RIF+PLGA1:1 ratio mixture (F₁)

TIME	%Degradation of RIF	%Formation of 3FRSV
0	-	-
15	1.92	1.42
30	6.51	5.51
45	8.19	7.19
60	11.35	10.96

Dissolution stability study of rifampicin with PLGA 1:2 ratio at ph 1.2

The results of dissolution stability study of RIF with plga 1:2 ratio. The percentage degradation of RIF was increased gradually from 1.12, 5.51, 7.19 and 9.35 in the time period of 15, 30, 45 and 60 mins respectively. Hence, it was indicated that the percentage degradation of RIF caused by plga 1:2 was reversed significantly ($P < 0.05$). The percentage formation of 3FRSV was also decreased significantly ($P < 0.05$) when compared with percentage formation of 3FRSV in RIF+PLGA 1; 2 ratio mixture. The concentrations of 3FRSV were found to be 1.10, 4.51, 6.19 and 8.35. Addition of plga 1:2 did not cause much change in the degradation of FDC (Table 38, 39 and 40 and Figure 30 and 31).

Table: 38 Percent degradation of rifampicin in rifampicin +plga1:2 ratio at pH 1.2buffer (F₂)

TIME (min)	Percent degradation of RIF			MEAN \pm S.D
	TRIAL1	TRIAL2	TRIAL3	
0	-	-	-	-
15	1.12	1.01	1.12	1.12 \pm 0.130
30	5.51	5.50	5.50	3.85 \pm 1.009
45	7.19	7.20	7.19	6.9 \pm 1.141
60	9.34	9.35	9.35	9.5 \pm 1.060

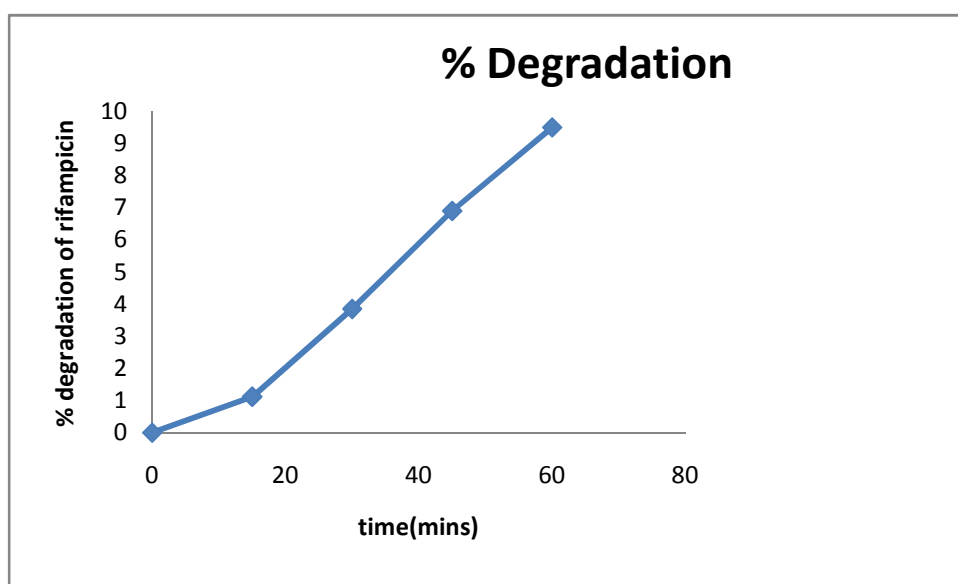


Fig: 30

Table: 39 Percent formation of metabolite (3FRSV) of rifampicin in RIF+PLGA1:2ratio mixture (F₂)

TIME (min)	Percent formation of 3FRSV			MEAN \pm S.D
	TRIAL1	TRIAL2	TRIAL3	
0	0	0	0	0
15	1.10	1.09	1.10	1.10 \pm 0.130
30	3.51	4.00	3.51	3.5 \pm 1.009
45	5.9	5.0	5.9	5.9 \pm 1.141
60	8.34	8.35	8.35	8.35 \pm 0.04583

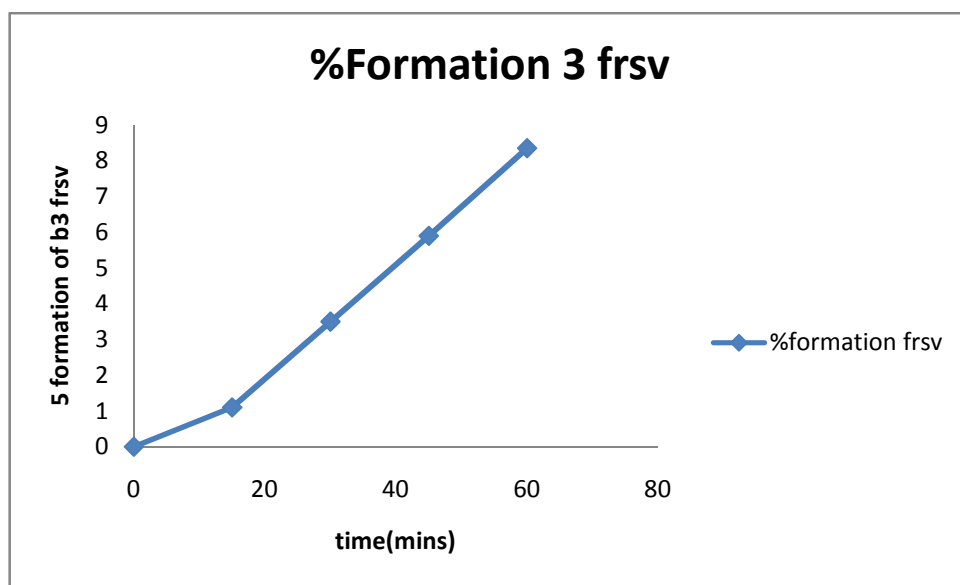


Fig: 31

Table: 40 Comparison of %degradation of rifampicin and % formation of 3FRSV in RIF+PLGA1:2 ratio mixture (F₂)

TIME	%Degradation of RIF	%Formation of 3FRSV
0	-	-
15	1.12	1.10
30	5.51	4.51
45	7.19	6.19
60	9.35	8.35

Dissolution stability study of rifampicin with PLGA 1:3 ratio at ph 1.2

The results of dissolution stability study of RIF with plga 1:3 ratio. The percentage degradation of RIF was increased gradually from 0.59, 3.51, 5.19 and 7.35 in the time period of 15, 30, 45 and 60 mins respectively. Hence, it was indicated that the percentage degradation of RIF caused by plga 1:3 was reversed significantly ($P < 0.05$). The percentage formation of 3FRSV was also decreased significantly ($P < 0.05$) when compared with percentage formation of 3FRSV in RIF+PLGA 1:3 ratio mixture. The concentrations of 3FRSV were found to be 0.09, 2.51, 4.19 and 6.35. Addition of plga 1:3 did not cause much change in the degradation of FDC (Table 41, 42 and 43 and Figure 32 and 33).

Table: 41 Percent degradation of rifampicin in rifampicin +plga1:3 ratio at pH 1.2buffer (F₃)

TIME (min)	Percent degradation of RIF			MEAN \pm S.D
	TRIAL1	TRIAL2	TRIAL3	
0	-	-	-	-
15	0.59	0.58	0.57	1.09 \pm 0.130
30	3.0	2.85	2.85	2.85 \pm 1.009
45	5.20	5.19	5.19	5.19 \pm 1.141
60	7.34	7.35	7.35	7.35 \pm 1.060

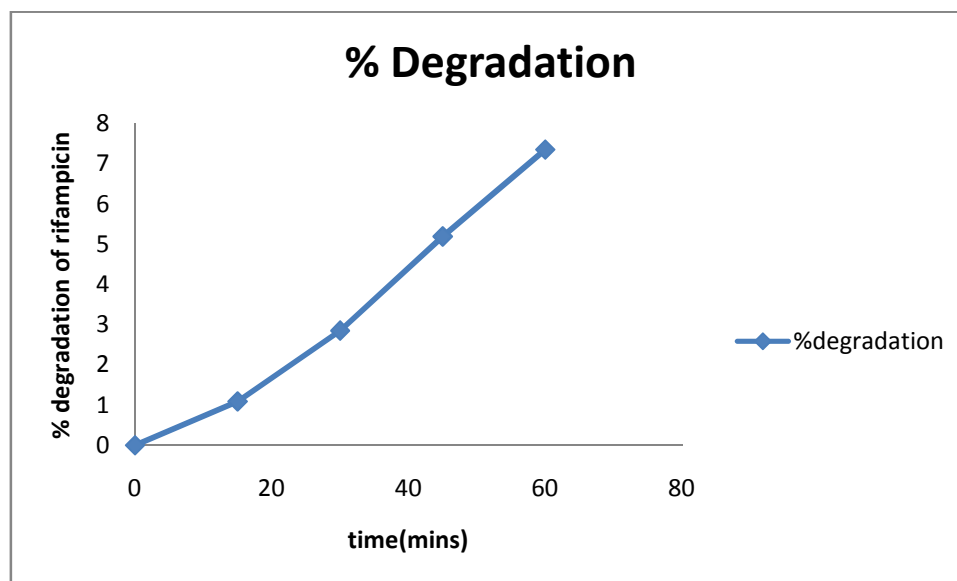


Fig: 32

Table: 42 Percent formation of metabolite (3FRSV) of rifampicin in RIF+PLGA1:3ratio mixture (F₃)

TIME (min)	Percent formation of 3FRSV			MEAN \pm S.D
	TRIAL1	TRIAL2	TRIAL3	
0	0	0	0	0
15	0.09	0.08	0.09	1.01 \pm 0.130
30	2.51	2.50	2.51	2.51 \pm 1.009
45	4.19	4.20	4.19	4.19 \pm 1.141
60	6.35	6.34	6.35	6.35 \pm 0.04583

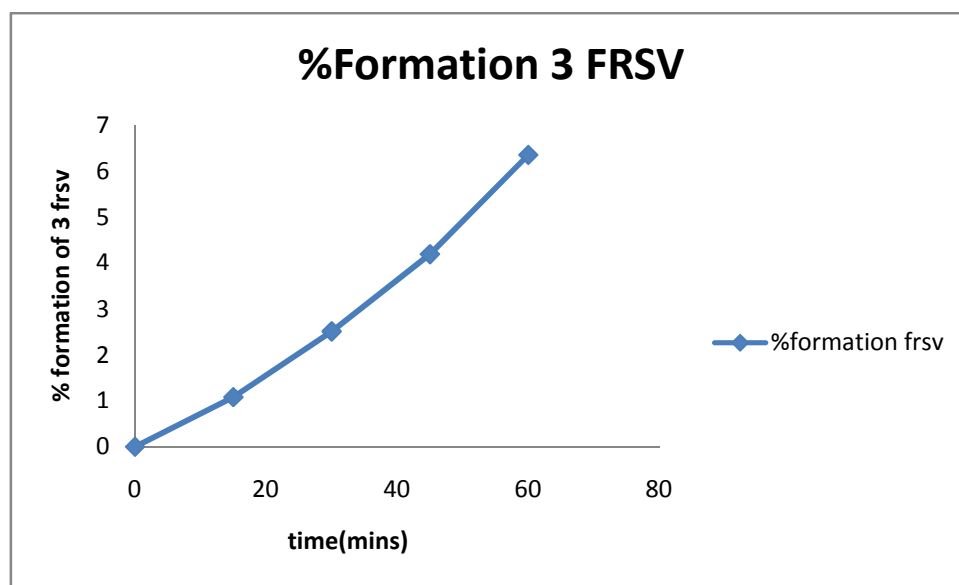


Fig: 33

Table: 43 Comparison of %degradation of rifampicin and % formation of 3FRSV in RIF+PLGA1:3 ratio mixture (F₃)

TIME	%Degradation of RIF	%Formation of 3FRSV
0	-	-
15	0.59	0.09
30	3.51	2.51
45	5.19	4.19
60	7.35	6.35

Dissolution stability study of rifampicin with plga 1:1 ratio in the presence of fdc at pH 1.2 buffer

The results of dissolution stability study of RIF with plga 1:1 ratio in the presence of FDC at pH 1.2 buffer was shown Tables , and and Figures , and . The percentage degradation of RIF was increased gradually from 4.97, 11.31, 14.53 and 18.09 in the time period of 15, 30, 45 and 60mins respectively. Hence, it was indicated that the percentage degradation of RIF caused by FDC was reversed significantly ($P<0.05$) by the addition of PLGA 1:1 ratio . The percentage formation of 3FRSV was also decreased significantly ($P<0.05$) when compared with percentage formation of 3FRSV in RIF+FDC mixture. The concentrations of 3FRSV were found to be 4.82, 10.96, 14.07 and 17.52. Addition of 1:1 ratio of plga did not cause much change in the degradation of FDC (Table 44,45 and 46 and Figure 34 and 35).

Table: 44 Percent Degradation of rifampicin with 1:1 PLGA in the presence of FDC at pH 1.2 buffers (F₄)

TIME (min)	Percent degradation of RIF			MEAN \pm S.D
	TRIAL1	TRIAL2	TRIAL3	
0	-	-	-	-
15	4.95	4.99	4.97	4.97 \pm 0.02
30	11.37	11.35	11.22	11.31 \pm 0.08
45	14.56	14.52	14.49	14.53 \pm 0.035
60	18.07	18.10	18.10	18.09 \pm 0.017

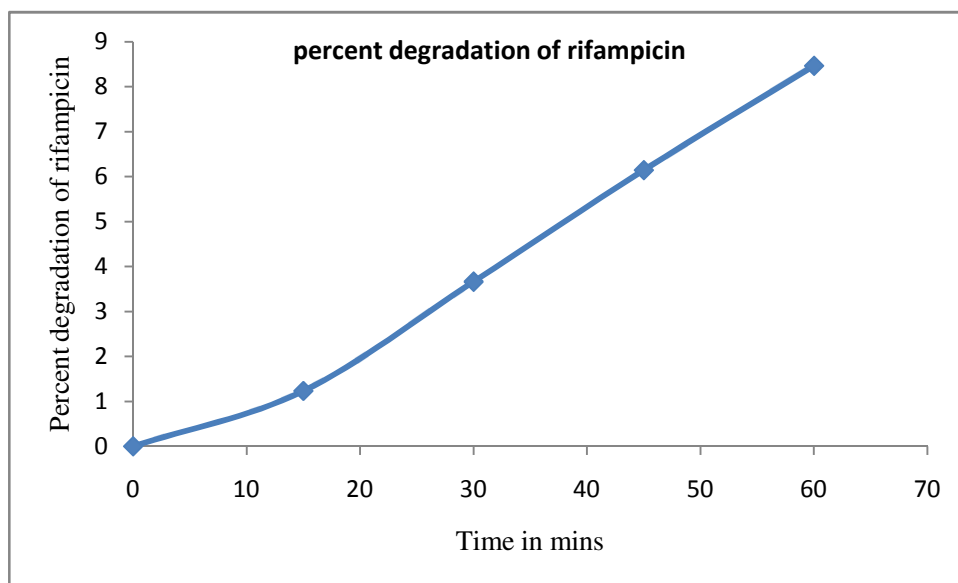


Fig: 34 Percent Degradation of rifampicin with 1:1 PLGA in the presence of FDCat pH 1.2 buffers

Table: 45 Percentage formation of metabolite (3FRSV) of rifampicin with 1:1 PLGA in the presence of FDCat pH 1.2 buffers (F₄)

TIME (min)	Percent formation of 3FRSV			MEAN \pm S.D
	TRIAL1	TRIAL2	TRIAL3	
0	0	0	0	0
15	4.79	4.81	4.86	4.82 \pm 0.03606
30	10.96	10.95	10.97	10.96 \pm 0.01000
45	14.0	14.09	14.12	14.07 \pm 0.06245
60	17.48	17.51	17.57	17.52 \pm 0.04583

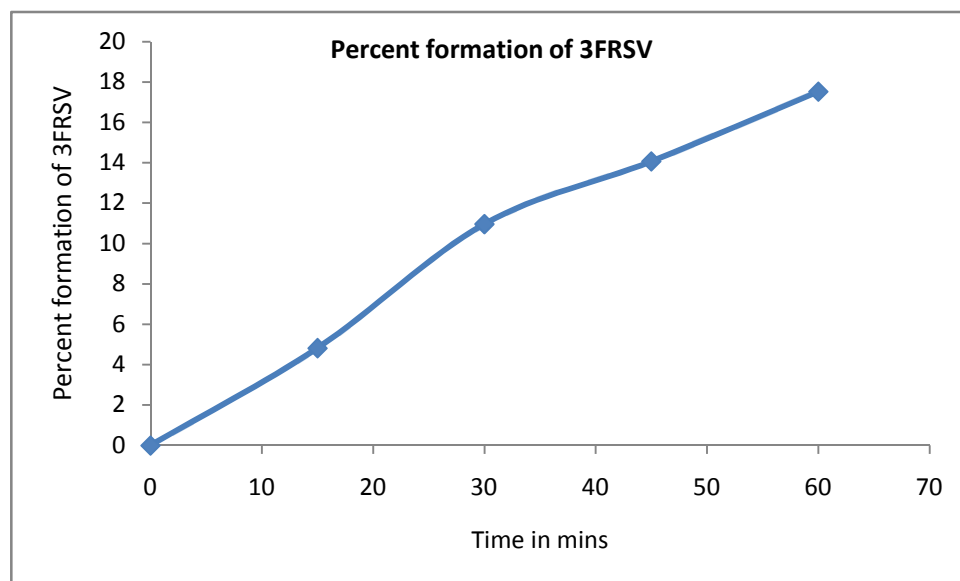


Fig: 35 Percentage formation of metabolite (3FRSV) of rifampicin with 1:1 PLGA in the presence of FDCat pH 1.2 buffers

Table: 46 Comparison of %degradation of RIF and % formation of 3FRSV in the mixture of rifampicin PLGA NPS in 1:1 ratio along with FDC (F₄)

TIME	%Degradation of RIF	%Formation of 3FRSV
0	-	-
15	4.97	4.82
30	11.31	10.96
45	14.53	14.07
60	18.09%	17.52

Dissolution stability study of rifampicin with plga 1:2 ratio in the presence of fdc at pH 1.2 buffers

The results of dissolution stability study of RIF with PLGA 1:2 ratio in the presence of FDC at pH 1.2 buffer was shown in Tables , and and Figures , and . The percent degradation of RIF was increased gradually from 3.97, 9.20, 11.23 and 14.29 in the time period of 15, 30, 45 and 60mins respectively. The percent degradation of RIF was decreased significantly ($p < 0.01$) with increase in concentration of PLGA 1:1 to 1:2. The percent formation of 3FRSV was also decreased significantly ($p < 0.01$) with increased concentration of plga. The values were 3.85, 8.92, 10.89 and 13.86 in the time period of 15, 30, 45 and 60mins respectively. Increase in concentration of plga 1:2 ratio did not cause much change in the degradation of FDC (Table 47,48and 49 and Figure36 and 37).

Table: 47 Percent degradation of rifampicin in rifampicin PLGA 1:2 NPS in the presence of FDC at pH 1.2 buffer (F₅)

TIME (min)	Percent degradation of rifampicin			MEAN \pm S.D
	TRIAL1	TRIAL2	TRIAL3	
0	-	-	-	-
15	4.07	3.96	3.79	3.97 \pm 0.14
30	9.23	9.19	9.20	9.20 \pm 0.02
45	11.29	11.25	11.17	11.23 \pm 0.06
60	14.37	14.32	14.40	14.29 \pm 0.04

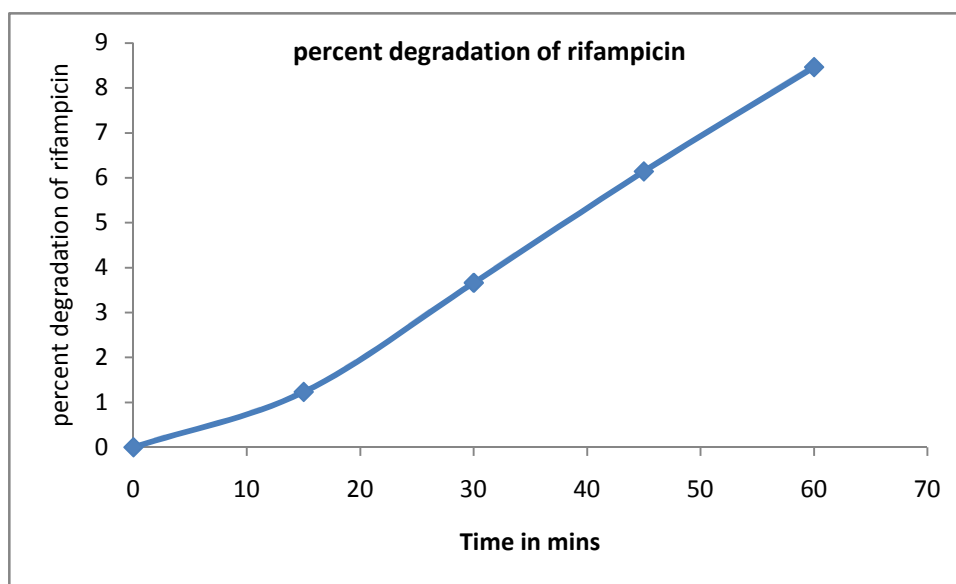


Fig: 36 Percent degradation of rifampicin in rifampicin PLGA 1:2 NPS in the presence of FDC at pH 1.2 buffer

Table: 48 Percentage formation of metabolite (3FRSV) of rifampicin with 1:2 PLGA in the presence of FDCat pH 1.2 buffers

TIME (min)	Percent formation of 3FRSV			MEAN \pm S.D
	TRIAL1	TRIAL2	TRIAL3	
0	0	0	0	0
15	3.80	3.81	3.94	3.85
30	8.90	8.91	8.95	8.92
45	10.81	10.87	10.99	10.89
60	13.83	13.85	13.90	13.86

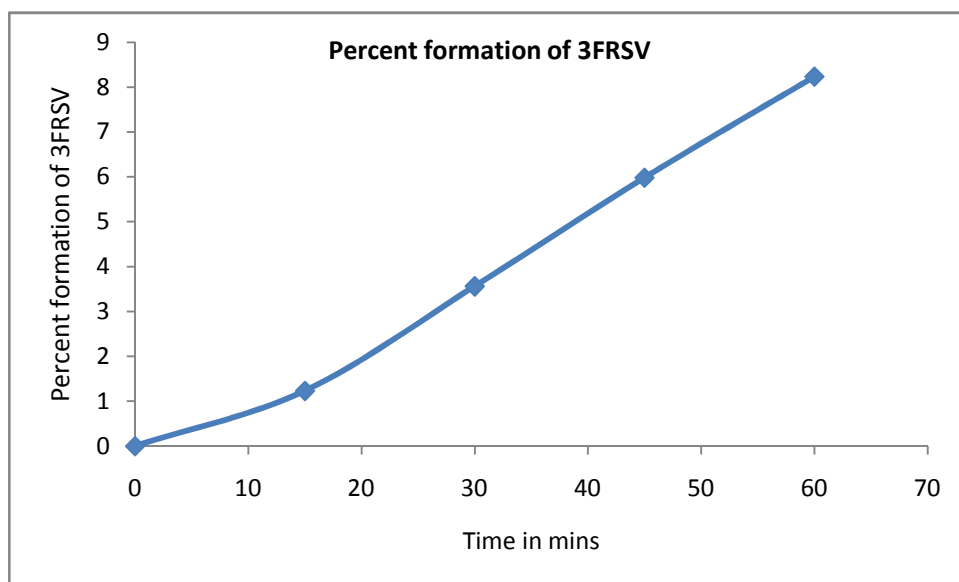


Fig: 37 Percentage formation of metabolite (3FRSV) of rifampicin with 1:2 PLGA in the presence of FDCat pH 1.2 buffers

Table: 49 Comparison of %degradation of RIF and % formation of 3FRSV in the mixture of rifampicin in rifampicin PLGA 1:2 ratio along with FDC (F₅)

TIME(min)	%Degradation of RIF	%Formation of 3FRSV
0	-	-
15	3.97	3.85
30	9.20	8.92
45	11.23	10.89
60	14.29	13.86

Dissolution stability study of rifampicin with plga 1:3 ratio in the presence of fdc at pH 1.2 buffers

The result of dissolution stability study of RIF in the presence of FDC and PLGA 1:3 ratio was shown in Tables , and and Figures , and . The percent degradation of RIF was increased gradually from 1.46, 4.07, 6.46 and 8.92 in the time period of 15, 30, 45 and 60mins respectively. The percent degradation of RIF was decreased significantly ($P<0.01$) with increase in concentration of plga 1:2 to plga 1:3 ratio. The percent formation of 3FRSV was also decreased with increased significantly ($P<0.01$) concentration of plga. The values were 1.37, 3.96, 6.28 and 8.67 in the time period of 15, 30, 45 and 60mins respectively. Increase in concentration of plga 1:3 did not cause much change in the degradation of FDC(Table 50,51 and 52 and Figure38 and 39).

Table: 50 Percent Degradation of rifampicin in rifampicin PLGA 1:3 ratio in the presence of FDC at pH 1.2 buffers (F₆)

TIME (min)	Percent degradation of rifampicin			MEAN \pm S.D
	TRIAL1	TRIAL2	TRIAL3	
0	-	-	-	-
15	2.15	2.17	2.12	1.46 \pm 0.025
30	4.11	4.05	4.04	4.07 \pm 0.037
45	6.48	6.42	6.48	6.46 \pm 0.034
60	9.40	9.34	9.40	8.92 \pm 0.034

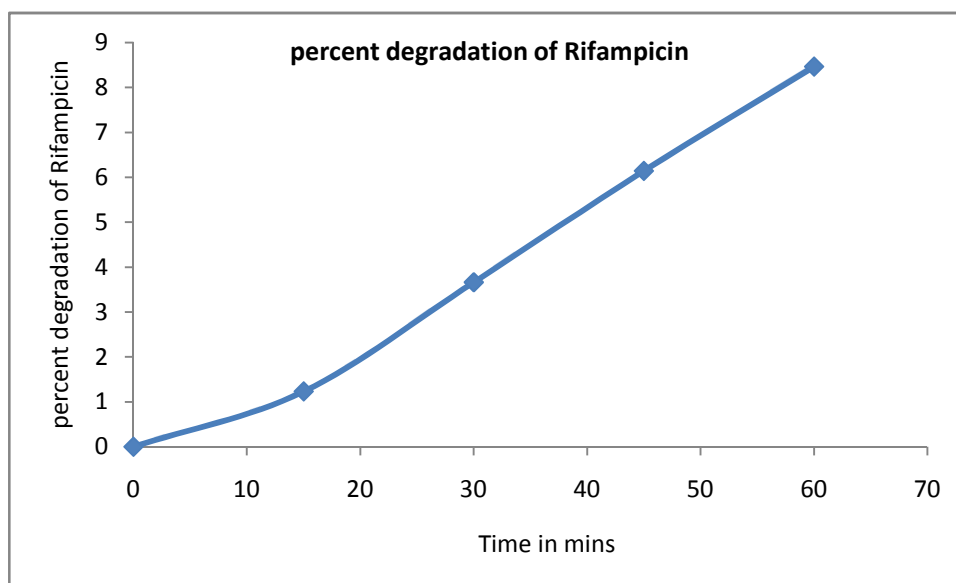


Fig: 38 Percent Degradation of rifampicin in rifampicin PLGA 1:3 ratio in the presence of FDC at pH 1.2 buffers

Table: 51 Percent formation of metabolite (3FRSV) of Rifampicin in rifampicin PLGA 1:3 ratio in the presence of FDC at pH 1.2 buffers (F₆)

TIME (min)	Percent formation of 3FRSV			MEAN \pm S.D
	TRIAL1	TRIAL2	TRIAL3	
0	0	0	0	0
15	1.32	1.38	1.41	1.37 \pm 0.04583
30	3.91	3.95	4.02	3.96 \pm 0.05568
45	6.25	6.29	6.30	6.28 \pm 0.02646
60	8.60	8.65	8.76	8.67 \pm 0.08185

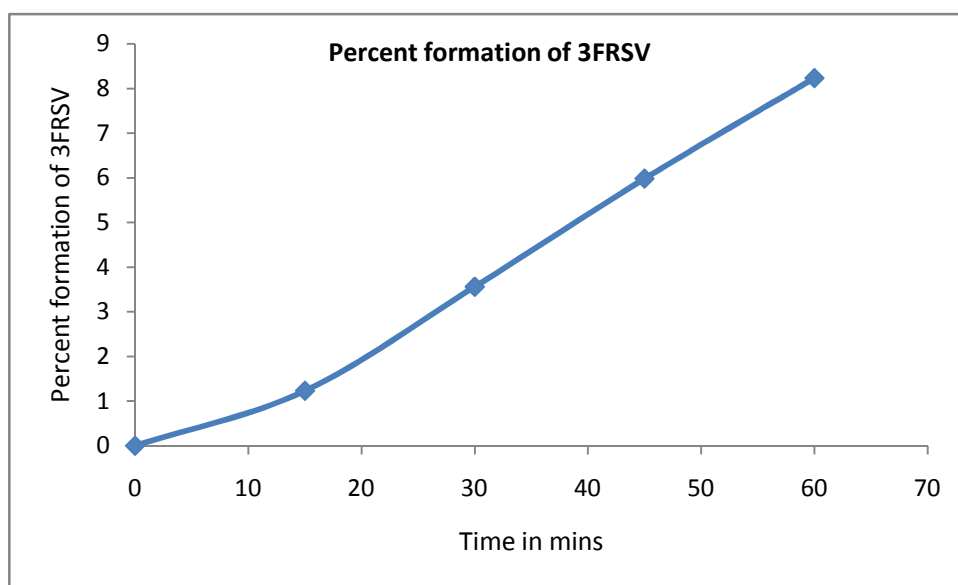


Fig: 39 Percent formation of metabolite (3FRSV) of rifampicin in rifampicin PLGA 1:3 ratio in the presence of FDC at pH 1.2 buffers

Table: 52 Comparison of % degradation of RIF and % formation of 3FRSV in the mixture of rifampicin in rifampicin PLGA 1:3 ratio along with FDC (F₆)

TIME	%Degradation of RIF	%Formation of 3FRSV
0	-	-
15	1.46	1.37
30	4.07	3.96
45	6.46	6.28
60	8.92	8.67

8.10. Table :53 COMPARITIVE % DEGRADATION

Time	RIF ALONE	RIF+FDC	RIF+PLG A 1:1	RIF+PLG A 1:2	RIF+PLG A 1:3	RIF+PLGA 1:1+FDC	RIF+PLG A 1:2+FDC	RIF+PLG A 1:3+FDC
0	0	0	0	0	0	0	0	0
15	2.42±0.130	7.97±0.546	1.92±0.130	1.12±0.3	0.59±0.513	4.97±0.02	3.97±0.14	1.46±0.025
30	7.51±1.009	13.07±0.05 0	6.51±1.009	5.51±1.00 9	3.51±0.513	11.31±0.08	9.20±0.02	4.07±0.037
45	10.19±1.141	16.95±0.01	8.19±1.141	7.19±1.14 1	5.19±0.208	14.53±0.35	11.23±0.0 6	6.46±0.034
60	13.35±1.060	21.40±0.02	11.35±1.06 0	9.35±1.06 0	7.35±0.513	18.09±0.017	14.29±0.0 4	8.92±0.034

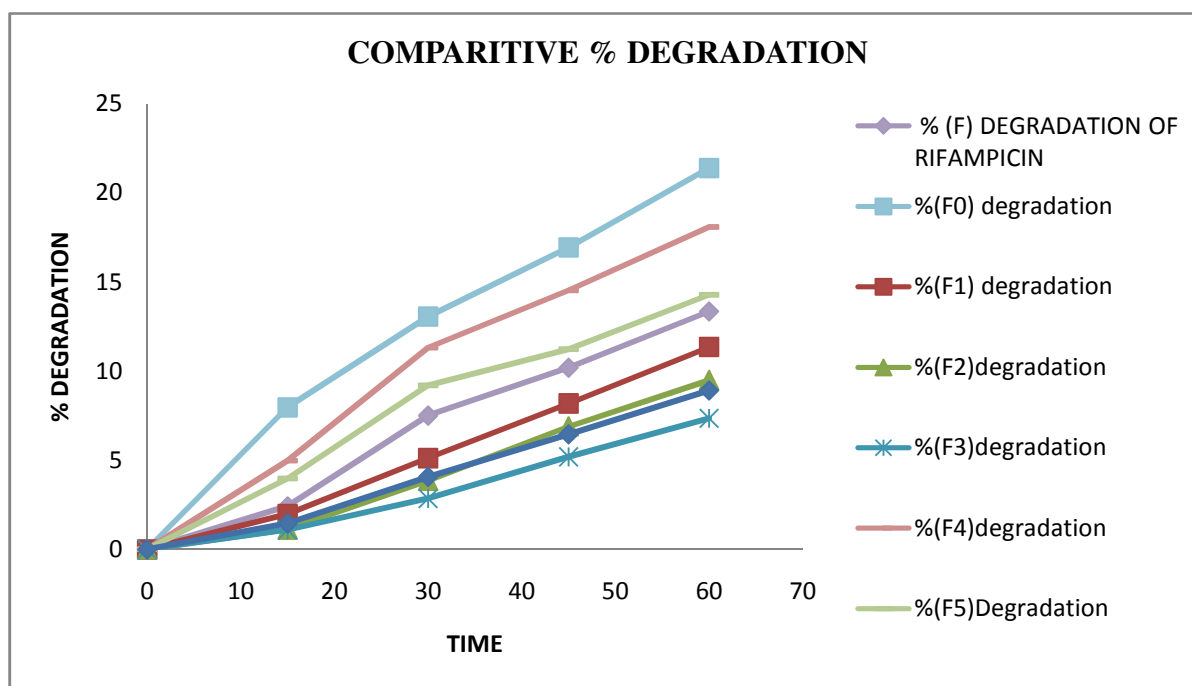


Fig: 40

8.11. Table: 54 COMPARITIVE % FORMATION OF 3 FRSV

Time	RIF ALONE	RIF+FDC	RIF+PLG A 1:1	RIF+PLG A 1:2	RIF+PL GA 1:3	RIF+PLGA 1:1+FDC	RIF+PLG A 1:2+FDC	RIF+PLGA 1:3+FDC
0	0	0	0	0	0	0	0	0
15	2.35±1.00 0	7.77±0.060	1.42±0.130	1.10±0.3	0.09±0.5 13	4.82±0.036	3.85±0.14	1.37±0.045
30	7.29±0.09 0	12.74±0.04 1	5.51±1.009	4.51±1.009	2.51±0.5 13	10.96±0.010	8.92±0.02	3.96±0.055
45	9.89±0.01 5	16.52±0.05 2	7.19±1.141	6.19±1.141	4.19±0.2 08	14.07±0.062	10.89±0.06	6.28±0.026
60	12.96±0.0 45	20.86±0.08 7	10.35±1.06	8.35±1.060	6.35±0.5 13	17.52±0.045	13.86±0.04	8.67±0.081

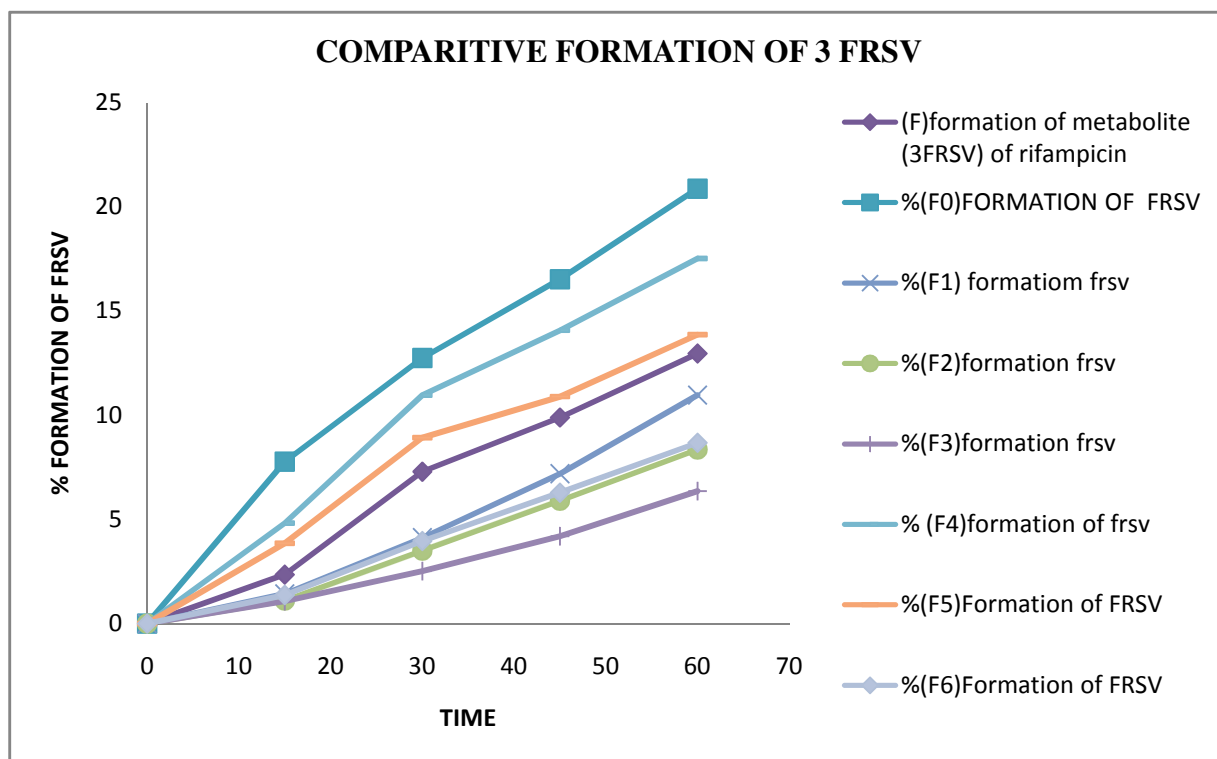
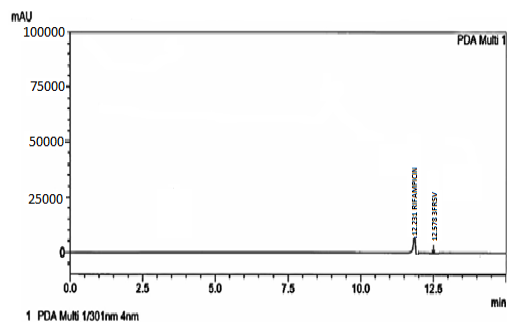


Fig: 41

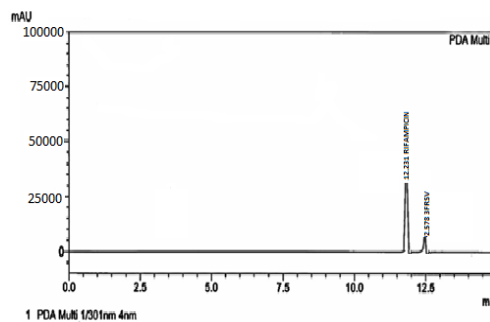
Chromatograms of GroupI animals (Rifampicin alone):

0.5 hr



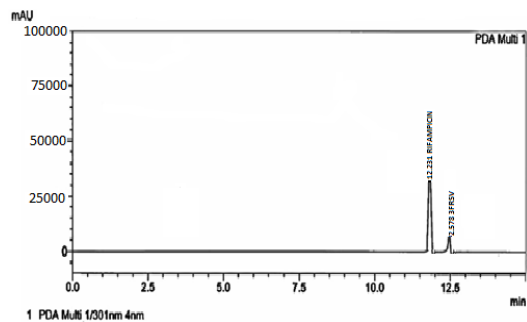
RETENTION	12.231	12.578
TIME(MIN)		
AREA	6513	724

1.0 hr



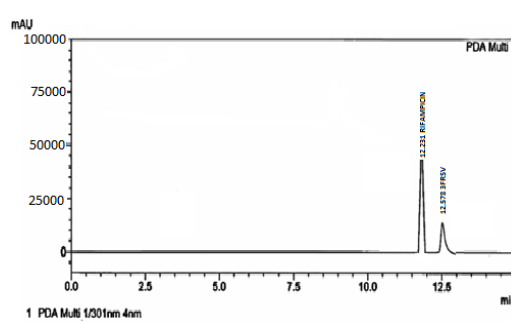
RETENTION	12.231	12.578
TIME(MIN)		
AREA	30397	4451

1.5hr



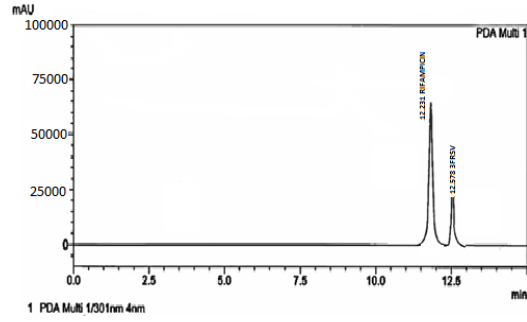
RETENTION	12.231	12.578
TIME(MIN)		
AREA	36911	5283

2.0hr



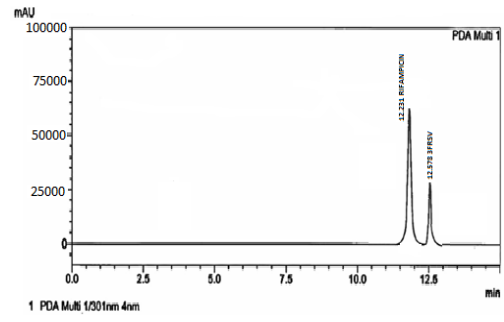
RETENTION	12.231	12.578
TIME(MIN)		
AREA	47043	15198

2.5hr



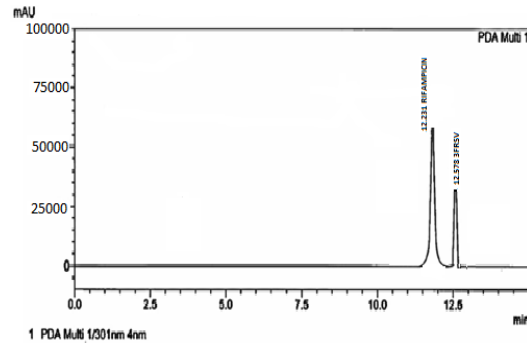
RETENTION TIME(MIN)	12.231	12.578
AREA	66585	23160

3.0hr



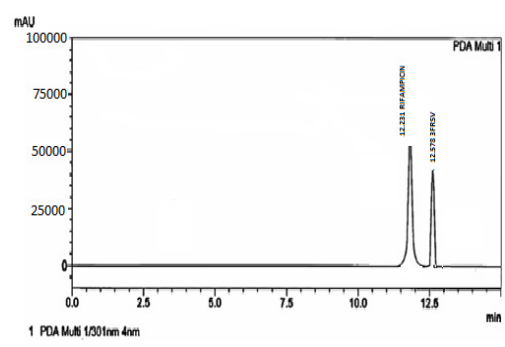
RETENTION TIME(MIN)	12.231	12.578
AREA	62966	30397

3.5hr



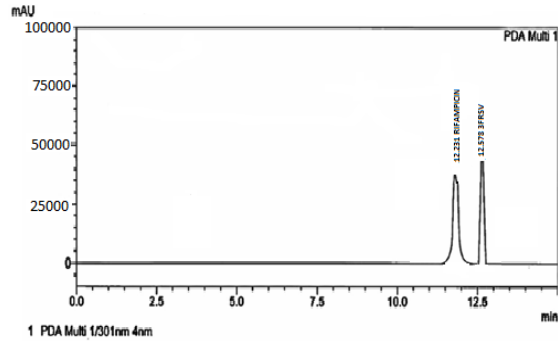
RETENTION TIME(MIN)	12.231	12.578
AREA	56452	36911

4.0hr



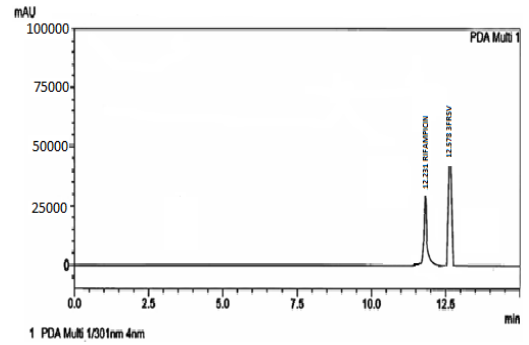
RETENTION TIME(MIN)	12.231	12.578
AREA	51386	42977

5.0hr



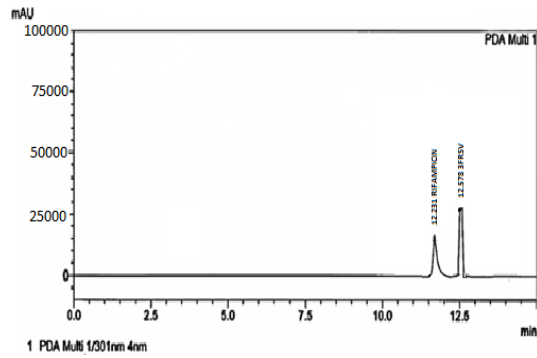
RETENTION TIME(MIN)	12.231	12.578
AREA	38358	47043

6.0hr



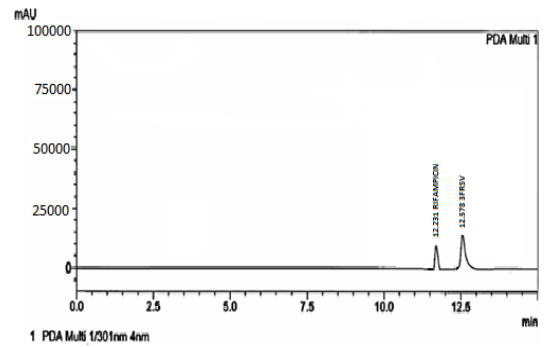
RETENTION TIME(MIN)	12.231	12.578
AREA	31568	41977

8.0hr



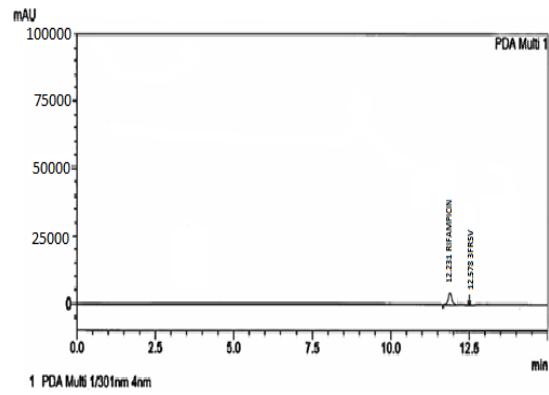
RETENTION TIME(MIN)	12.231	12.578
AREA	18817	29673

10.0hr

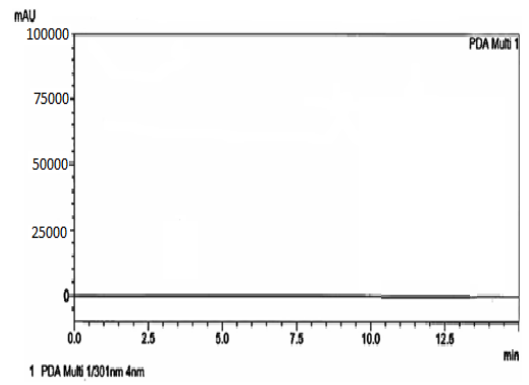


RETENTION TIME(MIN)	12.231	12.578
AREA	9408	15922

12.0hr



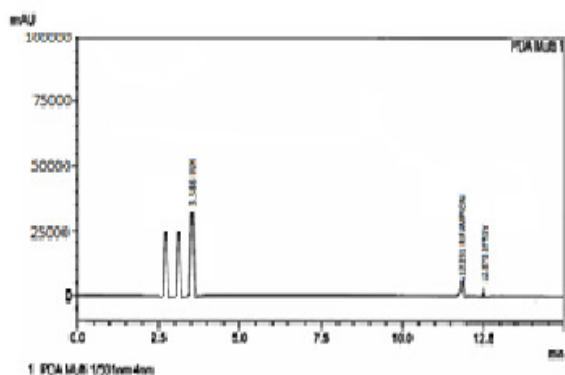
24.0hr



RETENTION TIME(MIN)	12.231	12.578
AREA	2895	724

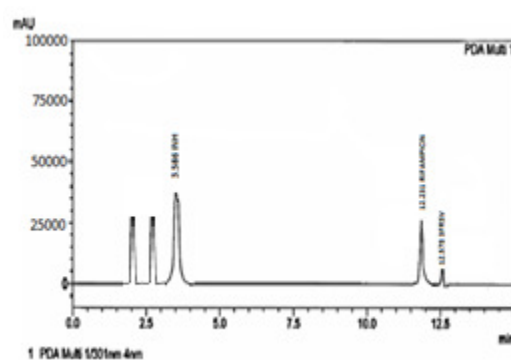
Chromatograms of GroupII (Rifampicin+FDC)

0.5 hr



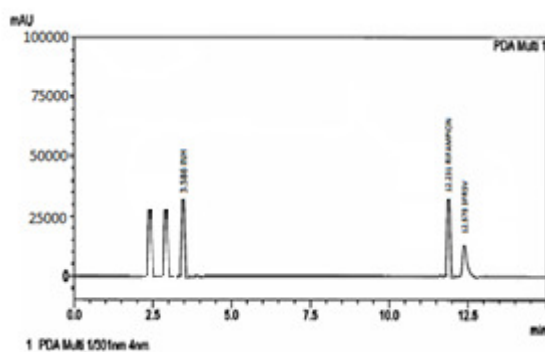
RETENTION TIME(MIN)	3.586	12.231	12.578
AREA	34740	6513	724

1.0hr



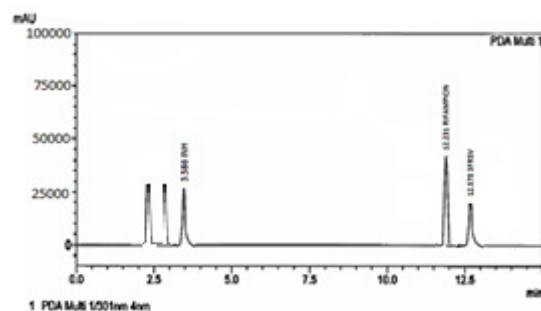
RETENTION TIME(MIN)	3.586	12.231	12.578
AREA	38358	27504	5790

1.5hr



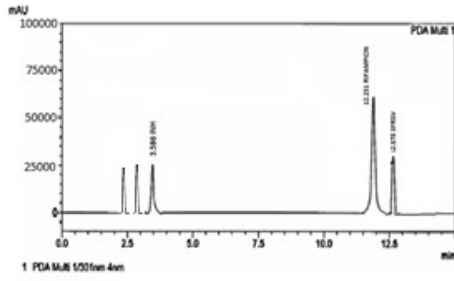
RETENTION TIME(MIN)	3.586	12.231	12.578
AREA	34740	34016	12303

2.0hr



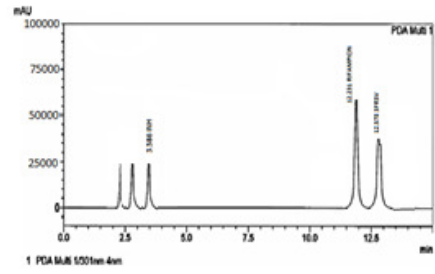
RETENTION TIME(MIN)	3.586	12.231	12.578
AREA	2967 3	42700	20264

2.5hr



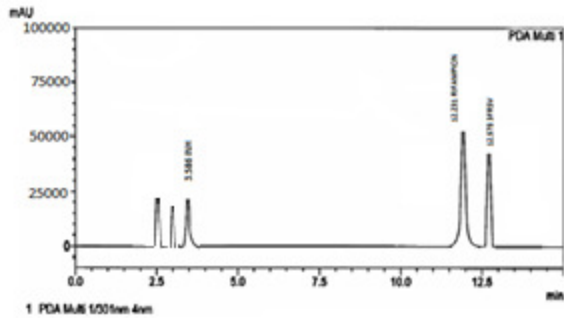
RETENTION TIME(MIN)	3.586	12.231	12.578
AREA	27502	60071	29673

3.0hr



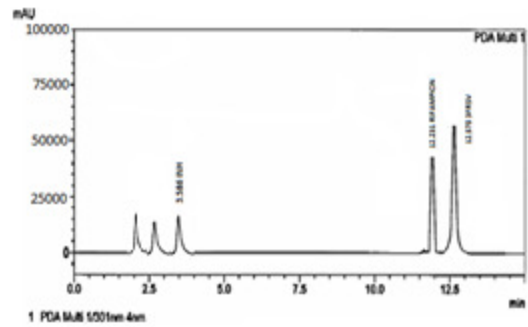
RETENTION TIME(MIN)	3.586	12.231	12.578
AREA	24607	57176	39806

3.5hr



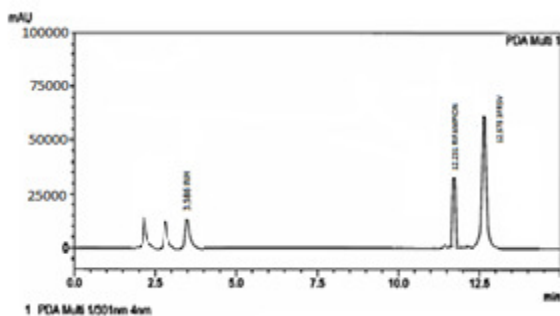
RETENTION TIME(MIN)	3.586	12.231	12.578
AREA	20988	51386	46320

4.0hr



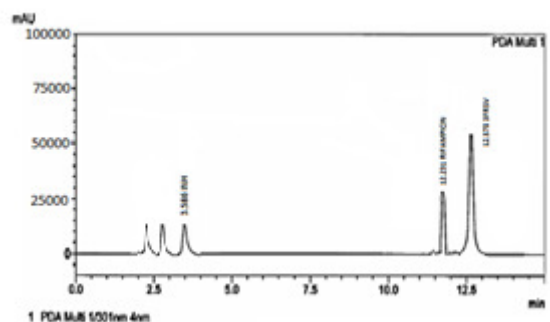
RETENTION TIME(MIN)	3.586	12.231	12.578
AREA	18817	46320	54381

5.0hr



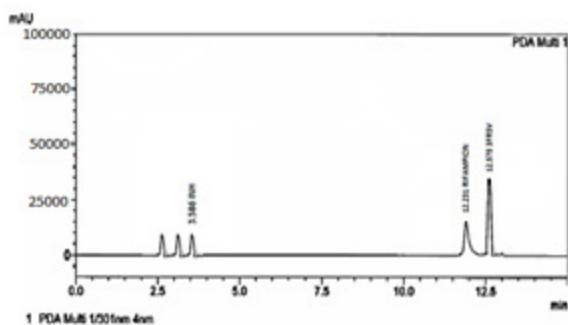
RETENTION TIME(MIN)	3.586	12.231	12.578
AREA	11580	34740	58623

6.0hr



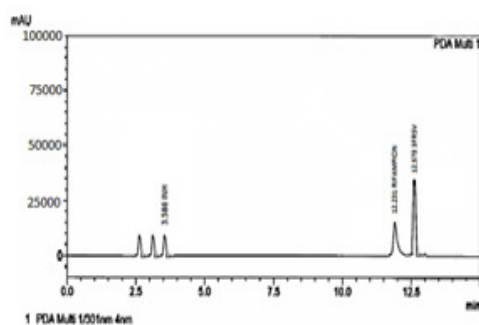
RETENTION TIME(MIN)	3.586	12.231	12.578
AREA	11219	28950	51386

8.0hr



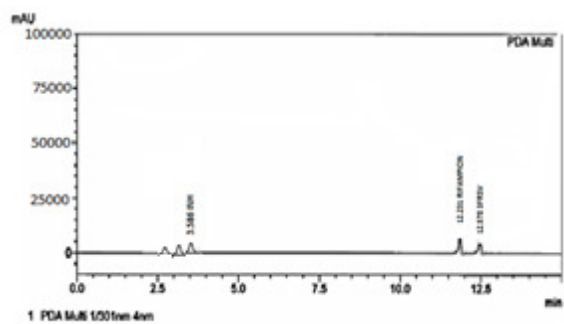
RETENTION TIME(MIN)	3.586	12.231	12.578
AREA	7961	17370	37635

10.0hr

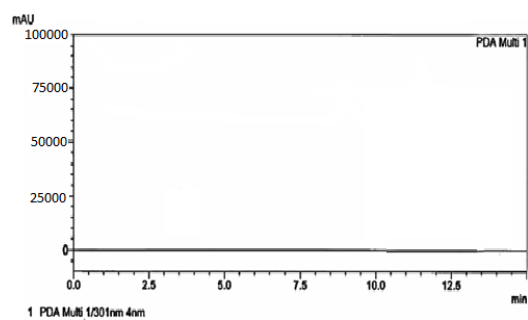


RETENTION TIME(MIN)	3.586	12.231	12.578
AREA	5066	8684	18817

12.0hr



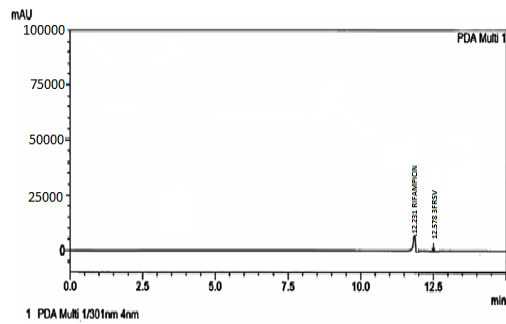
24.0hr



RETENTION	3.586	12.231	12.578
TIME(MIN)			
AREA	3618	2896	1448

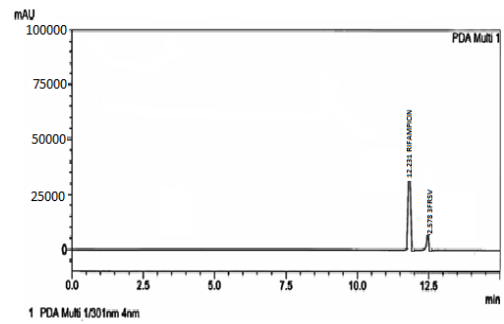
Chromatograms of GroupIII animals (Rifampicin + PLGA):

0.5 hr



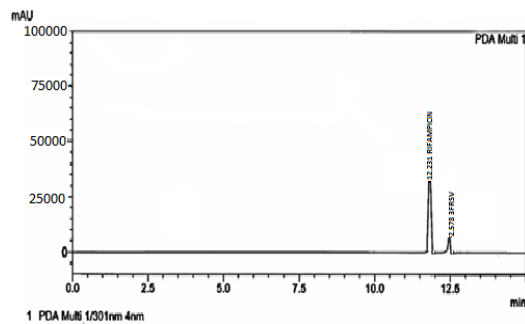
RETENTION	12.231	12.578
TIME(MIN)		
AREA	9513	424

1.0 hr



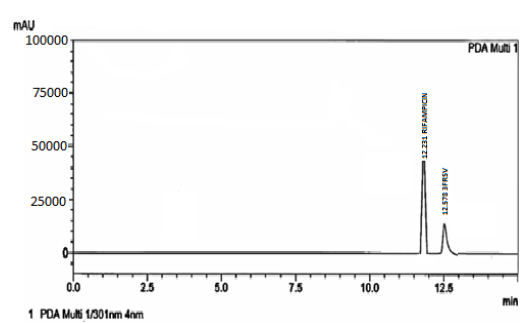
RETENTION	12.231	12.578
TIME(MIN)		
AREA	3397	4151

1.5hr



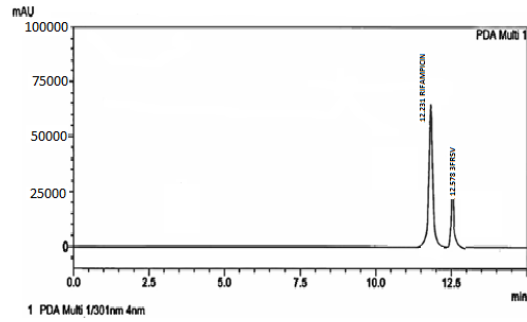
RETENTION	12.231	12.578
TIME(MIN)		
AREA	39911	4983

2.0hr



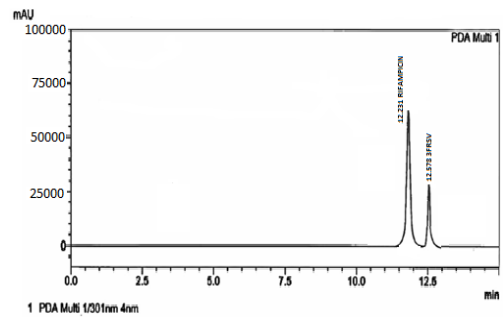
RETENTION	12.231	12.578
TIME(MIN)		
AREA	44043	12198

2.5hr



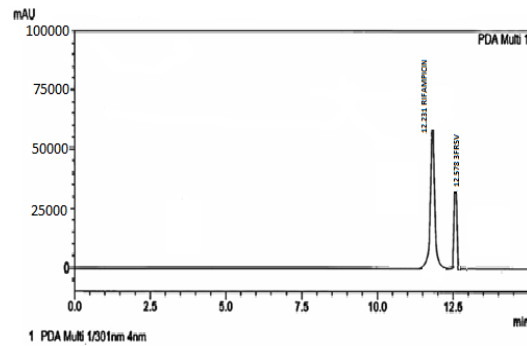
RETENTION TIME(MIN)	12.231	12.578
AREA	69585	20160

3.0hr



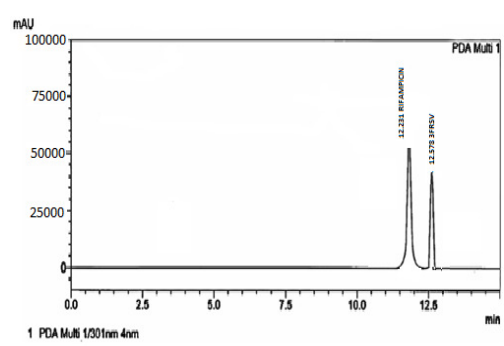
RETENTION TIME(MIN)	12.231	12.578
AREA	65966	27397

3.5hr



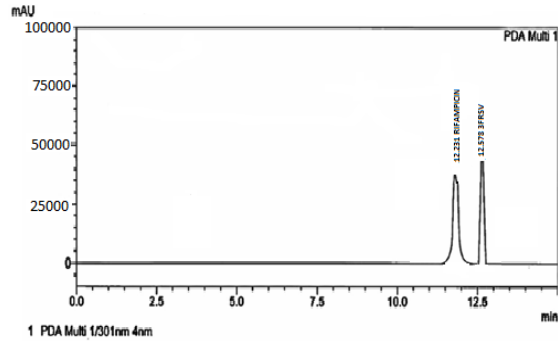
RETENTION TIME(MIN)	12.231	12.578
AREA	59452	33911

4.0hr



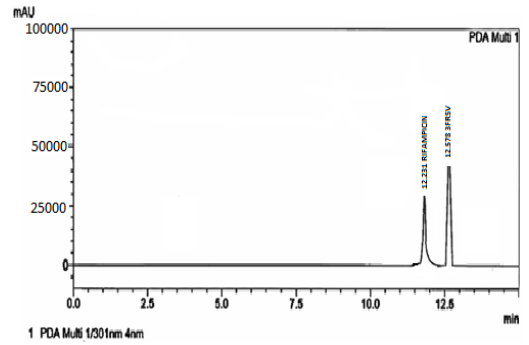
RETENTION TIME(MIN)	12.231	12.578
AREA	54386	39977

5.0hr



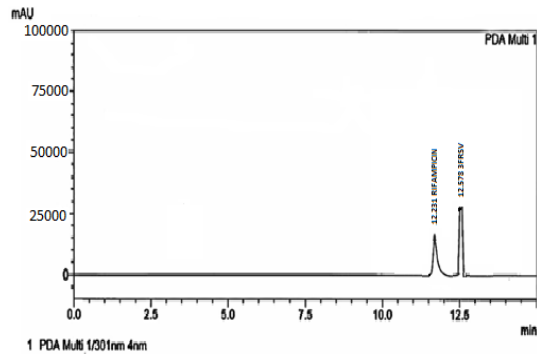
RETENTION TIME(MIN)	12.231	12.578
AREA	35358	44043

6.0hr



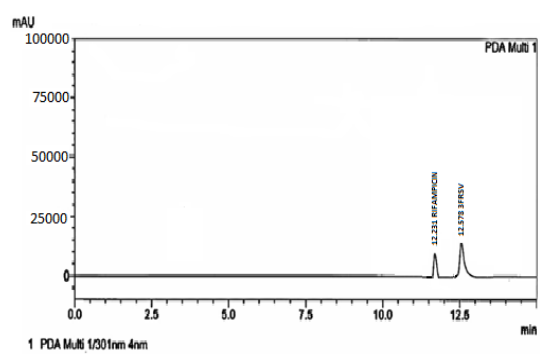
RETENTION TIME(MIN)	12.231	12.578
AREA	34568	38977

8.0hr



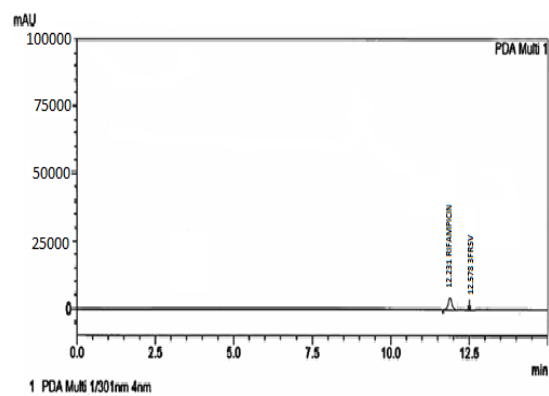
RETENTION TIME(MIN)	12.231	12.578
AREA	21817	26673

10.0hr

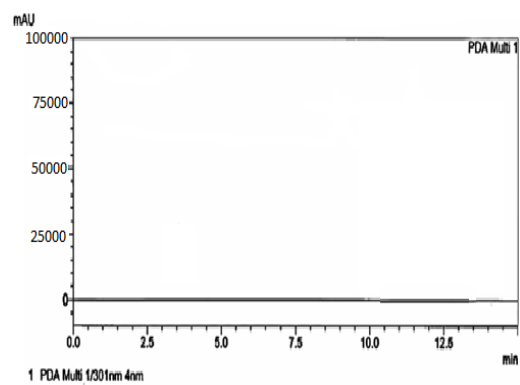


RETENTION TIME(MIN)	12.231	12.578
AREA	9708	12922

12.0hr



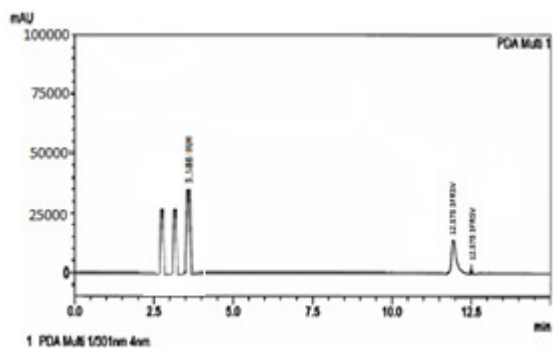
24.0hr



RETENTION	12.231	12.578
TIME(MIN)		
AREA	3195	694

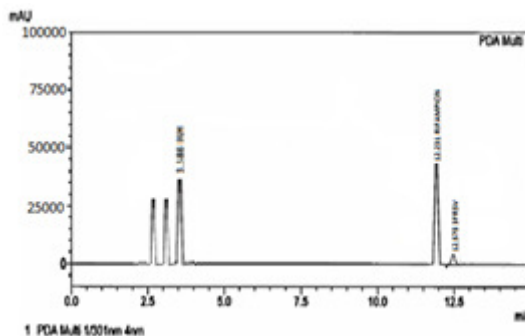
Chromatograms of Group IV animals (RIF+FDC+PLGA)

0.5 hr



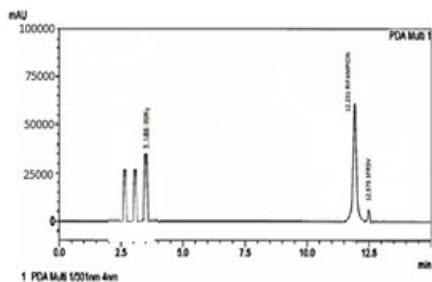
RETENTION TIME(MIN)	3.586	12.231	12.578
AREA	35463	15922	742

1.0hr



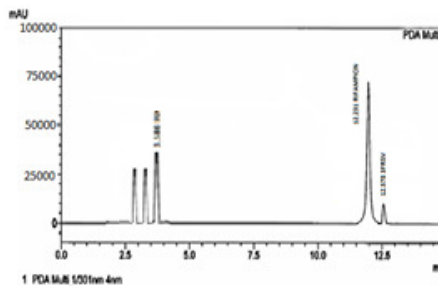
RETENTION TIME(MIN)	3.586	12.231	12.578
AREA	39806	47767	2714

1.5hr



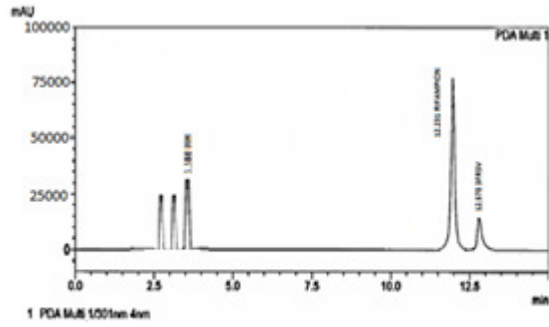
RETENTION TIME(MIN)	3.586	12.231	12.578
AREA	35463	60795	5066

2.0hr



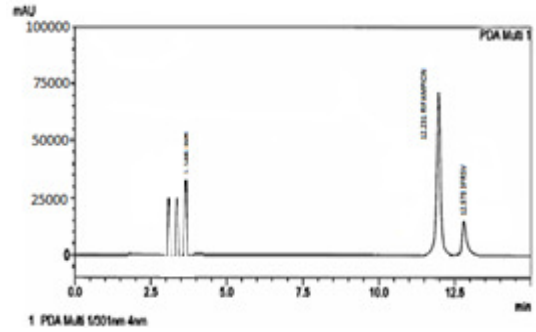
RETENTION TIME(MIN)	3.586	12.231	12.578
AREA	29673	73098	9408

2.5hr



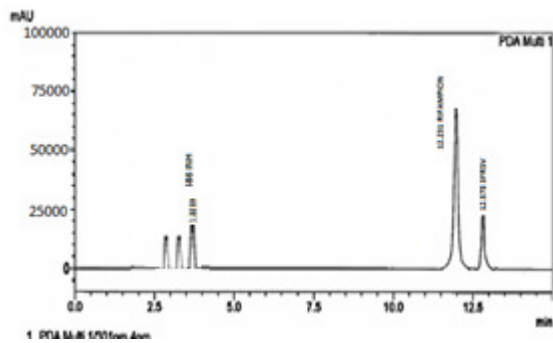
RETENTION TIME(MIN)	3.586	12.231	12.578
AREA	28225	76718	14475

3.0hr



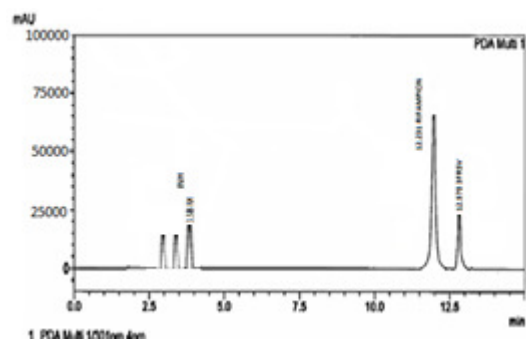
RETENTION TIME(MIN)	3.586	12.231	12.578
AREA	25331	75270	18817

3.5hr



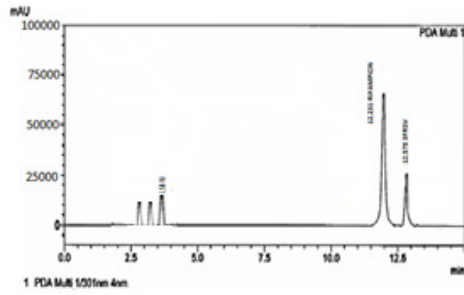
RETENTION TIME(MIN)	3.586	12.231	12.578
AREA	22436	73822	21712

4.0hr



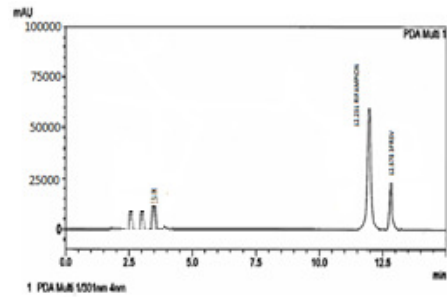
RETENTION TIME(MIN)	3.586	12.231	12.578
AREA	19541	70921	25331

5.0hr



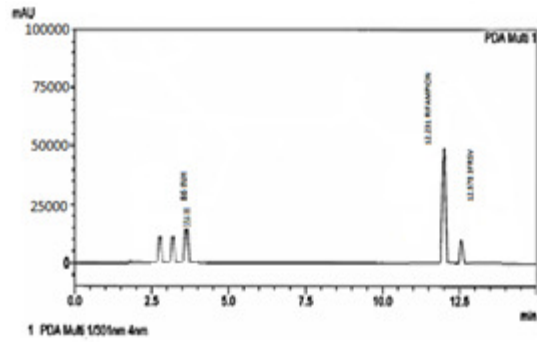
RETENTION TIME(MIN)	3.586	12.231	12.578
AREA	13027	66585	28950

6.0hr



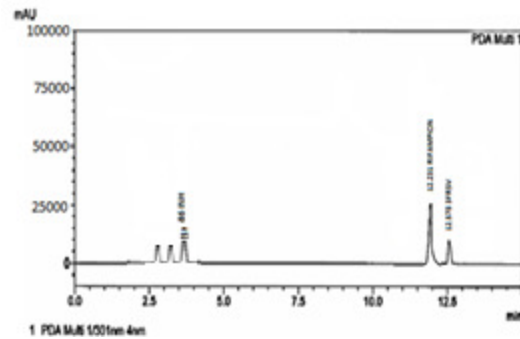
RETENTION TIME(MIN)	3.586	12.231	12.578
AREA	10856	60795	24607

8.0hr



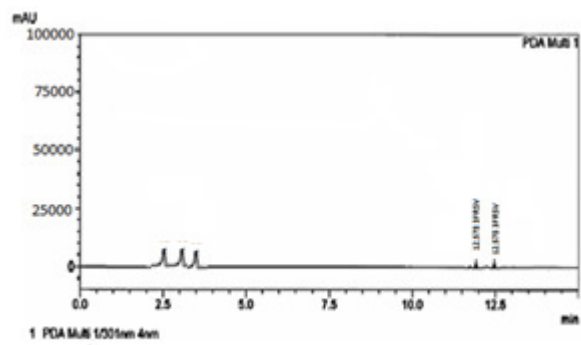
RETENTION TIME(MIN)	3.586	12.231	12.578
AREA	18817	49215	8684

10.0hr

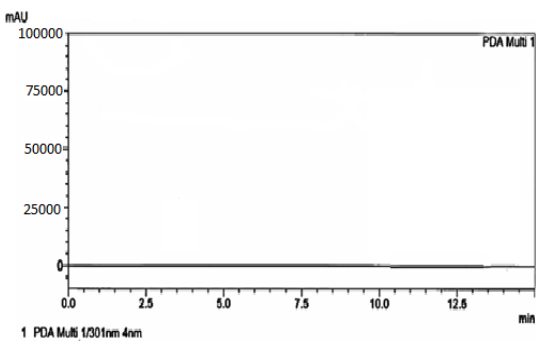


RETENTION TIME(MIN)	3.586	12.231	12.578
AREA	5790	28950	9408

12.0 hr



24.0hr



RETENTION TIME(MIN)	3.586	12.231	12.578
AREA	5428	724	742

Table: 55 Peak area of rifampicin in Group I animals at various time intervals; n=6

0.5	1.0	1.5	2.0	2.5	3.0	3.5	4.0	5.0	6.0	8.0	10.0	12.0
7273.5	28950	35463	49215	73099	64413	53557	49938	36911	34740	20948	8685	4342
4342	31161	38358	46320	64413	62242	55728	57176	39806	33292	21712	7237	2171
5066	28226	36187	47767	62966	63690	55005	48491	36186	31121	14475	10856	14330
7961	32568	39082	49938	71651	60795	59347	47043	40530	32568	16646	79691	4342
8685	29673	34740	44872	68032	57900	57900	54241	37635	30397	14475	11580	36187
5790	31845	37635	43425	66585	62242	57176	51386	39082	28950	17370	10132	14330

Table: 56 Peak area of 3FRSV in Group I animals at various time intervals; n=6

0.5	1.0	1.5	2.0	2.5	3.0	3.5	4.0	5.0	6.0	8.0	10.0	12.0
362	2171	7237	13389	21712	28950	36187	43425	49215	40530	28950	13389	36187
1086	6514	14475	19541	24607	31845	35463	41977	46320	43425	30397	19541	1086
434	3618	10132	14475	20988	29674	34740	41254	47767	41254	28226	14475	434
1013	5066	11580	13751	25331	31121	39082	44148	49939	39806	31121	13751	1013
282	2895	9409	16646	22436	28226	38358	44872	44872	44149	27502	16646	282
282	5790	12304	14330	23884	32568	37635	40530	43425	42701	31845	14330	282

Table: 57 Peak area of rifampicin in Group II animals at various time intervals; n=6

0.5	1.0	1.5	2.0	2.5	3.0	3.5	4.0	5.0	6.0	8.0	10.0	12.0
7237	30397	38359	43425	61518	56452	54281	44872	33292	27502	15922	5790	2171
4342	28950	31121	41977	58623	57900	48491	47767	36187	30397	18817	1158	36187
5066	26778	29674	41253	56452	55728	49938	43425	34016	28226	16646	7961	14330
7961	24607	33292	44148	60071	58623	51386	49215	35463	29673	18093	6513	4342

8685	26778	34740	44872	57176	55005	52833	44149	32569	30397	14475	9408	72
5790	26055	39082	40530	62966	59347	50662	48491	36911	27502	20265	7237	506

Table: 58 Peak area of 3FRSV in Group II animals at various time intervals; n=6

0.5	1.0	1.5	2.0	2.5	3.0	3.5	4.0	5.0	6.0	8.0	10.0	12.0
362	5066	11580	18817	28950	39082	44872	57900	62966	54281	36187	18094	7237
1085	6514	13027	21712	30397	44872	47767	54281	54281	48491	40530	19541	21712
434	4342	10856	19541	28226	41253	43425	49215	56452	49938	37635	17370	21712
1013	7237	13751	20989	31121	35463	49215	47043	60795	51386	39082	2026	7237
287	6514	13027	18094	27502	37635	44149	57900	57538	52833	36911	16646	21712
287	5066	11580	22436	31845	40530	48491	48491	58623	50662	39806	20989	21712

Table: 59 Peak area of rifampicin in Group III animals at various time intervals; n=6

Time(h)	0.5	1.0	1.5	2.0	2.5	3.0	3.5	4.0	5.0	6.0	8.0	10.0	12.0	24.0
1	9273.5	58950	65463	79215	93099	94413	83557	79938	66911	64740	50948	10685	7342	
2	6342	61161	68358	76320	94413	92742	85728	87176	69806	63292	51712	9237	5171	
3	7066	58226	66187	77767	92966	93690	85005	78491	66186	61121	44475	40856	44475	
4	9961	62588	69082	79938	91651	98795	89347	77043	60530	64568	46646	109691	7342	
5	10685	32673	37740	47872	98032	60900	87900	84241	67635	60397	44475	14580	7618	

	6	7790	34845	39635	46425	99587	65245	87176	81386	69082	58950	47370	13132	4447	
--	---	------	-------	-------	-------	-------	-------	-------	-------	-------	-------	-------	-------	------	--

Time(h)	0.5	1.0	1.5	2.0	2.5	3.0	3.5	4.0	5.0	6.0	8.0
---------	-----	-----	-----	-----	-----	-----	-----	-----	-----	-----	-----

Table: 60 Peak area of 3FRSVin Group III animals at various time intervals; n=6

Peak area	1	162	1771	4237	10389	18712	25950	33187	40425	46215	37530	25950
	2	786	3514	11475	16541	21607	28845	32463	38977	43320	40425	27397
	3	134	1618	7132	11475	17988	26674	31740	38254	44767	38254	25226
	4	713	2066	8580	10751	23331	28121	36082	41148	46939	36806	29121
	5	182	1895	6409	13646	19436	25226	35358	41872	43872	43949	24502
	6	182	2790	9304	9330	20884	29568	34635	37530	40425	39701	28845

Table: 61 Peak area of rifampicin in Group IV animals at various time intervals; n=6

0.5	1.0	1.5	2.0	2.5	3.0	3.5	4.0	5.0	6.0	8.0	10.0	1
14475	47044	60071	76717	75994	74546	73099	70204	65861	57900	46320	28226	13
17370	48491	61518	70204	77441	75994	74546	71651	65137	63690	54281	29674	19
15199	46320	59347	75270	75270	73822	72375	69480	66585	58623	44148	27502	14
16646	49215	62242	73099	78165	76715	75270	72375	70927	62966	49938	30397	13
13751	45596	58624	71651	74546	73099	71651	68756	64413	59345	53557	26778	16
17370	49939	62966	73822	78889	77441	75993	73099	65137	62242	50662	31121	14

Table: 62 Peak area of 3FRSV in Group IV animals at various time intervals; n=6

0.5	1.0	1.5	2.0	2.5	3.0	3.5	4.0	5.0	6.0	8.0	10.0	1
-----	-----	-----	-----	-----	-----	-----	-----	-----	-----	-----	------	---

362	1447	4342	8685	18817	18094	20989	24607	27502	23883	20988	8685	3
1086	2895	5790	7238	12303	19541	22436	26055	30397	25331	21712	7238	1
435	724	3619	10856	15198	17370	20265	23884	28226	23160	14475	10856	4
1013	3619	6514	79691	17370	20265	23160	26779	29673	26055	16646	79691	1
287	2895	2895	11580	13751	16646	19541	23160	30397	22436	14475	11580	2
287	1448	7238	10133	11580	20989	23884	27503	27503	26779	17370	10133	2

Table: 63 Plasma concentration of rifampicin in Group I animals at various time intervals; n=6

0.5	1.0	1.5	2.0	2.5	3.0	3.5	4.0	5.0	6.0	8.0	10.0	
1.0	4.0	4.9	6.8	10.1	8.9	7.4	6.9	5.1	4.8	2.9	1.2	
0.6	4.3	5.3	6.4	8.9	8.6	7.7	7.9	5.5	4.6	3.0	1.0	
0.7	3.9	5.0	6.6	8.7	8.8	7.6	6.7	5.0	4.3	2.0	1.5	
1.1	4.5	5.4	6.9	9.9	8.4	8.2	6.5	5.6	4.5	2.3	1.1	
1.2	4.1	4.8	6.2	9.4	8.0	8.0	7.5	5.2	4.2	2.0	1.6	
0.8	4.4	5.2	6.0	9.2	8.6	7.9	7.1	5.4	4.0	2.4	1.4	
0.9±0.09	4.2±0.96	5.1±0.96	6.5±0.14	9.3±0.22	8.6±0.13	7.8±0.11	7.1±0.21	5.3±0.09	4.4±0.11	2.5±0.17	1.3±0.09	0

Table: 64 Plasma concentration of 3FRSV in Group I animals at various time intervals; n=6

0.5	1.0	1.5	2.0	2.5	3.0	3.5	4.0	5.0	6.0	8.0	10.0	
0.05	0.3	1.0	1.85	3.0	4.0	5.0	6.0	6.8	5.6	4.0	1.85	
0.15	0.9	2.0	2.7	3.4	4.4	4.9	5.8	6.4	6.0	4.2	2.7	
0.06	0.5	1.4	2.0	2.9	4.1	4.8	5.7	6.6	5.7	3.9	2.0	
0.14	0.7	1.6	1.9	3.5	4.3	5.4	6.1	6.9	5.5	4.3	1.9	
0.05	0.4	1.3	2.3	3.1	3.9	5.3	6.2	6.2	6.1	3.8	2.3	
0.15	0.8	1.7	1.98	3.3	4.5	5.2	5.6	6.0	5.9	4.4	1.98	
I 0.1±0.02	0.6±0.09	1.5±0.14	2.1±0.13	3.2±0.09	4.2±0.09	5.1±0.09	5.9±0.09	6.5±0.14	5.8±0.09	4.1±0.09	2.1±0.13	

Table: 65 Plasma concentration of rifampicin in Group II animals at various time intervals; n=6

	0.5	1.0	1.5	2.0	2.5	3.0	3.5	4.0	5.0	6.0	8.0	10.0	
	1.0	4.2	5.3	6.0	8.5	7.8	7.5	6.2	4.6	3.8	2.2	0.8	
	0.6	4.0	4.3	5.8	8.1	8.0	6.7	6.6	5.0	4.2	2.6	1.6	
	0.7	3.7	4.1	5.7	7.8	7.7	6.9	6.0	4.7	3.9	2.3	1.1	
	1.1	3.4	4.6	6.1	8.3	8.1	7.1	6.8	4.9	4.1	2.5	0.9	
	1.2	3.7	4.8	6.2	7.9	7.6	7.3	6.1	4.5	4.2	2.0	1.3	
	0.8	3.6	5.4	5.6	8.7	8.2	7.0	6.7	5.1	3.8	2.8	1.0	
1	0.9±0.09	3.8±0.11	4.7±0.21	5.9±0.09	8.3±0.14	7.9±0.09	7.1±0.11	6.4±0.13	4.8±0.09	4.0±0.77	2.4±0.11	1.2±0.11	

Table: 66 Plasma concentration of 3FRSV in Group II animals at various time intervals; n=6

	0.5	1.0	1.5	2.0	2.5	3.0	3.5	4.0	5.0	6.0	8.0	10.0	
	0.05	0.7	1.6	2.6	4.0	5.4	6.2	8.0	8.7	7.0	5.0	2.5	
	0.15	0.9	1.8	3.0	4.2	6.2	6.6	7.5	7.5	7.5	5.6	2.7	
	0.06	0.6	1.5	2.7	3.9	5.7	6.0	6.8	7.8	7.3	5.2	2.4	
	0.14	1.0	1.9	2.9	4.3	4.9	6.8	6.5	8.4	6.7	5.4	2.8	
	0.05	0.9	1.8	2.5	3.8	5.2	6.1	8.0	7.9	7.1	5.1	2.3	
	0.15	0.7	1.6	3.1	4.4	5.6	6.7	6.7	8.1	6.9	5.5	2.9	
1	0.1±0.02	0.8±0.06	1.7±0.06	2.8±0.09	4.1±0.09	5.5±0.18	6.4±0.13	7.2±0.27	8.1±0.17	7.1±0.11	5.3±0.09	2.6±0.09	

Table: 67 Plasma concentration of rifampicin in Group III animals at various time

Time(h)		0.5	1.0	1.5	2.0	2.5	3.0	3.5	4.0	5.0	6.0	8.0	10.0
Time(h)		0.5	1.0	1.5	2.0	2.5	3.0	3.5	4.0	5.0	6.0	8.0	10.0
Peak area	1	1.8	5.1	5.9	7.8	11.1	9.9	8.4	7.9	6.1	5.8	3.9	3.0
	2	1.8	5.0	6.3	7.4	9.9	9.6	8.7	7.9	6.5	5.6	4.0	3.0
Peak area	3	1.6	5.3	6.0	7.7	9.7	9.5	8.6	7.7	6.0	5.3	3.0	
	4	1.7	4.9	6.4	7.9	10.9	9.4	9.2	7.5	6.6	5.5	3.3	
	5	1.7	5.5	5.8	7.2	10.4	9.0	9.0	8.5	6.2	5.2	3.0	
	6	1.8	5.4	6.2	7.0	10.2	9.6	8.9	8.1	6.4	5.0	3.4	
Mean±SEM		1.9±0.09	5.2±0.96	6.1±0.96	7.5±0.14	10.3±0.22	9.6±0.13	8.8±0.11	8.1±0.21	6.3±0.09	4.4±0.11	3.5±0.17	2.0±0.09

intervals; n=6

Table: 68 Plasma concentration of 3FRSV in Group III animals at various time intervals; n=6

	3	0.06	0.6	2.0	1.0	1.9	2.1	3.8	4.7	5.6	4.7	2
	4	0.14	0.6	1.4	0.9	2.5	2.3	3.4	5.1	5.9	4.5	3
	5	0.05	0.3	1.6	1.3	2.1	2.9	3.3	5.2	5.2	5.1	2
	6	0.15	0.7	1.3	0.98	2.3	3.5	3.2	4.6	5.0	4.9	3
Mean+SEM		0.1 ±0.02	0.5± 0.09	1.4± 0.014	1.1± 0.14	2.2± 0.09	3.2± 0.09	4.1± 0.09	4.9± 0.09	5.5± 0.14	4.8± 0.09	3.0± 0.09

Table: 69 Plasma concentration of rifampicin in Group IV animals at various time intervals; n=6

0.5	1.0	1.5	2.0	2.5	3.0	3.5	4.0	5.0	6.0	8.0	10.0
2.0	6.5	8.3	10.6	10.5	10.3	10.1	9.7	9.1	8.0	6.4	3.9
2.4	6.7	8.5	9.7	10.7	10.5	10.3	9.9	9.0	8.8	7.2	4.1
2.1	6.4	8.2	10.4	10.4	10.2	10.0	9.6	9.2	8.1	6.1	3.8
2.3	6.8	8.6	10.1	10.8	10.6	10.4	10.0	9.8	8.7	6.9	4.2
1.9	6.3	8.1	9.9	10.3	10.1	9.9	9.5	8.9	8.2	7.4	3.7
2.4	6.9	8.7	10.2	10.9	10.7	10.5	10.1	9.0	8.6	7.0	4.3
2.2±0.8	6.6±0.09	8.4±0.09	10.0±0.13	10.6±0.09	10.4±0.09	10.2±0.09	9.8±0.09	9.2±0.13	8.4±0.13	6.8±0.02	4.0±0.09

Table: 70 Plasma concentration of 3FRSV in Group IV animals at various time intervals; n=6

0.5	1.0	1.5	2.0	2.5	3.0	3.5	4.0	5.0	6.0	8.0	10.0
-----	-----	-----	-----	-----	-----	-----	-----	-----	-----	-----	------

	0.05	0.2	0.6	1.2	2.6	2.5	2.9	3.4	3.8	3.3	2.9	1.2
	0.15	0.4	0.8	1.0	1.7	2.7	3.1	3.6	4.2	3.54	3.0	1.0
	0.06	0.1	0.5	1.5	2.1	2.4	2.8	3.3	3.9	3.2	2.0	1.5
	0.14	0.5	0.9	1.9	2.4	2.8	3.2	3.7	4.1	3.6	2.3	1.1
	0.05	0.4	0.4	1.6	1.9	2.3	2.7	3.2	4.2	3.1	2.0	1.6
	0.15	0.2	1.0	1.4	1.6	2.9	3.3	3.8	3.8	3.7	2.4	1.4
	0.1±0.02	0.3±0.06	0.7±0.09	1.3±0.09	2.0±0.16	2.6±0.09	3.0±0.09	3.5±0.09	4.0±0.07	3.4±0.09	2.5±0.017	1.3±0.09

9.1. Pharmacokinetic calculations

Table: 71 Pharmacokinetics of rifampicin in Group I (Rifampicin alone) animals;n=6

S.No	Parameters	Trials						Mean±S.E.M
		1	2	3	4	5	6	
1	C_{max}(µg/ml)	10.10	8.90	8.80	9.90	9.40	9.20	9.38±0.2151
2	T_{max}(hr)	2.50	2.50	3.00	2.50	2.50	2.50	2.58±0.083
3	AUC₀₋₂₄	53.90	50.95	48.82	53.17	52.15	49.70	51.448±0.81
4	k_{eli}(hr⁻¹)	0.289	0.234	0.295	0.255	0.318	0.245	0.272±0.013
5	AUC_{0-∞}	96.87	111.94	95.25	102.96	98.15	105.82	101.83±2.59
6	t_{1/2}(hr)	2.182	2.251	2.196	2.150	2.140	2.324	1.942±0.098

Table: 72 Pharmacokinetics of 3FRSV in Group I (Rifampicin alone) animals;n=6

S.No	Parameters	Trials						Mean±S.E.M
		1	2	3	4	5	6	
1	C_{max}(µg/ml)	6.8	6.4	6.6	6.9	6.2	6	6.48±0.1424
2	T_{max}(hr)	4.5	4.5	4.5	4.5	4.0	4.5	4.42±0.08
3	AUC₀₋₂₄	23.95	27.65	22.2	23.08	21.2	29.415	24.585±1.3
4	k_{eli}(hr⁻¹)	0.344	0.335	0.322	0.358	0.339	0.345	0.304±0.004
5	AUC_{0-∞}	45.44	54.51	46.27	51.90	46.07	50.13	49.05±1.514
6	t_{1/2}(hr)	1.559	2.411	1.932	2.342	1.579	2.005	1.97±0.148

Table: 73 Pharmacokinetics of RIF in Group II (Rifampicin in the presence of FDC); n=6

S.No	Parameters	Trials						Mean±S.E.M
		1	2	3	4	5	6	
1	C_{max}(µg/ml)	8.50	8.10	7.80	8.30	7.90	8.70	8.22±0.1424
2	T_{max}(hr)	2.50	2.5	2.50	2.50	2.50	2.50	2.5±0.0
3	AUC₀₋₂₄	36.50	40.40	34.92	39.52	35.50	41.2	38.0±1.10
4	k_{eli}(hr⁻¹)	0.383	0.308	0.403	0.316	0.464	0.298	0.36±0.027
5	AUC_{0-∞}	58.67	66.70	54.3	65.83	52.54	70.37	61.4±2.97
6	t_{1/2} (hr)	1.808	1.794	1.722	1.702	1.495	1.681	1.97±0.138

Table: 74 Pharmacokinetics of 3FRSV in Group II (Rifampicin in the presence of FDC); n=6

S. No	Parameters	Trials						Mean±S.E.M
		1	2	3	4	5	6	
1	C_{max}(µg/ml)	8.7	7.5	7.8	8.4	8	8.1	8.1±0.17400
2	T_{max}(hr)	4.5	4	4.5	4.5	4	4.5	4.3±0.10540
3	AUC₀₋₂₄	39.675	43.45	40.405	40.745	38.4	41.85	40.75±0.71410
4	k_{eli}(hr⁻¹)	0.2040	0.2047	0.2997	0.2970	0.2660	0.2636	0.255±0.0174
5	AUC_{0-∞}	61.17	68.06	66.42	61.89	55.53	64.12	62.9±1.81500
6	t_{1/2} (hr)	1.713	2.275	2.312	1.744	1.485	1.906	1.9±0.13440

Table: 75 Pharmacokinetics of rifampicin in Group III (Rifampicin in the presence of PLGA); n=6

S.No	Parameters	Trials						Mean±S.E.M
		1	2	3	4	5	6	
1	C_{max}(µg/ml)	11.10	9.90	9.80	10.90	10.40	10.20	11.38± 0.2151
2	T_{max}(hr)	2.86	2.85	2.86	2.86	2.86	2.87	2.865±0.003
3	AUC₀₋₂₄	97.90	90.95	88.82	97.17	96.15	89.70	97.448±0.081
4	k_{eli}(hr⁻¹)	0.136	0.135	0.134	0.135	0.136	0.136	0.136±0.013
5	AUC_{0-∞}	161.87	16.80	16.85	160.87	160.87	160.87	161.4±2.97
6	t_{1/2} (hr)	2.541	2.542	2.543	2.542	2.542	2.541	2.542±0.098

Table: 76 Pharmacokinetics of 3FRSV in Group III (Rifampicin in the presence of PLGA); n=6

S.No	Parameters	Trials						Mean±S.E.M
		1	2	3	4	5	6	
1	C_{max}(µg/ml)	2.8	2.4	2.6	2.9	2.2	2.2	2.48±0.1424
2	T_{max}(hr)	4.61	4.60	4.60	4.61	4.62	4.61	4.62±0.008
3	AUC₀₋₂₄	3.58	3.59	3.58	3.51	3.52	3.58	3.585±1.3
4	k_{eli}(hr⁻¹)	0.384	6.380	0.382	0.384	0.382	384	0.384±0.044
5	AUC_{0-∞}	24.44	34.51	26.27	32.90	28.07	29.13	24.05±514
6	t_{1/2} (hr)	2.559	3.411	2.932	3.342	2.579	1.005	2.18±0.148

Table: 77 Pharmacokinetics of rifampicin in Group IV (RIF+FDC+PLGA); n=6

S.No	Parameters	Trials						Mean±S.E.M
		1	2	3	4	5	6	
1	C _{max} (µg/ml)	10.6	10.7	10.4	10.8	10.3	10.9	10.62±0.09
2	T _{max} (hr)	2.0	2.50	2.00	2.50	2.50	2.50	2.33±0.1054
3	AUC ₀₋₂₄	80.65	90.15	80.875	84.375	84.20	84.75	84.2±1.407
4	k _{eli} (hr ⁻¹)	0.195	0.160	0.188	0.194	0.173	0.193	0.18±0.01
5	AUC _{0-∞}	135.07	157.18	136.21	140.10	143.81	141.3	142.27±3.261
6	t _{1/2} (hr)	3.559	4.342	3.688	3.577	4.012	3.595	3.795±0.1292

Table: 78 Pharmacokinetics of 3FRSV in Group IV (RIF+FDC+PLGA) animals; n=6

S.No	Parameters	Trials						Mean±S.E.M
		1	2	3	4	5	6	
1	C _{max} (µg/ml)	3.8	4.2	3.9	4.1	4.2	3.8	4.0±0.07746
2	T _{max} (hr)	4.5	4.5	4.5	4.5	4.5	4.5	4.5±0.000
3	AUC ₀₋₂₄	19.45	20.15	18.71	19.99	18.9	20.85	19.68±0.33
4	k _{eli} (hr ⁻¹)	0.406	0.405	0.472	0.422	0.481	0.491	0.446±0.016
5	AUC _{0-∞}	28.81	34.12	29.17	32.72	29.92	33.87	31.44±0.98
6	t _{1/2} (hr)	2.032	2.908	2.156	2.152	2.086	2.375	2.28±0.134

9.2. Pharmacokinetic parameters of rifampicin

C_{\max} of rifampicin in RIF alone, RIF+FDC, RIF+PLGA and RIF+FDC+PLGA

The mean C_{\max} values of RIF in RIF alone, RIF+FDC, RIF+PLGA and RIF+FDC+PLGA are respectively 9.383 ± 0.2151 , 8.216 ± 0.1424 , 11.38 ± 0.2151 and 10.616 ± 0.0945 . The C_{\max} of RIF was decreased in the presence of FDC significantly ($p < 0.001$) and C_{\max} of RIF+FDC+PLGA was decreased compared to RIF+PLGA significantly ($p < 0.001$).

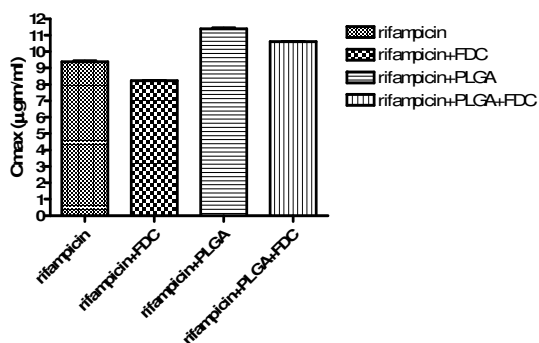
Table: 79

C_{\max} of rifampicin in RIF alone, RIF+FDC, RIF+FDC+PLGA $n=6$, Mean \pm S.E.M

S.NO	GROUP	$C_{\max}(\mu\text{g/ml})$
1	RIF alone	9.38 ± 0.2151
2	RIF+FDC	8.22 ± 0.1424
3	RIF+PLGA	11.38 ± 0.2151
4	RIF+FDC+PLGA	10.616 ± 0.0945

$a=p < 0.001$, $b=p < 0.001$, $c=p < 0.001$ $d=p < 0.001$ when compared with RIF alone, RIF+FDC, RIF+PLGA and RIF+FDC+PLGA groups respectively followed by one way ANOVA followed by Tukey's multiple comparison test. $P < 0.05$ was considered as significant.

Fig: 42 C_{\max} of RIF alone, RIF+FDC, RIF+PLGA, RIF+FDC+PLGA



T_{max} of RIF in RIF alone, RIF+FDC, and RIF+FDC+PLGA

The mean T_{max} values of RIF, RIF+FDC, RIF+PLGA, RIF+FDC+PLGA are respectively 2.583±0.0083, 2.5±0.00, 2.865±0.003 and 2.33±0.1054. There is no significant difference in T_{max} of RIF alone, RIF+FDC, RIF+PLGA and RIF+FDC+PLGA

Table: 80

T_{max} of rifampicin in RIF alone, RIF+FDC, RIF+PLGA and RIF+FDC+PLGA n=6, Mean±S.E.M

S.NO	GROUP	T _{max} (hr ⁻¹)
1	RIF alone	2.58±0.083
2	RIF+FDC	2.5±0.00
3	RIF+PLGA	2.865±0.003
4	RIF+FDC+PLGA	2.33±0.1054

There is no significant difference in p values of T_{max} in RIF alone, RIF+FDC, RIF+PLGA, RIF+FDC+PLGA followed by one way ANOVA followed by Tukey's multiple comparison test. P<0.05 was considered as significant.

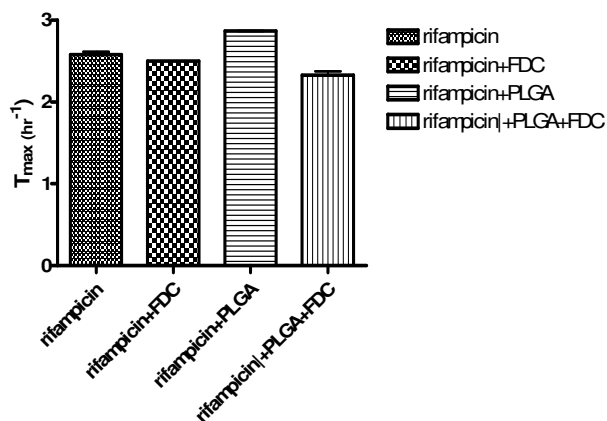


Fig: 43 T_{max} of rifampicin in RIF alone, RIF+FDC, RIF+PLGA and RIF+FDC+PLGA

AUC₀₋₂₄ of rifampicin in RIF alone, RIF+FDC, RIF+PLGA, RIF+FDC+PLGA

The mean AUC₀₋₂₄ values of RIF, RIF+FDC, RIF+PLGA, RIF+FDC+PLGA are respectively 51.448±0.8099, 38.008±1.100, 97.448±0.081 and 84.166±1.407. AUC₀₋₂₄ of RIF was decreased in the presence of FDC significantly (p<0.001) and the AUC of RIF+FDC+PLGA was decreased compare to RIF+PLGA was significantly (p<0.001).

Table: 81

AUC₀₋₂₄ of rifampicin in RIF alone, RIF+FDC, RIF+FDC+PLGA n=6, Mean±S.E.M

S.NO	GROUP	AUC ₀₋₂₄ (µg/ml.hr)
1	RIF alone	51.448±0.8099
2	RIF+FDC	38.008±1.100
3	RIF+PLGA	97.448±0.081
4	RIF+FDC+PLGA	84.166±1.407

a=p<0.001; b=p<0.001, c=p<0.001 d=p<0.001 when compared with RIF alone, RIF+FDC, RIF+PLGA and RIF+FDC+PLGA groups respectively followed by one way ANOVA followed by Tukey's multiple comparison test. P<0.05 was considered as significant.

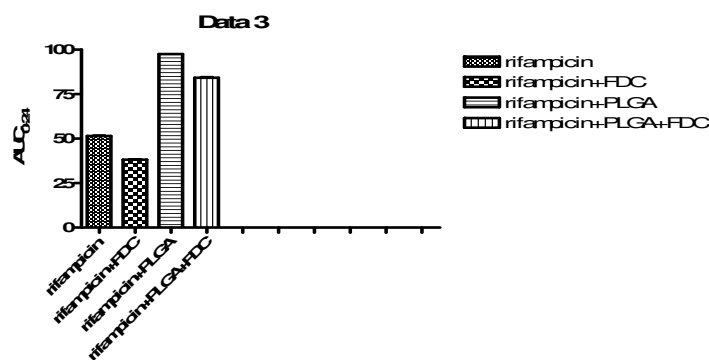


Fig: 44 AUC₀₋₂₄ of rifampicin in RIF alone, RIF+FDC, RIF+PLGA, RIF+FDC+PLGA

$K_{el}(\text{hr}^{-1})$ of Rifampicin in RIF alone, RIF+FDC, RIF+PLGA, RIF+FDC+PLGA

The mean $K_{el}(\text{hr}^{-1})$ values of RIF, RIF+FDC, RIF+PLGA, RIF+FDC+PLGA are respectively 0.2726 ± 0.0134 , 0.362 ± 0.0268 , 0.136 ± 0.013 and 0.1838 ± 0.006 . K_{el} of RIF was increased in the presence of FDC significantly ($p < 0.001$). RIF+FDC+PLGA was increased compared to RIF+PLGA and this increase was significantly ($p < 0.001$).

Table: 82

$K_{el}(\text{hr}^{-1})$ of rifampicin in RIF alone, RIF+FDC, RIF+PLGA, RIF+FDC+PLGA $n=6$, Mean \pm S.E.M

S.NO	GROUP	$K_{el}(\text{hr}^{-1})$
1	RIF alone	0.2726 ± 0.0134
2	RIF+FDC	0.362 ± 0.0268
3	RIF+PLGA	0.136 ± 0.013
4	RIF+FDC+PLGA	0.1838 ± 0.006

$a=p < 0.01$; $b=P < 0.01$, $b=p < 0.001$, $c=p < 0.01$, $c=p < 0.001$, $d=p < 0.001$ when compared with RIF alone, RIF+FDC, RIF+PLGA and RIF+FDC+PLGA groups respectively followed by one way ANOVA followed by Tukey's multiple comparison test. $P < 0.05$ was considered as significant

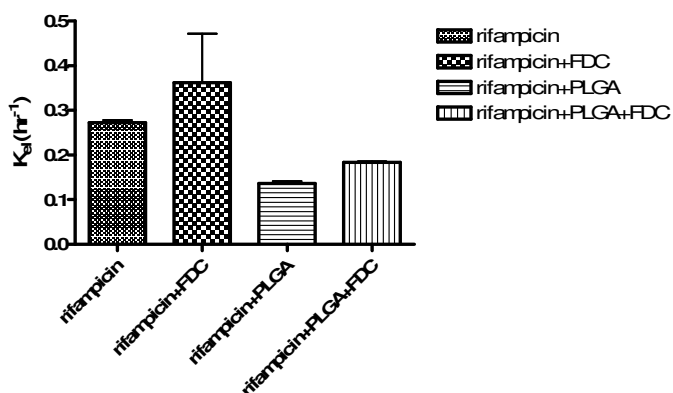


Fig: 45 $K_{el}(\text{hr}^{-1})$ of rifampicin in RIF alone, RIF+FDC, RIF+PLGA, RIF+FDC+PLGA.

AUC_{0-∞} of rifampicin in RIF alone, RIF+FDC,RIF+PLGA,RIF+FDC+PLGA

The mean AUC_{0-∞} values of RIF, RIF+FDC,RIF+PLGA,RIF+FDC+PLGA are respectively 101.8316±2.587, 61.407±2.970,161.4±2.97 and 142.27±2.361.AUC_{0-∞} of RIF was decreased in the presence of FDC significantly (p<0.001) and AUC of RIF+FDC+PLGA was decreased compared to RIF+PLGA this decrease was significantly (p<0.001).

Table: 83

AUC_{0-∞}of rifampicin in RIF alone, RIF+FDC,RIF+PLGA, RIF+FDC+PLGA n=6, Mean±S.E.M

S.NO	GROUP	AUC _{0-∞} (µg/ml.hr)
1	RIF alone	101.8316±2.587
2	RIF+FDC	61.407±2.970
3	RIF+PLGA	161.4±2.97
4	RIF+FDC+PLGA	142.27±2.361

a=p<0.001; b=P<0.001, c=p<0.001 d=p<0.001 when compared with RIF alone, RIF+FDC,RIF+PLGA and RIF+FDC+PLGA groups respectively followed by one way ANOVA followed by Tukey's multiple comparison test. P<0.05 was considered as significant.

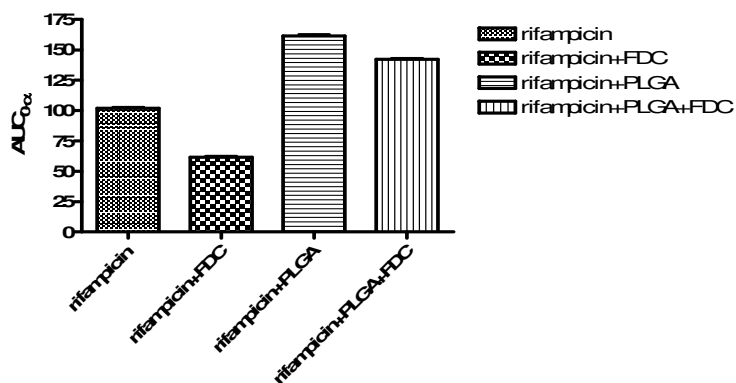


Fig: 46 AUC_{0-∞}of rifampicin in RIF alone, RIF+FDC,RIF+PLGA,RIF+FDC+PLGA

9.3. Pharmacokinetic parameters of 3FRSV

C_{max} of 3FRSV in RIF alone, RIF+FDC, RIF+PLGA and RIF+FDC+PLGA

The mean C_{max} values of 3FRSV in RIF, RIF+FDC, RIF+PLGA, RIF+FDC+PLGA are respectively 6.483 ± 0.1424 , 8.0808 ± 0.174 , 2.48 ± 0.1424 and 4.0 ± 0.077 . The C_{max} of RIF was increased in the presence of FDC significantly ($p < 0.001$) and this increase was also seen in the RIF+FDC+PLGA when compared to RIF +PLGA significantly ($p < 0.001$).

Table: 84

C_{max} of 3FRSV in RIF alone, RIF+FDC, RIF+PLGA, RIF+FDC+PLGA $n=6$, Mean \pm S.E.M

S.NO	GROUP	$C_{max}(\mu\text{g/ml})$
1	RIF alone	6.483 ± 0.1424
2	RIF+FDC	8.0808 ± 0.174
3	RIF+PLGA	2.48 ± 0.1424
4	RIF+FDC+PLGA	4.0 ± 0.077

$a=p < 0.001$; $b=P < 0.001$, $c=p < 0.001$ $d=p < 0.001$ when compared with RIF alone, RIF+FDC, RIF+PLGA and RIF+FDC+PLGA groups respectively followed by one way ANOVA followed by Tukey's multiple comparison test. $P < 0.05$ was considered as significant

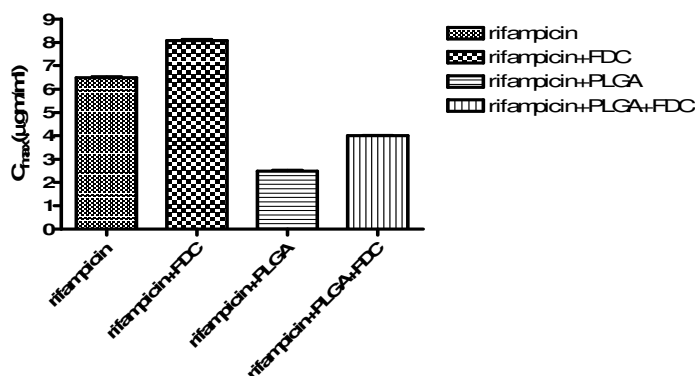


Fig: 47 C_{max} of 3FRSV in RIF alone, RIF+FDC, RIF+PLGA, RIF+FDC+PLGA

T_{max} of 3FRSV in RIF alone, RIF+FDC, RIF+PLGA and RIF+FDC+PLGA

The mean T_{max} values of 3FRSV in RIF, RIF+FDC, RIF+PLGA, RIF+FDC+PLGA are respectively 4.416±0.0083, 4.33±0.1054, 4.62±0.008 and 4.5±0.001. There is no significance difference in T_{max} of 3FRSV in RIF alone, RIF+FDC, RIF+PLGA and RIF+FDC+PLGA

Table: 85

T_{max} of 3FRSV in RIF alone, RIF+FDC, RIF+PLGA and RIF+FDC+PLGA n=6, Mean±S.E.M

S.NO	GROUP	T _{max} (hr ⁻¹)
1	RIF alone	2.58±0.083
2	RIF+FDC	2.5±0.004
3	RIF+PLGA	4.62±0.008
4	RIF+FDC+PLGA	4.5±0.001

There is no significant difference in p values of RIF alone, RIF+FDC, RIF+PLGA, RIF+FDC+PLGA followed by one way ANOVA followed by Tukey's multiple comparison test. P<0.05 was considered as significant

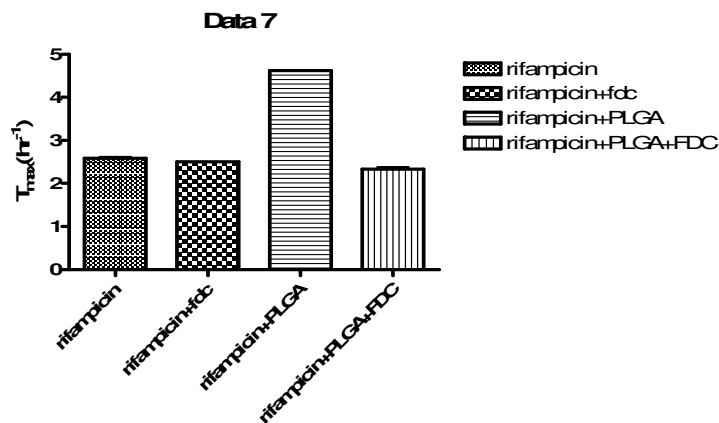


Fig: 48 T_{max} of 3FRSV in RIF alone, RIF+FDC, RIF+PLGA and RIF+FDC+PLGA

AUC₀₋₂₄ of 3FRSV in RIF alone, RIF+FDC, RIF+PLGA, RIF+FDC+PLGA

The mean AUC₀₋₂₄ values of 3FRSV in RIF alone, RIF+FDC, RIF+PLGA, RIF+FDC+PLGA are respectively 24.585±1.322, 40.754±0.7141, and 19.675±0.0311. AUC₀₋₂₄ of 3FRSV was increased in the presence of FDC significantly (p<0.001) AUC was increased in case of RIF+PLGA+FDC compared to RIF+PLGA and this increase was significantly (p<0.001).

Table: 86

AUC₀₋₂₄ of 3FRSV in RIF alone, RIF+FDC, RIF+PLGA, RIF+FDC+PLGA n=6, Mean±S.E.M

S.NO	GROUP	AUC ₀₋₂₄ (µg/ml.hr)
1	RIF alone	24.585±1.322
2	RIF+FDC	40.754±0.7141
3	RIF+PLGA	3.585±1.3
4	RIF+FDC+PLGA	19.675±0.0311

a=p<0.001; b=P<0.001, c=p<0.001 d=p<0.001 when compared with RIF alone, RIF+FDC, RIF+PLGA and RIF+FDC+PLGA groups respectively followed by one way ANOVA followed by Tukey's multiple comparison test. P<0.05 was considered as significant

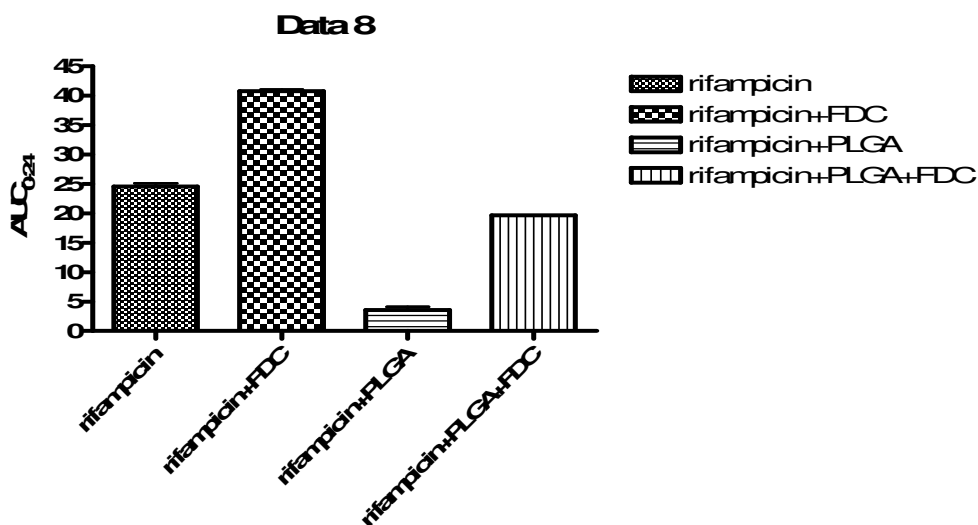


Fig: 49 AUC₀₋₂₄ of 3FRSV in RIF alone, RIF+FDC, RIF+PLGA, RIF+FDC+PLGA

$K_{el}(\text{hr}^{-1})$ of 3FRSV in RIF alone, RIF+FDC, RIF+PLGA, RIF+FDC+PLGA

The mean $K_{el}(\text{hr}^{-1})$ values 3FRSV in RIF, RIF+FDC, RIF+PLGA, RIF+FDC+PLGA are respectively 0.3405 ± 0.00487 , 0.2558 ± 0.0174 , 0.384 ± 0.004 and 0.4461 ± 0.01611 . K_{el} of 3FRSV was decreased in the presence of FDC significantly ($p < 0.001$) and the k_{el} of RIF+PLGA+FDC was increased when compare to RIF+PLGA this increase was significantly ($p < 0.001$).

Table: 87

$K_{el}(\text{hr}^{-1})$ of 3FRSV in RIF alone, RIF+FDC, RIF+FDC+PLGA

S.NO	GROUP	$K_{el}(\text{hr}^{-1})$
1	RIF alone	0.3405 ± 0.00487
2	RIF+FDC	0.2558 ± 0.0174
3	RIF+PLGA	0.384 ± 0.004
4	RIF+FDC+PLGA	0.4461 ± 0.01611

$a = p < 0.01$; $b = P < 0.01$, $c = p < 0.001$, $d = p < 0.001$ when compared with RIF alone, RIF+FDC, RIF+PLGA and RIF+FDC+PLGA groups respectively followed by one way ANOVA followed by Tukey's multiple comparison test. $P < 0.05$ was considered as significant

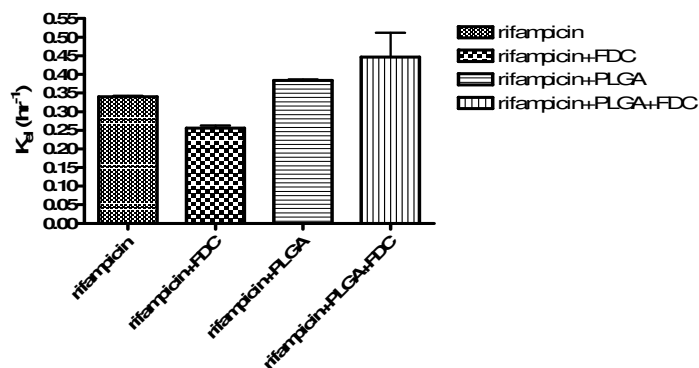


Fig: 50 $K_{el}(\text{hr}^{-1})$ of 3FRSV in RIF alone, RIF+FDC, RIF+PLGA, RIF+FDC+PLGA

AUC_{0-∞} of 3FRSV in RIF alone, RIF+FDC, RIF+PLGA, RIF+FDC+PLGA

The mean AUC_{0-∞} values of 3FRSV of RIF, RIF+FDC, RIF+PLGA, RIF+FDC+PLGA are respectively 49.053±1.514, 62.865±1.815, 24.05±514 and 31.435±0.985. AUC_{0-∞} of 3FRSV was increased in the presence of FDC significantly (p<0.001) and this increase was also seen in RIF+FDC+PLGA a when compared to RIF+PLGA significantly (p<0.001).

Table: 88

AUC_{0-∞} of 3FRSV in RIF alone, RIF+FDC, RIF+PLGA, RIF+FDC+PLGA n=6, Mean±S.E.M.

S.NO	GROUP	AUC _{0-∞} (µg/ml.hr)
1	RIF alone	49.053±1.514
2	RIF+FDC	62.865±1.815
3	RIF+PLGA	24.05±514
4	RIF+FDC+PLGA	31.435±0.985

a=p<0.001; b=P<0.001, c=p<0.001 d=p<0.001 when compared with RIF alone, RIF+FDC, RIF+PLGA and RIF+FDC+PLGA groups respectively followed by one way ANOVA followed by Tukey's multiple comparison test. P<0.05 was considered as significant

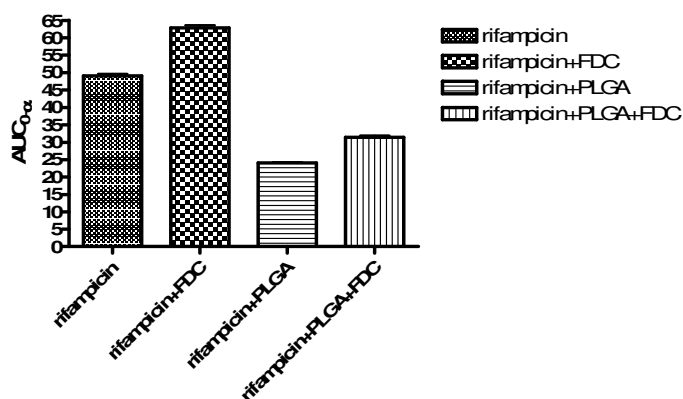


Fig: 51 AUC_{0-∞} of 3FRSV in RIF alone, RIF+FDC, RIF+PLGA, RIF+FDC+PLGA

10. DISCUSSION

Treatment of tuberculosis remains challenge due to resistance to the drug treatment rifampicin, isoniazid, pyrazinamide, ethambutol, are drugs of choice due to resistance to the drug treatment of tuberculosis as recommended by WHO. They are administered as a fixed dose combination in order to avoid drug resistance to separately administered drugs. This fixed dose combination (FDC) is widely used in india and elsewhere due to better patient compliance, reduction in viable bacterial population in minimization of drug resistance. Reports indicate poor bioavailability of rifampicin from a number of dosage forms of rifampicin and its combination with INH⁷⁵. This may be responsible for the treatment failure and consequent development of resistance.

Degradation of rifampicin is another issue that affects bioavailability of rifampicin. Rifampicin degrade in acidic condition of the stomach and the degradation of rifampicin is pH dependend⁷⁶. Another report says the problem of poor absorption of rifampicin from combination products is perhaps due to increased decomposition in stomach condition and the decomposition of rifampicin is enhanced by presence of INH.

In acidic medium rifampicin hydrolyses to 3 formyl rifampicin SV (3-FRSV) and it undergoes air oxidation in alkaline medium to form in active quinone derivative rifampicin quinone, 3-FRSV precipitates in acidic condition. It shows high antimicrobial activity⁷⁷ but is inactive in invivo (USP DI,1996). Therefore formation of 3-FRSV in the acidic condition environment of stomach can be an important factor affecting bioavailability of rifampicin and cannot be overlooked.

Rifampicin has been reported rapidly absorbed from the stomach however undergoes degradation and so results as in poor bioavailabilty of rifampicin. The normal gastric empty time is 2-3 hrs. several fixed dose combination of rifampicin are available however it has been reported that these formulation showed varied release rate of rifampicin in the stomach and so resulting in prolonged resident time in the gastric pH.

Any attempt that can be prevent or minimize the degradation of rifampicin either as a single drug or in combination of other anti tubercular drug is therapeutically beneficial to overcome resistance to tuberculosis treatment and there by achive effective control of tuberculosis with improved bioavailabilty of rifampicin.

Based on the above factors present study was aimed to study the decomposition effect of rifampicin in a pH stimulating the condition in stomach and also how rifampicin nanoparticles addition protects rifampicin against degradation in the gastric pH. The stability was extended to 3 hrs considering the gastric empty time (3 hrs).

The result of the stability indicate that rifampicin nanoparticles minimizes degradation of rifampicin and at low level concentration rifampicin nanoparticles could reduce the rifampicin degradation from 2% to 12% (statistically significant; $P < 0.001$) as the rifampicin nanoparticles concentration was increased the degradation of rifampicin was further reduced significantly. This may the probable mechanism for protective effect of rifampicin against degradation in the stomach.

Rifampicin degraded 13.35% at 60min and the degradation was increased to 21.4% in the presence of FDC. Rifampicin nanoparticles Incorporation reduced the RIF's degradation in the presence of FDC in a dose dependent manner. Maximum inhibition of degradation of RIF in the presence and absence of FDC was found with 1:3 ratios with rifampicin nanoparticles. Beyond this concentration no significant ($p > 0.05$) inhibition of RIF degradation in presence of FDC (8.46%) was observed. The inhibition of RIF's degradation in presence of FDC by rifampicin nanoparticles was well reflected in the percent formation of 3FRSV, the metabolite of RIF. Rifampicin nanoparticles dose dependently inhibit the formation of 3FRSV was observed with 1:3 ratios of rifampicin nanoparticles. There was no significant ($p > 0.05$) inhibit of 3FRSV formation (8.23%) beyond the concentration 1:3 ratio of plga (Tables 53, 54 and Figs 40, 41). The above findings clearly suggest that Icorporation of rifampicin nanoparticles reduces RIF degradation, formation of the metabolite 3FRSV in the presence of FDC.

The encapsulation efficiency and percentage yield of the nanoparticles were found influenced by rifampicin nanoparticles (PLGA) concentration; both parameters were increased with increasing rifampicin nanoparticles(PLGA) concentration. During the formation of

nanoparticles the RIF might be undergoing shift from crystallinity to amorphous in the polymer PLGA and therefore the increasing encapsulation efficiency and percentage yield with increase in PLGA concentration. The DSC thermogram showed characteristic change in the endothermic peak of rifampicin showing amorphous form of the drug that helps in influencing the encapsulation efficiency and percentage yield of nanoparticles. The particle was found smooth and spherical at all concentration of polymer, however with increase in size of particles as the concentration of PLGA increased. The particle size increased with increase in PLGA concentration. The particle size of nanoparticles depend upon that techniques followed for preparation of nanoparticles and other factors such as the type of crosslinking agent and the desolvating agent used. The size of the nanoparticles ranged from 298 ± 0.25 nm to 892 ± 0.12 nm (Table 9). An increase in particle size was evident with increase in PLGA concentration..

The PDI of nanoparticles ranged between 0.195 and 0.541 (Table 9) which indicates a homogenous dispersion of the drug; the PDI was found increased with increasing the PLGA concentration indicating that higher concentration of the polymer detrimental to homogenous dispersion of the drug. This may be another reason pointing to suggest that the particle size of the nanoparticles depending on the PLGA concentration.

Surface characteristics of the nanoparticles greatly influence their interaction with the biological membrane, besides the stability of nanoparticles. Zeta potential is an index of the stability of the nanoparticles under most conditions, the higher the absolute value of the zeta potential of the nanoparticles, the larger the charge on their surface, leading to stronger repulsive interaction between the dispersed nanoparticles and higher stability and more uniform size. It has also been demonstrated that a high potential value of above ± 25 mV, ensures a high energy barrier that stabilizes the nanosuspension (Muller R.H. et al)⁷⁸. A lower zeta potential (less than 0.25 mV) observed in the formulations F₂, F₃, F₄, F₅ & F₆ may be another factor influencing the particle size of nanoparticles in these formulations. The nano size initially formed during the preparation of nanoparticles formed aggregates to grow in size due to instability of the nanoparticles with low zeta potential which was evident in F₂, F₃, F₄, and F₅ & F₆.

A variable dissolution profile of formulations F₁, F₂, F₃, F₄, F₅ and F₆ was observed. All formulations showed slow dissolution of Rifampicin. However the percentage of rifampicin release was highest 35% (Table 14 and fig 17) from F₁, and lowest 17.2% (Table 24 and fig 22) from

F₆ formulation. The percentage of rifampicin release from F₂ was 31.4 (Table 16 and fig 18). The percentage of rifampicin release from F₃ was 28 % (Table 18 and fig 19). The percentage of rifampicin release from F₄ was 22.4% (Table 20 and fig 20). The percentage of rifampicin release from F₅ was 20.4 (Table 22 and fig 21). All the formulations showed zero order release kinetic with r^2 value about 0.99. The variation in percent drug release at different time point intervals, in different formulations may be due to the PLGA concentration used. The factors influencing the dissolution of rifampicin can be stated as follows. 1. Particle size plays an important role in influencing the dissolution of the drug in the environment. The particle size was least in F₁ 298 nm as compared to that in F₂ 495 nm and F₃ 596 nm and F₄ 698 nm, F₅ 859 nm and F₆ 892 nm. Therefore it is obvious that a higher percent of Rifampicin was released from F₁ as compared to F₂, F₃, F₄, F₅ and F₆. Other factors such as pH of the environment can also influence the dissolution of drug. However in the present study all formulations showed slow dissolution which was found to be independent of pH of the environment. These observations suggest that PLGA nanoparticles release the drug at a rate independent of the pH of the environment.

The in-vitro dissolution profile of F₁, F₂, F₃, F₄, F₅ and F₆ was also reflected in the diffusion study. The percentage drug diffused from F₁, F₂, F₃, F₄, F₅ and F₆ was 35%, 31%, 28%, 22.4%, 20.4% and 17.2% (Table 14, 16, 18, 20, 22 and 24) respectively. These findings propose that factors particularly particle size of nanoparticles did also influence the diffusion of drug which was found to be dependent upon the PLGA concentration. There was no burst release of drug from all the formulations and showed a near perfect zero order release of the nanoparticles.

Based on the dissolution and diffusion characteristics the formulation F₆ was found to be the ideal formulation for further in-vivo study. According to FDA guidelines a controlled release formulation should release 0-20% at 4 h, 15-70% at 12 h and > 85% at 24h. Accordingly a formulation F₆ was found to satisfy the above requirement compared to F₂, F₃, F₄, F₅ and F₆ as such the formulation F₆ was selected for the in-vivo pharmacokinetic study.

The result of *in-vitro* study was examined in the *in-vivo* study. The *in-vivo* study was limited to the influence of Rifampicin PLGA in 1:3 ratios along with FDC on the pharmacokinetic of RIF and FDC because PLGA at this concentration was found to inhibit RIF degradation in the presence of FDC to maximum. The C_{max} of RIF was significantly decreased from 9.38-8.22 μ g/ml and Increased to 11.38 when rifampicin along with PLGA this was reversed to 10.61 μ g/ml by PLGA along with FDC (Table 79 and Fig 42). The bioavailability of the drug is normally reflected in the AUC values of the drug. The $AUC_{(0-24)}$ of RIF was significantly ($p<0.001$) reduced from 51.44 to 38.00 in the presence of FDC ,and increased to 94.44 in the presence of PLGA along with rifampicin which was reverse to 84.16 by PLGA in the presence of FDC (Table 81 and Fig 44). Similarly there was significant difference in $AUC_{(0-\infty)}$ of RIF as compared to RIF +FDC and RIF+PLGA and RIF +PLGA+FDC. The $AUC_{(0-\infty)}$ of RIF was 101.83 which was significantly decreased to 61.40 by FDC.164.4 when rifampicin along with PLGA. Rifampicin nanoparticles Incorporation reversed the $AUC_{(0-\infty)}$ values from 164.4 of RIF+PLGA to 142.27 of RIF +FDC+PLGA (Table 83 and Fig 46) significantly ($p<0.001$). The changes in C_{max} , AUC_{0-24} , and $AUC_{0-\infty}$ clearly indicate that PLGA significantly improve the bioavailability of RIF. Comparison of C_{max} , $AUC_{(0-24)}$ and $AUC_{0-\infty}$ of RIF with that of 3FRSV reveal that Incorporation of Rifampicin nanoparticles PLGA significantly inhibit the formation of 3FRSV, the metabolite of RIF.

The C_{max} of 3FRSV with RIF alone was 6.48 which was increased to 8.08 significantly ($p<0.001$) that was significantly ($p<0.001$) reversed to 4.0 by PLGA co administration (Table 89 and Fig 51). The $AUC_{(0-24)}$ of 3FRSV with RIF+FDC was 40.75 and 3.58 with RIF+PLGA which was reduced significantly ($p<0.001$) to 19.67 by Incorporation of PLGA along with FDC (Table 91 and Fig 53). Similar pattern was observed with $AUC_{0-\infty}$ of 3FRSV which was 62.86 with RIF in the presence of FDC and it was significantly ($p<0.001$) reduced to 31.43 with Incorporation of PLGA along with FDC (Table 88 and Fig 51). The T_{max} of RIF was not significantly affected in the presence of FDC as well as with Incorporation of rifampicin nanoparticles . The K_{el} of RIF was significantly ($p<0.01$) influenced and decreased from 0.36 hr^{-1} to 0.183 hr^{-1} by Incorporation of rifampicin nanoparticles in the presence of FDC (Table 82 and Fig 45). The underlying mechanism for change in K_{el} value of RIF in the presence of FDC by Incorporation of rifampicin nanoparticles was not clearly understood. Presence of 3FRSV

formation we observed similar K_{el} of 3FRSV is increased significantly ($p<0.01$) with Incorporation of rifampicin nanoparticles (Table 87 and Fig 50).

11. CONCLUSION

The present study reveals that FDC promotes degradation of rifampicin in the acidic environment. Incorporation of rifampicin nanoparticles in fixed dose combinations resulted more rifampicin concentration availability in the acidic environment for absorption. Further work in humans may help to understand the beneficial effects of rifampicin nanoparticles in fixed dose combination instead of rifampicin.

11. REFERENCES

1. Dye C, Garnett GP, Sleeman K, Williams BG. Prospects for worldwide tuberculosis control under the WHO DOTS strategy. Directly observed short-course therapy. *Lancet* 1998;352:1886-91.
2. Mariappan TT, Saranjit Singh. Gastrointestinal permeability studies using combinations of rifampicin and nucleoside analogue reverse transcriptase inhibitors in rats. *Ind J Pharmacol* 2007;39:284-90.
3. Jianfang Liu, Jin Sun, Wei Zhang, Kun Gao, Zhonggui He. HPLC determination of rifampicin and related compounds in pharmaceuticals using monolithic column. *J Pharm Biomed Anal* 2008;46:405–09.
4. Hemanth Kumar A. Chandra IK, Geetha R, Silambu Chelvi K, Lalitha V, Prema G. A validated high-performance liquid chromatography method for the determination of rifampicin and desacetyl rifampicin in plasma and urine. *Ind J Pharmacol* 2004;36:231-33.
5. Subhash Agal, Rajiv Baijal, Snehanishu Pramanik, Nikhil Patel, Parijat Gupte, Praful Kamani, Deepak Amarapurkar. Monitoring and management of antituberculosis drug induced hepatotoxicity. *J Gastroenterol Hepatol* 2005;20:1745-52.
6. Heifects LB, Lindholm-Levy P. Comparison of bacterial activities of streptomycin, amikacin, kanamycin, and capreomycin against *Mycobacterium avium* and *M tuberculosis*. *Antimicrob Agents Chemother* 1989;33:1298-1301.
7. Garg RK. Classic diseases revisited: Tuberculosis of the central nervous system. *Postgrad Med J* 1999;75:133-140.
8. Mitchison DA. Mechanism of drug action in short-course chemotherapy. *Bull Int Union Tuberc* 1985;65:30-7.
9. Iseman MD, Madsen LA. Drug-resistant tuberculosis. *Clin chest Med* 1989;10:341-53.

10. Panchagnula R, Rungta S, Sancheti P, Agrawal S, Kaul C. In vitro evaluation of food effect on the bioavailability of rifampicin from antituberculosis fixed dose combination formulations. *Farmaco*. 2003;58:1099-1103.
11. Acocella G. Clinical Pharmacokinetics of Rifampicin. *Clin Pharmacokinet* 1978;3:108-27.
12. Peloquin CA, Namdar R, Singleton MD, Nix DE. Pharmacokinetics of Rifampin Under Fasting Conditions, With Food, and With Antacids. *Chest* 1999;115:12-18.
13. Satish Balkrishna Bhise, Sevukarajan Mookkan. Formulation and Evaluation of Novel FDCs of Antitubercular Drugs. *J Pharm Res* 2009;2:437-44.
14. Akansha Tripathi, Ranjana Gupta, Subhini A. Saraf. PLGA Nanoparticles of Anti Tubercular Drug: Drug Loading And Release Studies Of a Water Insoluble Drug. Faculty of Pharmacy, BBDNITM, Sector-1, Dr. Akhilesh Das Nagar, Fazabad Road, Lucknow, 227105 (UP), India July – September 2010..
15. [Raviglione](#) MC, [Dixie ES Jr](#), [Kochi](#) A. Global Epidemiology of Tuberculosis. *JAMA* 1995;273:220-6.
16. De Jong BC, Antonio M, Gagneux S. *Mycobacterium africanum*-review of an important cause of human tuberculosis in West Africa. *PLoS Negl Trop Dis* 2010;4:744
17. Dye C, Garnett GP, Sleeman K, Williams BG. Prospects for worldwide tuberculosis control under the WHO DOTS strategy. Directly observed short-course therapy. *Lancet* 1998;352:1886-91. (I -1)
18. Chakraborty AK. Epidemiology of tuberculosis: Current status in India. *Indian J Med Res* 2004;120:248-76.
19. Walls T, Shingadia D. Global epidemiology of paediatric tuberculosis. *J Infect* 2004;48:13-22.
20. Dye C. Global epidemiology of tuberculosis. *Lancet* 2006;367:938–40.
21. Burzynski J, Schluger NW. The epidemiology of tuberculosis in the United States. *Semin Respir Crit Care Med* 2008;29:492-8.

22. Pepper DJ, Meintjes GA, McIlleron H, Wilkinson RJ. Combined therapy for tuberculosis and HIV-1: the challenge for drug discovery. *Drug Discov Today* 2007;12:980-9.
23. Mitchison DA. Mechanism of drug action in short-course chemotherapy. *Bull Int Union Tuberc* 1985;65:30-7.
24. Iseman MD, Madsen LA. Drug-resistant tuberculosis. *Clin chest Med* 1989;10:341-53.
25. Heifets LB, Lindholm-Levy P. Comparison of bacterial activities of streptomycin, amikacin, kanamycin, and capreomycin against *Mycobacterium avium* and *M tuberculosis*. *Antimicrob Agents Chemother* 1989;33:1298-1301.
26. Garg RK. Classic diseases revisited: Tuberculosis of the central nervous system. *Postgrad Med J* 1999;75:133-140
27. Ragno R, Marshall GR, Di Santo R, Costi R, Massa S, Rompei R, *et al*. Antimycobacterial pyrroles: synthesis, anti-*Mycobacterium tuberculosis* activity and QSAR studies. *Bioorg Med Chem* 2000;8:1423–32.
28. Hu Y, Coates AR, Mitchison DA. Sterilising activities of fluoroquinolones against rifampintolerant populations of *Mycobacterium tuberculosis*. *Antimicrob Agents Chemother* 2003;47:653–7.
29. Cole ST, Alzari PM. TB-a new target, a new drug. *Science* 2005;307:214–5.
30. Matsumoto M, Hashizume H, Tomishige T, Kawasaki M, Tsubouchi H, Sasaki H, *et al*. OPC-67683, a nitro-dihydro-imidazoazole derivative with promising action against tuberculosis in vitro and in mice. *PLoS Med* 2006;3:2131–44.
31. Ginsberg AM, Spigelman M. Challenges in tuberculosis drug research and development. *Nat Med* 2007;13:290–94.
32. Nuermberger E, Tyagi S, Williams KN, Rosenthal I, Bishai WR, Grosset JH. Rifapentine, moxifloxacin, or DNA vaccine improves treatment of latent tuberculosis in a mouse model. *Am J Respir Crit Care Med* 2005;172:1452–6.

33. Chen P, Gearhart J, Protopopova M, Einck L, Nacy CA. Synergistic interactions of SQ109, a new ethylene diamine, with front-line antitubercular drugs in vitro. *J Antimicrob Chemother* 2006;58:332–7.
34. Panchagnula R, Rungta S, Sancheti P, Agrawal S, Kaul C. In vitro evaluation of food effect on the bioavailability of rifampicin from antituberculosis fixed dose combination formulations. *Farmaco*. 2003;58:1099-1103.
35. Koup JR, Williams-Warren J, Viswanathan CT, Weber A, Smith AL. Pharmacokinetics of Rifampin in Children II. Oral bioavailability. *Ther Drug Monit* 1986;8:17-22.
36. Saranjit Singh, Mariappan TT, Sankar R, Sarda N, Baljinder Singh. A critical review of the probable reasons for the poor/variable bioavailability of rifampicin from anti- tubercular fixed-dose combination (FDC) products, and the likely solutions to the problem. *Int J Pharm* 2001;228:5-17.
37. C.J.Shishoo,S.A.Shah, I.S. Rathod, S.S. Savale, M.J. Vora .Impaired bioavailability of rifampicin in presence of isoniazid from fixed dose combination formulation, *int J Pharm*. 2001; 228:53–67.
38. Singh S, Mariappan TT, Sankar R, Sarda N, Singh B. A critical review of the probable reasons for the poor/variable bioavailability of rifampicin from anti-tubercular fixed dose combination (FDC) products, and the likely solutions to the problem. *Int J Pharm* 2001;228:5-17.
39. Shishoo CJ, Shah SA, Rathod IS, Savale SS, Kotecha JS, Shah PB. Stability of rifampicin in dissolution medium in presence of isoniazid. *Int J Pharm* 1999;190:109-23.
40. Jindal KC, Chaudhary RS, Singla AK. Gangwal, SS Khanna S. Dissolution test method for rifampicin–isoniazid fixed dose formulations. *J Pharm Biomed Anal* 1994;12:493-97.
41. Sankar R, Sharda N, Singh S. Behavior of decomposition of rifampicin in the presence of isoniazid in the pH range of 1-3. *Drug Dev Ind Pharm*. 2003;29:733-8.

42. [Mariappan](#) TT, [Singh](#) S. Regional gastrointestinal permeability of rifampicin and isoniazid (alone and their combination) in the rat. [Int J Tuberc Lung Dis](#) 2003;7:797-803.
43. .Gambhire Vaishali , Bhalekar Mangesh , Gambhire Makarand . Development of rifampicin nanoparticles by 3^2 factorial design. International Journal of Pharmaceutical Sciences and nanotechnology 2010 ; 3(3) : 1085-1091
44. . Magdalena Stevanovi,Dragan Uskokovi.Poly(lactide-co-glycolide)-based Micro and Nanoparticles for the Controlled DrugDelivery of Vitamins.
45. . L. Zhang , D. Pornpattananangkul, C.-M.J. Hu and C.-M. Huang. Development of Nanoparticles for Antimicrobial Drug Delivery .Current Medicinal Chemistry, 2010; 17: 585-594.
46. Prabakaran D, Singh P, Jaganathan KS, Vyas SP: Osmotically regulated asymmetric capsular systems for simultaneous sustained delivery of anti-tubercular drugs. *J Contr Rel* 2004, 95(2):239-248.
47. Pandey R, Sharma A, Zahoor A, Sharma S, Khuller GK, Prasad B: Poly (DL-lactide-co-glycolide) nanoparticle-based inhalable sustained drug delivery system for experimental tuberculosis. *J Antimicrob Chemother* 2003, 52:981-986.
48. Kailasam S, Daneluzzi D, Gangadharam PRJ: Maintenance of therapeutically active levels of isoniazid for prolonged periods in rabbits after a single implant of biodegradable polymer. *Tuber Lung Dis* 1994, 75(5):361-365.
49. Dutt M, Khuller GK: Sustained release of isoniazid from a single injectable dose of poly (DL-lactide-co-glycolide) microparticles as a therapeutic approach towards tuberculosis. *IntJ Antimicrob Agents* 2001, 17:115-122.
50. Ain Q, Sharma S, Garg SK, Khuller GK: Role of poly [DL-lactide-co-glycolide] in development of a sustained oral delivery system for antitubercular drug(s). *Int J Pharm* 2002, 239(1-2):37-46.

51. Pandey R, Sharma A, Zahoor A, Sharma S, Khuller GK, Prasad B: Poly (DL-lactide-co-glycolide) nanoparticle-based inhalable sustained drug delivery system for experimental tuberculosis. *J Antimicrob Chemother* 2003, 52:981-986.
52. Zhou H, Zhang Y, Biggs DL, Manning MC, Randolph TW, Christians U, Hybertson BM, Ng K: Microparticle-based lung delivery of INH decreases INH metabolism and targets alveolar macrophages. *J Contr Rel* 2005, 107(2):288-299.
53. Barrow EL, Winchester GA, Staas JK, Quenelle DC, Barrow WW. Use of microsphere technology for targeted delivery of rifampin to *Mycobacterium tuberculosis*-infected macrophages. *Antimicrob Agents Chemother* 1998; 42:2682-2689.
54. Sharma R, Saxena D, Dwivedi AK, Misra A. Inhalable microparticles containing drug combinations to target alveolar macrophages for treatment of pulmonary tuberculosis. *Pharm Res* 2001; 18:1405-1410.
55. Suarez S, O'Hara P, Kazantseva M, Newcomer CE, Hopfer R, McMurray DN, Hickey AJ: Airways delivery of rifampicin microparticles for the treatment of tuberculosis. *J Antimicrob Chemother* 2001, 48:431-434.
56. O'Hara P, Hickey AJ: Respirable PLGA microspheres containing rifampicin for the treatment of tuberculosis: manufacture and characterization. *Pharm Res* 2000, 17:955-961.
57. Zahoor A, Pandey R, Sharma S, Khuller GK: Pharmacokinetic and pharmacodynamic behaviour of antitubercular drugs encapsulated in alginate nanoparticles at two doses. *Int J Antimicrob Agents* 2006, 27(5):409-416.
58. Pandey R, Khuller GK: Solid lipid particle-based inhalable sustained drug delivery system against experimental tuberculosis. *Tuberculosis* 2005, 85(4):227-234.

59. Vyas SP, Kannan ME, Sanyog Jain, Mishra V, Singh P: Design of liposomal aerosols for improved delivery of rifampicin to alveolar macrophages. *Int J Pharm* 2004, 269(1):37-49.
60. Walter Wehrli. Rifampin: Mechanisms of Action and Resistance. *Rev Infect Dis* 1983;5:407-11.
61. Goodman and Gilman: The pharmacological basis of therapeutics. 10th ed. edited by Joel G. Hardman and Lee E. Limbird, published by McGraw-Hill Medical Publishing Division; .p1706.
62. Van Scoy RE, Wilkowske CJ. Antituberculosis agents. *Mayo Clin Proc* 1987;**62**:1129-36.
63. Chow AW, Jewesson PJ. Pharmacokinetics and Safety of Antimicrobial Agents during Pregnancy. *Rev Infect Dis* 1985;**7**:287-313.
64. Erlich Henry, Doolittle WF, Volker Neuhoﬀ. Molecular Biology of Rifomycin. New York, NY: MSS Information Corporation, 1973. pp. 44-45, 66-75, 124-130.
65. Meyer H, Mally J. Über Hydrazinderivate der Pyridincarbonsäuren. *Monatshefte für Chemie und verwandte Teile anderer Wissenschaften* 1912; 23: 393-414.
66. Indian Pharmacopeia 2010 volume II page 1515-1517.
67. Winder FG, Collins PB. Inhibition by isoniazid of synthesis of mycolic acids in *Mycobacterium tuberculosis*. *J Gen Microbiol* 1970; 63: 41-8.
68. Baciewicz AM & Self TH: Isoniazid interactions. *South Med J* 1985; 78:714-718.
69. Siskind MS, Thienemann D, Kirlin L. Isoniazid-induced neurotoxicity in chronic dialysis patients: report of three cases and a review of the literature. *Nephron* 1993; 64: 303-6.
70. Jimenez-Lucho VE, Del Busto R, Odel J. Isoniazid and ethambutol as a cause of optic neuropathy. *Eur J Respir Dis* 1987; 71: 42-5.
71. Parasuram S, Ravendran R, kesavan R. Blood sample collection in small laboratory animals. *J Pharmacol Pharmacother* 2010;1:87-93.

72. Karan RS, Bhargava VK, Garg SK. Effect of trikatu, an Ayurvedic prescription, on the pharmacokinetic profile of rifampicin in rabbits. *J Ethnopharmacol* 1999;64:259-64.
73. Bhavika Mohan, Nishi Sharda, Saranjit Singh, Evaluation of the recently reported USP gradient HPLC method for analysis of anti-tuberculosis drugs for its ability to resolve degradation products of rifampicin, *J.pharm and biomedical analysis* 2003; 31:607-612.
74. Shargel L, Wu-Pong S, Yu ABC. *Applied Biopharmaceutics and Pharmacokinetics*. 5th ed. p. 46.
75. Doshi BS Bhate AD, Chauhan BL, Parkar TA, Kulkarni RD. Pharmacokinetics interaction of oral RIF and INH in normal subjects. *Indian Drugs* 1986;133:1076-80.
76. Gallo GG, Radaelli P. Rifampicin. Academic Press, New York, *Analytical profile of Drug substances* 1976;5:467-515.
77. Maggi N, Pasqualucci CR, Ballotta R, Sensi P. Rifampicin: A new orally active rifampicin. *Chemotherapy* 1966;11:285-92.
78. Muller RH, Souto EB, Goppert TM, Gohla S. Production of biofunctionalized solid lipid nanoparticles (SLN) for site-specific drug delivery. *Nanotechnologies for the life sciences Vol 2; Biological and pharmaceutical nanoparticles*. Weinheim; Kumar CSSR, WILEY-VCH Verlag GmbH & Co. KGaA; 2006.